NON-LINEAR FINITE ELEMENT ANALYSIS ON SINGLE-HEADED ANCHOR UNDER SHEAR LOADING IN CONCRETE COMPARED TO PREDICTIVE DESIGN MODELS

by

Mayembe Muledy

210527138

A thesis submitted in fulfillment of the requirements for the degree of

Master of Science in Civil Engineering

College of Agriculture, Engineering and Science

School of Civil Engineering, Surveying & Construction

University of KwaZulu-Natal

Date: 08/02/2023

Supervisor: Prof. G. Drosopoulos

Co-supervisors: Dr. O.B.Olalusi and Dr. Mcleod

Declaration

I hereby certify that the dissertation I have just finished is my original work, carried out under the guidance of Prof. G. Drosopoulos, Dr. O.B.Olalusi and Dr. McLeod It is submitted for the degree of Master of Science in Engineering in the College of Agriculture, Engineering and Science, School of Civil Engineering, Surveying & Construction, University of KwaZulu-Natal, Durban. I further declare that other than this submission, this dissertation has not been delivered or submitted to any institution for the award of any degree. All references used in the dissertation have received the appropriate credit.

Signature (Student): Muledy.M Date: 08/02/2023

Signature (Supervisor) Date: 08/02/2023

Dedication

I dedicate this work to God Almighty, who is the source of all my inspiration, knowledge, wisdom, and insight. It is only on his wings that have been able to fly. This work is also dedicated to my father and late mother. Also, to the memory of my brothers, who though affected in every way, yet made it a point of duty to always encourage and motivate me to keep fighting harder to finish the work I had started. God bless you all.

Acknowledgment

My supervisors Prof. Georgios Drosopoulos, Dr. O.B.Olalusi, and Dr. McLeod, have my undying gratitude. This project would not have been possible without your mentoring. Your immense contributions are indeed highly appreciated.

My deep gratitude also goes to my beloved daughter, Alegria Nkengue Mayembe and my fiancé, Mrs Zungu Nana. You stood firmly beside me to provide emotional support throughout the difficult journey, especially at moments when it seems impossible to move on.

Finally, I want to thank all my generous family members and friends who helped me achieve this dream in one way or another. You were instrumental in bringing me to the happy end of a difficult journey. Thank you all.

Table of Contents

Table of Figures

List of Tables

Notations and Units

Below is the list of the terms, acronyms, abbreviations, and symbols used in this dissertation are listed below. In this thesis, SI units are used unless a conversion factor has been applied. All anchor design parameters such as effective embedment depth, anchor nominal diameter, and edge distance are in mm. The mean compressive strength of concrete is in MPa, the concrete breakout capacity is in KN and all dimensions are given in mm.

ANCHOR DESIGN PARAMETERS

d_{nom}	Anchor nominal diameter
h_{ef}	Effective embedment depth
C_1	Edge distance
$f_{cc,200}$	Mean Compressive strength of concrete (using cube strength)

$f_{cc,150}$ Mean compressive strength using a cube with a side length of 150 mm can be calculated using the following expression:

$f_{cc,150} = \frac{f_{cc,200}}{0.95}$ in MPa

$\frac{h_{ef}}{d_{nom}}$	Stiffness Ratio

FURTHER NOTATIONS

V_U	Concrete breakout failure loads from the design predictive models in KN
$V_{u,Exp}$	Experimental concrete edge breakout failure loads in KN
$V_{u,pred}$	Predictive concrete edge breakout failure loads in KN
$\boldsymbol{V_{FEA}}$	Concrete edge breakout failure loads obtained from a numerical study in KN
β	Coefficient used to compute model uncertainties
f_{ctm}	Tensile strength of concrete in MPa
E_C	Young modulus in GPa
f	Stress in MPa
ε	Strain
CCD	Concrete capacity Design Method
MPC	Contact algorithm used in FE model to connect all the nodes
FEA	Finite element analysis
CoV	Coefficient of Variation
SD	Standard deviation
$\boldsymbol{R^2}$	Coefficient of determination
r	Correlation coefficient

FEM	Finite element model

Abstract

In recent years, advances in technology-aided design tools have made the construction of complex structures increasingly easier. Consequently, there is growing research interest in using different fastening techniques to understand how components of an engineering structure connect to ensure resilient designs. For instance, depending on the installation methods, the construction industry uses a variety of anchorage systems, such as cast-in-place anchors and post-in-place anchors. Previous studies have predominantly focused on understating the behavior of concrete anchors subjected to shear loading utilizing Finite Element Analysis (FEA) explicit dynamic solver. However, there is scanty evidence of work that analyzed the concrete behavior of a single cast-in-place headed anchor subjected to shear loading using an FEA static solver. Understanding the nonlinear behavior of a single concrete-headed anchor under loading and the consequent failure loads associated with concrete edge breakout depends heavily on the type of analysis. This dissertation examines the nonlinear behavior of a single concrete-headed anchor using a concrete model that was created using solid 65 element in Ansys static structural. The proposed model accuracy is validated by comparing numerical study results to experimental test results. However, the impact of the anchors in-group is not taken into account in this study because it solely addresses single-headed anchors loaded in shear. In addition, this study evaluated uncertainties and bias based on i) the Concrete Capacity Design (CCD) model, ii) the European standard (EN1994-2:2009), iii) the analytical predictive models from Anderson and Meinheit (2006), and iv) the Grosser model (2006). While the first two are drawn from the codes, the second two are derived from literature on anchorage with concrete edge breakout failure. The study employed statistical analysis and linear correlation to examine the uncertainties and biases of each predictive model. Overall, the failure loads derived from the numerical study were higher than the loads obtained from the findings of experimental test results. Nevertheless, in some instances, results obtained from numerical analysis were much lower than the experimental test results. This exception points to several assumptions made regarding the constitutive materials law of concrete and steel anchors. The statistical analysis and model uncertainties quantification of each predictive model indicates that the Grosser model is the most excellent predictor of concrete breakout capacity of single-headed anchor subject to shear loading, followed by Anderson and Meinheit (2006), EN2, and CCD.

Keywords: Cast-in-place headed anchor, finite element analysis (FEA), predictive models, concrete breakout capacity, and models uncertainties.

CHAPTER 1

INTRODUCTION

1.1 Background and Importance of the Study

There has been increasing demand for the design of an anchorage fastening system in concrete that resists static or dynamic loading in recent years. However, such connection systems become challenging to design without adequate information on the response of materials under loads. It has become critical to investigate how to design fasteners with sufficient load carrying and deformation capacity – that is fasteners that are, reliable, durable, and robust (Eligehausen et al., 2001).

Using numerical analysis, this study examined the behavior of a single cast-in-place headed anchor under shear loading in uncracked concrete (i.e., concrete devoid of reinforcing bars and while the tensile stress in the vicinity of the anchor is limited by the design standard: refer to section 2.1). Furthermore, this study investigated the applicability of the design models for anchorages namely, the Concrete Capacity Design (CCD) method, the European Standard model (EN1994-2:2009), the Anderson and Meinheit model (2006), and the Grosser Model (2012). These predictive design models apply only to single-headed anchors under shear loading.

The reason for using EC2 instead of the South African National Standard (SANS) for fastening design systems is because the SANS code is still under development and lack information in term of anchorage systems design. EC2 part 4 for structures and civil engineers provide more information which enables the designers to design and install anchors in such a way that our infrastructures and building are safe and more reliable.

Although experimental tests are widely used by designers to predict the structural response of a varied range of structures under different loading conditions (ranging from static to dynamics loading), such experiments are often cost-intensive and require a long time to complete compared to numerical analysis (Davidson et al., 2005; Wu et al., 2012). In contrast, numerical analysis has great flexibility in changing geometry, design parameters, materials properties, and loading conditions of a structural component (Al Saeab, 2019).

Despite its numerous advantages, a numerical analysis can be challenging and may produce unrealistic results due to the absence of experimental tests, materials properties, and models adopted (Al Saeab, 2019). For example, despite concrete being the conventional construction material composed of cement, aggregate, and water, it displays a nonlinear behavior leading to difficulties in modelling and simulations. Furthermore, concrete has a complex structural response with significant non-linearities including stress-strain behavior, tensile cracking, and compression crushing materials properties (Al Saeab, 2019).

Previous studies show that several factors have significant impacts on the strength of the anchorage system to concrete (Al Saeab, 2019). These include factors that are associated with:

i. Anchor type (cast-in-place or post-install), anchors spacing (in the case of anchors in the group), embedment depth, anchor strength, and edge distance.
ii. The base material (such as concrete) strength and condition of the base material.
iii. The applied load’s nature and direction as well as the type of the loads, which can be static or dynamic; and
iv. The environmental conditions (e.g., temperature and corrosion)

Conventionally, concrete breakout failure loads of anchorage systems can be determined by experimental testing, numerical modelling, or analytical predictive models. Current literature suggests that most of the earlier studies mainly concentrated on anchorage systems loaded in tension. However, the results from experimental and numerical investigations have revealed that such studies do not always produce positive results (Grosser, 2012). Other studies on shear-loaded anchorages and predictive models have either used design standards such as the European standard (EN1992-4:2009), the American Concrete Institute (ACI 318), the Concrete Capacity Design (CCD) model, the international federation for structural concrete (fib 1998) and predictive design models from literature such as Wong (1980) and Cruz (1987), Shaikh and Yi (1985), Fuchs (1990), Anderson and Meinheit (2006) and Grosser method (2012).

Many questions related to anchorage systems loaded in shear remain open. Consequently, many experimental tests and numerical studies have examined the behavior of anchorage systems subjected to static loading under tension and their results implemented in design codes (ACI318, EN1992-4: 2009, Fib) to improve the formulation of the predictive design equations for the anchor design parameters (Wong (1980); Eligehausen et al. (1986); Cruz 1(987); Ling (1988); Zhao, Fuchs, and Dieterle (1988); Matupayont (1989)). Making reasonable assumptions about the stress-strain behavior of the concrete, and the stiffness of the fixture due to shear and tension-loaded anchors is necessary for the nonlinear analysis (Eligehausen et al, 2001).

In this study, the conservative numerical approach used to examine the behavior of a single concrete-headed anchor is to implement Finite Element Analysis (FEA) using Ansys static solver. A three-dimensional nonlinear finite element model (FEM) capable of predicting structural behavior and reliability of concrete anchor failure modes under different loading conditions ranging from static to dynamic. This approach enables the model to carefully implement simulation parameters such as geometry, materials, contact modelling, meshing technique, boundary conditions, and load level. Similarly, Li and Eligehausen (1994) carried out a numerical analysis to determine the load-bearing capacity of anchors in the group while explicitly accounting for the effect of the hole clearance. The authors used typical load-displacement response curves for individual anchors in their analysis and concluded that the calculated load-bearing capacity was in good agreement with results obtained from laboratory tests. Numerical modelling of a single cast-in-place headed anchor subjected to shear loading requires the concrete parameters and the steel anchor strength to be incorporated into the model. Following this approach, Lee et al. (2020) investigated the shear failure mode and concrete edge failure on a single cast-in-place anchor. The authors concluded that the shear capacity of a single cast-in-place anchor mainly depends on the steel anchor's tensile strength and concrete compressive strength.

As its contribution to the open questions on anchorage systems, this study focused on the numerical simulation of a single cast-in-headed anchor embedded in a concrete cube using finite element analysis and predictive models. This study adopted four predictive design models, namely, the Concrete Capacity Design (CCD) method, the European Standard model (EN1994-2:2009), the Anderson and Meinheit model (2006), and the Grosser Model (2012). These predictive models have gained wide recognition internationally for predicting the shear capacity of a single cast-in-place headed anchor. The first two models are drawn from the codes, while the last two are from previous analytical predictive publications related to concrete edge breakout failure. The study further evaluated the performance of the models via statistical analysis and model uncertainty quantifications. Furthermore, the mean, standard deviation (SD), coefficient of variation (COV), coefficient of determination and correlation coefficient of anchor design parameters were used to quantify the uncertainties and bias of each predictive model

1.2 Statement of the Problem

Designers utilize static structural analysis in Ansys workbench to understand the nonlinear behavior of reinforced concrete (RC) members such as beams, slabs, columns, and foundations under static or dynamic loads. However, such numerical studies cannot describe the full concrete damage to concrete anchorage systems. Therefore, it takes an explicit dynamic solver to understand concrete damage fully. As a result, studies have been conducted on reinforced concrete beams using static solvers in Ansys, but numerical investigations of anchorage systems using static structural analysis solver types have received little research attention. Specifically, the study of the nonlinear behavior of concrete anchors under shear loading using a static analysis solver is still lacking.

Therefore, it becomes imperative for this study to investigate the nonlinear behavior of concrete anchors subjected to shear loading in uncracked concrete using FEA static solver. The outcome of such an investigation will offer helpful insights that can enable researchers and structural engineers to understand the nonlinear behavior of concrete anchors using a simplify concrete model and consequently predict the anchor load-carrying capacity of the anchorage system subjected to shear loading, providing safety for the users and saving construction costs.

1.3 Aim and Objectives

This study aims to investigate the behavior of a single-headed anchor embedded in concrete subject to shear loading using nonlinear finite element analysis (FEA) in the Ansys static structural workbench.

The following objectives were established to achieve the goal:

i. To create a model that displays the nonlinear behavior of concrete in the Ansys workbench.
ii. To conduct a mesh sensitivity analysis using a load-displacement response curve.
iii. To verify results from the numerical model in comparison to experimental test results.
iv. To perform a statistical analysis and model uncertainties quantification of each predictive models
v. To investigate relevant parameters influencing the load-bearing capacity using linear correlation analysis.

1.4 Research Hypothesis

The following hypotheses were tested in this study regarding the behavior of a single-headed anchor in concrete:

I. Hypothesis 1: The shear capacity of a single cast-in-placed headed anchor with concrete breakout failure can be predicted using static structural analysis solver in Ansys workbench.

II. Hypothesis 2: The load-carrying of a single-headed anchor subjected to shear loading can be determined using the design standards from the codes of practice and predictive models from the literature.

1.5 Research Questions

The study sought to test the stated hypotheses by answering the following research questions:

Q 1: How can the nonlinear behavior of concrete-headed anchors be modelled in Ansys static structural?

Q 2: How can the current design models from the codes of practice and predictive models from previous research publications be used to predict the shear capacity of the headed anchor displaying concrete edge breakout failure?

1.6 Research Methodology

This study's methodology included the following steps: data collection and creating a model using principles of Finite Element Analysis (FEA) in Ansys static workbench. From the analysis, a simulation was performed to establish the trend and understand the nonlinear behaviour of the cast-in headed anchor and predict the corresponding concrete breakout capacity.

Then, the predictive models from the design standards and predictive models from previous publications were assessed based on statistical analysis and model uncertainties quantifications.

1.7 Research Limitations

The study consisted of numerical analyses on a single cast-in-place headed anchor under shear loading, evaluated selected predictive design models using statistical and model uncertainties quantification, and assessment of the sensitivity of anchor design parameters. Nevertheless, the research was subject to several limitations and assumptions:

i. The study only considered single anchors rather than multiple grouped anchors.

ii. The concrete model used in the FE analysis does not consider the crack sections

iii. The study was limited to considering uncracked concrete sections, rather than cracked.

1.8 Dissertation outline

This Master’s thesis is divided into five chapters which are as follows:

Chapter 1: Introduction

This chapter describes the thesis’s background, objectives, hypotheses to be tested and significance.

Chapter 2: Literature review

This chapter provides an overview of the Finite Element Model (FEM) and Predictive models that were used in this study. As a results, the chapter critically examines related previous studies, their conclusions and contributions, as well as their strengths and weaknesses.

Chapter 3: Research methodology

This chapter describes the methodological approach used in this study, source of data, FE model, statistical analysis and uncertainties quantification of different Predictive Models adopted in the study.

Chapter 4: Results and discussion

This chapter provides an overview of all simulations conducted using the principle of Finite Element Analysis (FEA) in Ansys static structural workbench. The chapter compares the experimental results to the various predictive models used in the study. Most importantly, the chapter reports how the study's hypothesis relates to the findings obtained.

Chapter 5: Conclusion and Future Work

This chapter is a summary of the research based on the findings obtained. Essentially, the chapter provides a brief conclusion, useful recommendations, and a possible direction for future work.

CHAPTER 2

LITERATURE REVIEW

2.1 An overview of anchorage systems

Engineers can use anchorage systems to connect concrete and steel or structural components. Essentially, the design of anchorages allows them to convey tension and shear forces in concrete that results from any combination of applied loads (Eligehausen et al., 2012). Due to this vital role of anchorage techniques, it becomes imperative to design such a technique according to required standards.

From the design point of view, there are two load types to which anchors can be subject, namely, static and dynamic loads. The sum of permanent and quasi-permanent loads is referred to as static loads. Permanent loads are referred to as dead and live loads in this context. Dynamic loads arise from the actions of earthquakes, impacts, explosions, or vibration of machinery that create a large inertia force (Eligehausen et al., 2012). The presence of inertia force and attenuation forces is the main technical difference between static and dynamic loads. These forces are primarily caused by induced acceleration and must be taken into account when determining the forces on the anchors (Eligehausen et al., 2012).

In the design of anchorage systems, two stages can arise: anchors embedded in concrete can leads to a cracked concrete section otherwise a non-cracked concrete section in the vicinity of the anchor (Meyer.R et.al, 1994). The main difference between cracked and uncracked concrete is well-defined in EN 1992-4. The various design verifications required for concrete anchorage design depend on whether the concrete is defined as cracked or uncracked (EN1992-4).

For a concrete member to be deemed uncracked, the designer must be able to show through stress analysis that the concrete in close proximity to the anchor will remain uncracked under all predicted loading circumstances for the duration of the member's design life.

If it can be demonstrated that, under service conditions, the fastener and its complete embedment depth are situated in non-cracked concrete, non-cracked concrete may be assumed (refer to CEN/TS1992-4-1: 2009), if the equation below is realized, then this will be satisfied:

$\alpha_L + \alpha_R \ll \alpha_{admin}$

where α_L denotes the stresses in the concrete caused by the applied external loads including fastener load; α_R denotes the stresses in the concrete caused by restriction, intrinsic imposed deformations, or extrinsically imposed deformations. If no detailed analysis is performed, then $\alpha_R = 3\ N/mm^2$should be assumed as stipulated in CEN/TS1992-4-1: 2009; α_{admin} is the permissible tensile stress defining non-cracked concrete stage. A suggested value of $\alpha_{admin} = 0\ N/mm^2$ is acceptable (CEN/TS1992-4-1: 2009).

The above equation can be expressed as follows: $\alpha_L + \alpha_R \ll 0$ and $\alpha_L \ll -3N/mm^2$. As a result, for non-cracked concrete, the stresses in the concrete caused by the applied external loads should be limited to $3N/mm^2$.

Several theoretical and experimental investigations have been conducted over the past last few decades to characterize and explain the failure mechanisms of cast-in-place headed anchors under tension load, as well as to determine their corresponding failure loads (Ottosen (1981), Elfgren et al. (1982), Stone and Carino (1983), Eligehausen and Sawade (1985), Krenchel and Shah (1985), Ballarini et al. (1986), Ožbolt and Eligehausen (1990), and Elfgren et al. (2001a)), the studies demonstrated that when an anchor bolt is subjected to tensile force, concrete in the anchoring zone experiences large circumferential tensile stresses. These stresses result in the formation of microcracks at the service condition. Even small service loads (about 30% of the ultimate peak load) cause circumferential tension cracks at the head of the anchor to spread to the concrete surface as the loads on the anchor bolt increase. After the peak load, the crack growth becomes unstable and causes more severe deformation. Additionally, the circumferential cracks slope changes from test to test and is not constant along their depth. The cone angles are typically between 30 and 40 degrees with an average value of 35 degrees with respect to the concrete surface (Eligehausen et al., 2012).

Due to the absence of experimental data, it was predicated that headed studs under tension and shear loads would exhibit a similar distribution of tensile stresses along the fracture surface. The 45-degree cone model, which was incorporated into ACI 349, was the first theoretical model for predicting the concrete cone failure load (1985). This model is based on the 45 degrees cone angle and constant concrete tensile stress f_{ct}= 0.3$\sqrt{f_{cc}}\, N/mm^2$ where f_{cc}denotes the mean concrete compressive stress using cube test.

The stresses in the concrete caused by external loads were restricted to $3N/mm^2$ in this study as stipulated in CEN/TS1992-4-1: 2009 for non-cracked concrete. Because the tensile stress in the concrete is limited to 3 MPa (Refer to CEN/TS1992-4-1: 2009), the mean concrete compressive strength ranging from 21.5 to 31.5 MPa yielded an uncracked concrete section in the numerical study. It is evident that from the model adopted in numerical analysis, the formation of micro-crack at low-stress levels is expected. The concrete model (solid 65 element) adopted in the numerical study does not display the full concrete damage and does not take into consideration the crack section.

2.1.1 Load transfer mechanisms

The fastening and connections system must be designed to meet one or more of the following performance criteria:

I. **Strength**: A fastening system must be capable of resisting all actions (or forces) that it will be subjected to during its lifetime, including those resulting from external actions and restraint of imposed deformations.

II. **Ductility**: The ability of a fastening system to accommodate large inelastic deformation without a major decrease in capacity. In other words, a fastening system is ductile if it can be drawn or plastically deformed without fracture (Ovid'ko et al., 2018). It also measures the anchor's capacity to sustain overloads without loss of strength. This performance criterion significantly impacts seismic applications (Shuvalov et al., 2021). This characteristic in seismic applications can be sufficiently enhanced for large anchors to provide energy absorption.

III. **Durability:** Resistance to the adverse effects of change in temperature, exposure to moisture and other corrosive agents.

Apart from these three main performance criteria, other design factors that need to be considered, such as cost of construction, maintenance (especially selection of corrosion protective methods), and appearance, may significantly influence the final design of fastenings. Therefore, the inability of a fastening system to satisfy one of the four criteria above has given rise to multiple fastening types.

It is crucial to understand the load transfer mechanism across the base material and the fastening in terms of the classification of fastening systems. Different fasteners transfer tension load to the base material, as shown in Figure 2.1. Load transfer mechanisms of tension fastenings can be identified in three ways, as shown in Figure 2.1: mechanical interlock, friction and bond (Eligehausen et al., 2006).

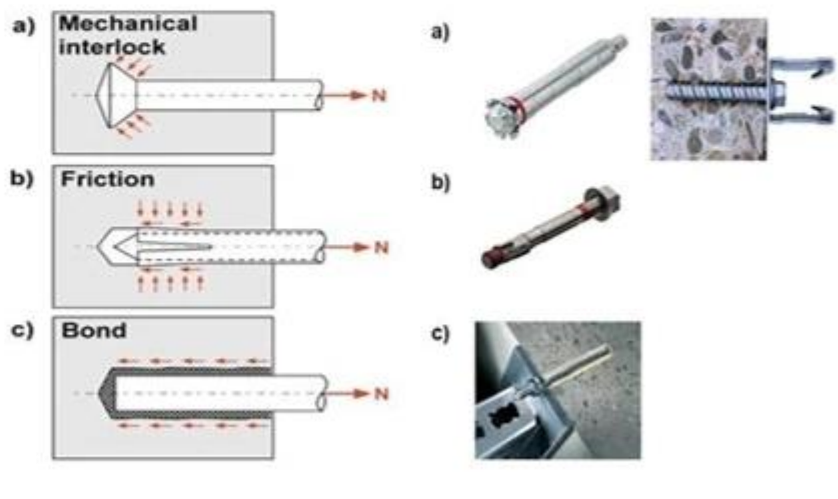

Figure 2.1: Anchor load-transfer mechanisms (Eligehausen et al, 2006)

I. Mechanical interlocks transfer load through bearing between the fasteners and the base materials. Such an approach applies mainly to headed anchors, screw anchors, undercut anchors and anchors channels.

II. Friction is a load transfer mechanism used primarily by expansion anchors. This mechanism allows an expansion force to be generated during the installation process, resulting in a frictional force between the drilled hole side and the anchors.

III. A bond is a load transfer mechanism that allows tension force to be transferred to the base material. Bounded anchors use chemical interlock as a load transfer mechanism.

The type of mortar used is the most important factor influencing bond strength. The bond stress distribution over the embedment depth is determined by the magnitude of the load, the stiffness of the mortar, and the embedment depth. Bond stresses are distributed unevenly across the embedment depth at peak load. For convenience, a uniform bond stress distribution is commonly assumed (Eligehausen et al, 2006). According to Cook et. al, 1998 bond strengths of most mortar products presently on the market do not vary considerably from the anchor rod nominal diameter. Nevertheless, some mortars exhibit diameter sensitivity in the form of significantly lower bond strength at specific diameters. For a wide range of concrete grades, the design value of the ultimate bond stress is provided in EC2, Cl 8.4.2 The basic required anchorage length is calculated using EC2, Cl 8.4.3 and is determined by the design yield stress of the steel bar, the maximum bond stress, the concrete grade, and the nominal diameter of the steel bar.

The effect of bond stresses between the concrete and the anchor is not considered in this study.

In the construction industry, most commercial fastening systems are designed to resist tension load via one or more load transfer mechanisms, as mentioned above. Depending on the fastening installation methods used for anchoring external load to concrete and reinforced concrete, two fastening methods are widely used in the construction industry. These fastening methods can be cast-in-place installation and post-installed installation systems.

2.1.2 Classification of anchors

a) **Cast-in-place installation systems**

Before the concrete is set, the anchors are secured in the formwork. External tension loads are transferred to cast-in place system via mechanical interlock between the embedded components and concrete (Eligehausen et at., 2006). One advantage of using this technique is that the expected external applied forces are known and can be accommodated in the reinforcement member design. Furthermore, cast-in-place anchors are more resistant to earthquakes (Liu et al., 2021). This thesis concentrated on shear-loaded cast-in-place headed anchors, as shown in Figure 2.2.

b) Post-installed installation systems

Drilling holes into the hardened concrete is used to Install. In some cases, large anchorage systems require the use of rock drills as well as rotary hammers and diamonds cores (which are less commonly used), as shown in Figure 2.2.

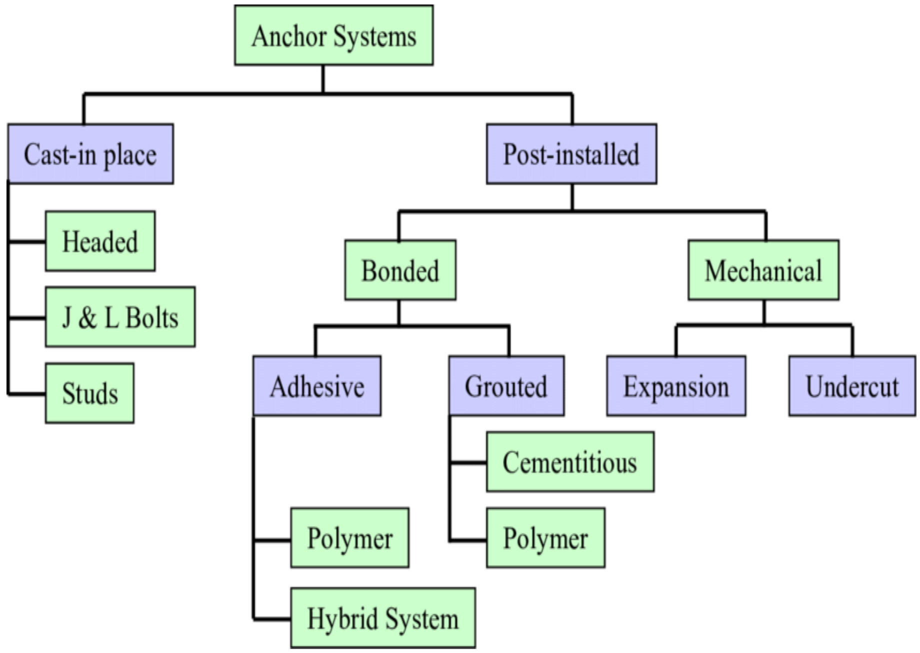

Figure 2.2: Fastening Methods: Cast-in-place installation and post-installed installation method (Eligehausen et al., 2006)

2.2 Cast-in-place headed anchor subjected to shear loading

Cast-in-place anchors subjected to a shear loading exhibits four major failure modes. The steel failure, concrete edge failure, concrete pry-out failure and pull-out failure are examples of these. These failure modes are discussed further below and illustrated in Figures 2-3.

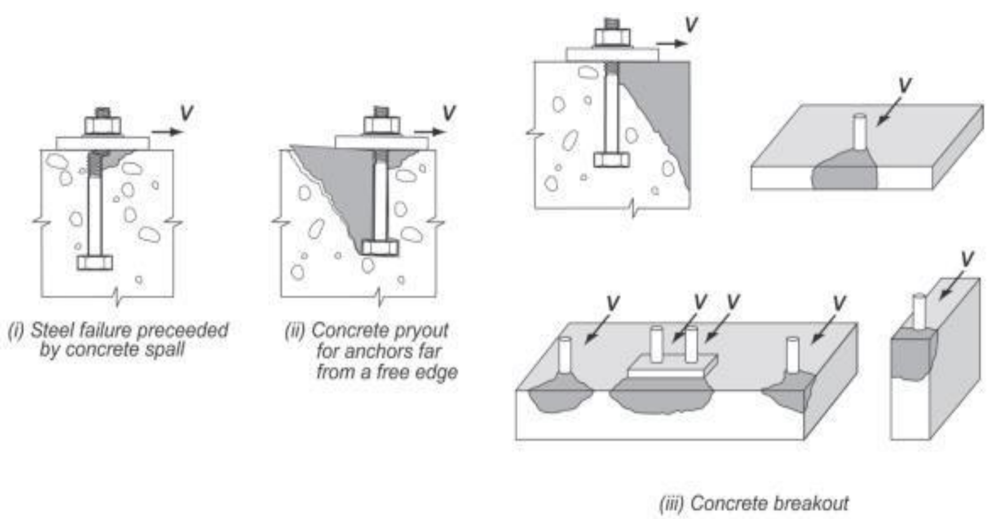

Figure 2.3: Mechanical fastener (Headed anchors) failure modes associated with shear loading (Eligehausen et al., 2006)

2.2.1 Pull-out Failure

The pull-out failure mode of cast-in-place headed anchor is typically associated with expansion anchors that are unable to develop sufficient frictional resistance to accommodate the tensile force generated in the anchor bolt as a result of lateral deformation. However, this failure mode is not discussed in depth because such failures are infrequently observed (Eligehausen et al., 2006).

2.2.2 Pry-out Fracture

Anchors subjected to shear loading with a limited embedment depth can rotate enough to cause a pry-out fracture. The primarily fracture surface forms behind the point of load application (Fig 2-3). This type of failure mode is not dependent on the presence of a free edge (Eligehausen et al., 2006).

Jebara et al. (2006) reported on the pry-out failure of a cast-in-place welded anchor subjected to shear loading in their investigation. The authors discovered as the anchor diameter increases, so does that the ultimate shear capacity.

2.2.3 Steel failure

Anchors subjected to shear load may exhibit steel failure if the embedment depth and edge distance are sufficiently large, resulting in conical spalling of the surface concrete and steel failure (as shown in Figure 2.3). Steel failure represents an upper limit on the shear capacity of the anchorage system for a given type of anchor Eligehausen et al., 2006).

2.2.4 Concrete breakout or concrete edge failure

The concrete edge breakout failure of a single cast-in-place headed anchor loaded in shear is central to this thesis. This emphasis is motivated by the fact that anchors subjected to shear loading toward the free edge may fail by forming a semi-conical fracture surface in the concrete that originates at the point of bearing and radiates to the free surface (Figure 2.3) (Eligehausen et al., 2006).

Ueda et al. (1990) investigated the shear strength of headed anchors embedded in concrete. Their experimental findings focused on concrete failure with wedge cone in the majority of the tested specimens, and the authors concluded that increasing the edge distance has a significantly impacts the shear strength of the anchors. As a results, increasing the edge distance increases the shear strength of single and double concrete anchors. When the load is applied perpendicular to the edge distance, the findings of Eligehausen et al. (2006) support the observation of Ueda et al. (1990). Ueda et al. (1991) and Eligehausen et al. (2006) maintained that the failure load remains constant up to some critical edge distance when the applied load is perpendicular to the edge distance.

Furthermore, Stichting & Bouwresearch (1971) and Fuchs & Eligehausen (1986/2) investigated the behavior of anchorage systems loaded in shear perpendicular to the edge distance. The authors proposed that the anchors could fail through the concrete fracture before reaching the load-carrying capacity of the steel anchors. The fracture cracks have an average angle of 35 degrees to the edge and propagates to a depth at the face of the edge and grow to a depth of approximately 1.3 to 1.5 times the edge distance. Zhao et al. (1988) and Zhao et al. (1988) conducted experimental tests to investigate the behavior of single anchor subjected to shear loading in concrete slabs with limited depth. These studies investigated the variation of the ratio between the embedment depth and the edge distance, given as $(\frac{h}{c_1})$. And, of the 76 total experimental tests performed on shear-loaded anchors, 37 tests were performed within the range of $0.5 \leq \frac{h_{ef}}{c_1} < 1.5$ and 39 tests within the range $1.5 \leq \frac{h_{ef}}{c_1} < 5.33$. According to their findings, the shear resistance of the anchor decreases when compared to slabs with suitable member thickness.

2.3 Load-displacement behavior and concrete edge failure of a headed anchor under shear load perpendicular to the edge

The load-displacement behavior of a shear-prone cast-in-place headed anchor is like to that of a post-installed anchor (Eligehausen et al., 2006).

Anchorages close to an edge under shear load perpendicular to the edge distance may fail via concrete fracture before the load-carrying capacity of the anchor steel is reached, according to Stichting & Bouwresearch (1971) and Fuchs & Eligehausen (1986/2). Furthermore, further investigation revealed that the fracture crack forms at an average of 35° to the edge and grows to a depth at the face of the edge of 1.5 times the edge distance.

The load-bearing behavior of such fasteners is strongly influenced by the tension behavior of crack concrete (Eligehausen et al., (2006). As a results, developing a reasonable analytical technique to calculate the concrete cone breakout load of anchors loaded in shear becomes difficult.

As a results, methods for determining the load-carrying capacity of headed anchors subjected to shear load near the edge have been developed. Utilising such methods requires the application of predictive models such as the Concrete Capacity Design model (CCD), EN1992-4: 2009 (European standard), Anderson and Meinheit (2006), and the Grosser Method (2011) as described in subsection 2.4.

2.4 Design Provisions and Predictive Models for a Single Cast-in-Place Headed Anchor Under Shear Load

The codes of practices and analytical predictive models have proposed many design methods in the literature. Essentially, these models are developed to predict the concrete breakout failure loads of a single cast-in-place headed anchor under shear load. Such predictive models comprise of but are not restricted to: i) the European standard (EN1992-4:2009), ii) the American Concrete Institute (ACI 318), iii) the Concrete Capacity model Design (CCD), iv) the International Federation for Structural Concrete (fib 1998), v) Fuchs et al. (1995), vi) Anderson and Meinheit (2006), and vii) Grosser Method (2011).

However, this study focuses on two common design methods proposed in the building codes for anchorages system subjected to shear loading and two analytical predictive models from the literature. These predictive models are the Concrete Capacity Design model (CCD), the European standard (EN1992-4: 2009), the Anderson and Meinheit (2006), and the Grosser Method (2011).

2.4.1 Concrete Capacity Design (CCD) Model

Fuchs (1984) proposed an equation for predicting the average concrete breakout capacity of a single headed anchor loaded in shear perpendicular to the edge of a member. The proposed equation is based on the results of approximately 80 experimental tests on post-installed and cast-in-place headed anchors with anchor nominal diameter (d) ≤ 25mm.

Based on additional experimental tests on various types of anchors, Zhao et al. (1989) confirmed the applicability of this equation, establishing the effect of the anchor geometry. Furthermore, Eligehausen et al. (1997) performed additional analysis on a database of shear tests on anchors. To aid their investigation, the authors developed an empirical model as described in Eq. 2.1.

$$V_u = 0.9 \times d_{nom}^{\ 0.5} \times \sqrt{f_{cc,200}} \left(\frac{hf}{d_{nom}}\right)^{0.2} \times C_1^{\ 1,5} \qquad \text{(Newton)} \qquad \text{(Eq.2.1)}$$

Where $d_{nom} \leq 25$ mm (Nominal diameter of the anchor)

$\frac{hf}{d_{nom}} \leq 8$

Figure 2.4. depicts the concrete breakout failure loads V_u for post-installed and headed anchors loaded perpendicular to the edge are plotted as a function of the edge distance C_1 .Using the relationship established in Eq2.1 Eligehausen et al. (2006) summarized the failure load measured in the tests to an outside diameter d_{nom} = 18mm, h_{ef} = 80 mm and a concrete strength ${f_{cc,200}}^{0.5}$ = 25N/mm^2.

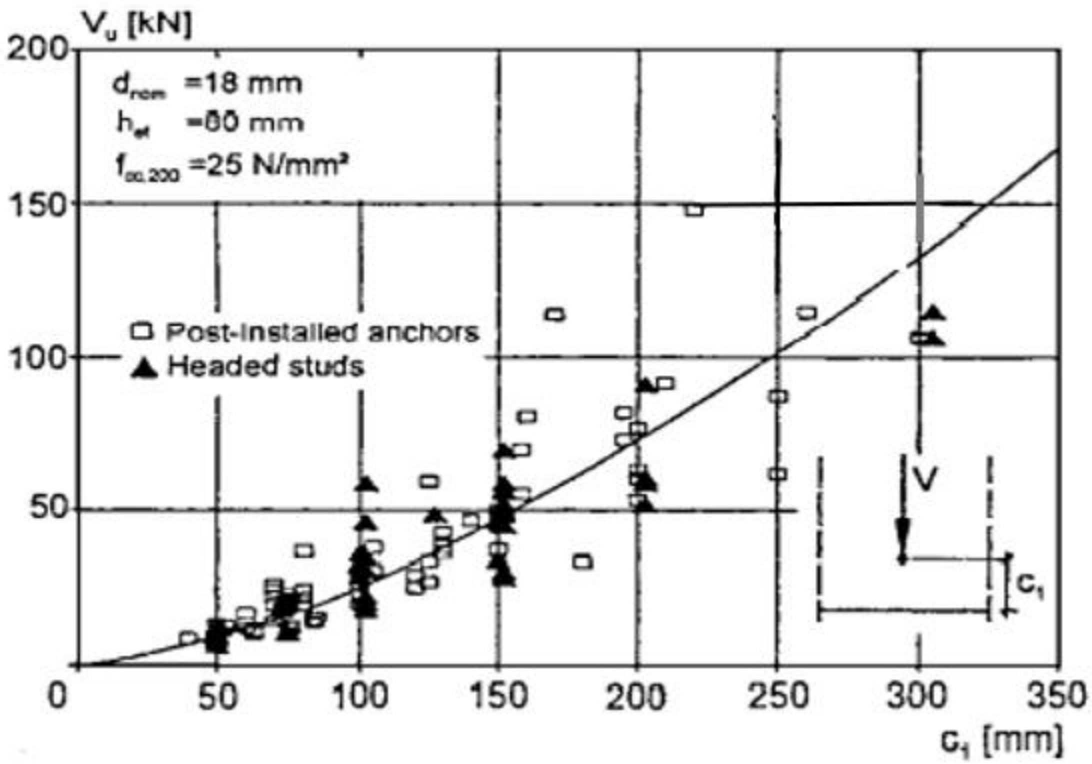

Figure 2.4: Effect of edge distance on the concrete cone breakout load due shear load towards the edge (Eligehausen et al., (1997))

From Fig.2.4, there seems to be a higher scatter as the concrete breakout failure loads increase. This trend can be attributed to the formulation and limitations of equation 2.1. It seems reasonable to limit the applicability of Eq.2.1 to an edge distance C_1 = 100 mm

According to Fuchs et al., 1995, the ratio of the measured to calculated concrete breakout failure load exhibits a normal distribution with a mean of 0.95 and a coefficient of variation of 17%.

According to Eligehausen et al. (2006), such scattering is slightly greater than that associated with concrete tensile strength.

According to Equation. 2.1, the edge distance has a significant influence on the concrete breakout failure load of a headed anchor loaded in shear near the edge. However, the failure concrete breakout load is proportional to ${C_1}^{1,5}$ whereas the area of the fracture surface is proportional to ${C_1}^2$. This relationship is most likely due to the size effect discussed by Fuchs (1990). Furthermore, according to Eq.2.1, the load-carrying capacity of the anchor is influenced by the tensile capacity of the concrete, which is assumed to be proportional to ${f_{cc,200}}^{0.5}$, as well as the distribution of bearing stresses along the anchor length, which is strongly dependent on the bearing stiffness of the concrete and the flexural stiffness of the steel anchor (Eligehausen et al., (2006).

More experimental and numerical studies have on post-installed bonded and headed anchors have been conducted. Eligehausen & Hofmann (2003), for example, demonstrated that Eq.2.1 overestimates the effect of the anchor diameter, particularly for anchors with a diameter greater than 25 mm. This study provided a more precise approach for computing the average concrete breakout failure load, as given by the following equation:

$$V_u = 3 \times {d_{nom}}^{\alpha} \times {l_f}^{\beta} \times \sqrt{f_{cc}} \times c^{1.5} \quad \text{(Newton)} \qquad \text{(Eq.2.2)}$$

Where $\alpha = 0.1 \left(\frac{l_f}{d_{nom}}\right)^{0.5}$ and $\beta = \left(\frac{d_{nom}}{C_1}\right)^{1.5}$

According to Equation 2.2, the effect of the anchor diameter and the value of the concrete breakout failure load are both affected by the edge distance (Eligehausen et al., (2006). The concrete breakout failure load for anchors with constant embedment depth, is roughly proportional to ${d_{nom}}^{0.15}$ for a small edge distance, and the anchor diameter has small influence on a large edge distance.

Fuchs (1990) explored the behavior of single and anchor groups under shear load in uncracked concrete and conducted various experimental and numerical studies on the anchorages system. Based on their findings of the authors, Fuchs et al. (1995) developed the Concrete Capacity Design (CCD) model which was published in the code.

The authors formulated Eq. 2.3. for the calculation of the shear strength of a single-headed anchor under shear load:

V_u= K×$d_{nom}{}^{o.5}$×$C_1{}^{1,6}$×$\sqrt{f_{cc,200}}$ (Newton) (Eq.2.3)

Where:

d_{nom} = anchor nominal diameter

C_1 = Edge distance

$f_{cc,200}$ = concrete compressive strength

K = Prefactor used to take into account the anchor design parameters

Furthermore, Grosser (2012) proposed a more simplified form of Equation 2, that takes into account the effect of the anchor t diameter, the edge distance, the embedment depth and the mean concrete compressive strength as shown below:

V_u= $(\frac{hf}{d_{nom}})^{0.2}$×$d_{nom}{}^{0.5}$×$C\ _1{}^{1,5}$×$\sqrt{f_{cc,200}}$ (Newton) (Eq.2.4)

Where:

h_f: Embedment depth (mm)

C_1: Edge distance

$f_{cc,200}$: Concrete compressive strength (Mpa)

2.4.2 The European standard (EN1992-4-2:2009)

Fuchs et al. (1995) and Hofmann (2005) contributed to the development of the predictive shear capacity equation of headed anchor in the concrete loaded in shear near the free edge according to the European standard (EN1992-4:2009). Fuchs et al. (1995) conducted a series of experimental tests on a single anchor under shear load with a nominal anchor diameter less or equal to 25 mm (d_{nom} ≤ 25 mm) and embedment depth less or equal to 8 times the nominal anchor diameter (l_f ≤ $8d_{nom}$) near the free edge in a thick uncracked concrete structural member. The authors proposed equation to calculate the shear capacity can be expressed as follows:

$V_{u,c}$ = K.$\sqrt{d_{nom}}$. $(\frac{l_f}{d_{nom}})^{0,2}\sqrt{f_{cc,200}}$. $C_1{}^{1,5}$ (Newton) (Eq.2.5)

K = Prefactor used to take into account the anchor design parameters

d_{nom} = anchor nominal diameter

$\frac{l_f}{d_{nom}}$ = stiffness Ratio

C_1 = Edge distance

$f_{cc,200}$ = concrete compressive strength

Because a few additional experimental tests have reported a better correlation with test results when Eq.2.5 is reduced by 10%, the above equation is frequently found with a prefactor k= 0.9. Essentially, a prefactor is a constant introduced into an analytical model in order to increase the accuracy of the concrete breakout capacity.

Other studies have called into question the equation (Eq.2.5) proposed by Fuchs et al. (1995). Hofmann (2005) for example, revised Eq2.5 to broaden the range of nominal anchor diameter and embedment depth. Hofmann's proposed equation, as shown in Eq. 2.6 is founded on numerical simulations with anchor diameter up to 190 mm and embedment depths equal to 16 times the nominal diameter.

$$V_u = 3 \times {d_{nom}}^{\alpha} \times {l_f}^{\beta} \times \sqrt{f_{cc}} \times c^{1.5} \qquad \text{(Newton)} \qquad \text{(Eq.2.6)}$$

Where:

$\alpha = 0.1 \left(\frac{l_f}{d_{nom}}\right)^{0.5}$ and $\beta = \left(\frac{d_{nom}}{C_1}\right)^{0.5}$

Both Eq. 2.3 and Eq.2.4 describe the mean concrete breakout load of a single anchor loaded near the free edge in non-cracked concrete which is not affected by the edges or member thickness. Equation 2.6 is the fundamental expression used in EN1992-4:2009 to determine the concrete breakout failure capacity of the anchor loaded in shear toward the free edge.

2.4.3 Anderson and Meinheit (2006)

The concrete breakout capacity of a single headed studs under shear load is determined by the mean concrete compressive strength and the edge distance. The concrete breakout capacity is computed using the equation below:

$$V_{u,c,o} = 14.47.C^{\frac{4}{3}}.\sqrt{f_{cc,200}} \qquad \text{(Newton)} \qquad \text{(Eq. 2.7)}$$

Where: C= edge distance (mm) and $f_{cc,200}$is the mean concrete compressive strength (MPa)

2.4.4 Grosser Method (2011b)

Grosser (2012a) proposed the mean concrete breakout for a single headed anchor subjected to shear load as given below:

$$V_u = 16.5.\sqrt{f_{cc,200}}.C^{\frac{4}{3}}.\psi_{d,v}.\psi_{l,v} \quad \text{(Newton)} \quad \text{(Eq. 2.8)}$$

Where:

$\psi_{d,v}$= (0.02d + 0.5) ≤ 1

$= 0.5\times(\frac{d}{d_o} + 1) \leq 1$ where d_o= 25 mm

$\psi_{l,v} = (\frac{h}{12d})^{x}$ with x = $(\frac{1}{C})^{0.4}$ more accurate approach (refer to Grosser 2011a)

X = 0.2 for $\frac{h}{d} < 12$

X = 0,1for $\frac{h}{d}$ >12

The simplified form of Grosser's equation is as given below:

$$V_u = 16.5\times\sqrt{f_{cc,200}}.\,C^{\frac{4}{3}}.\,(0.02d+0.5).(\frac{h}{12d})^{C^{-0.4}} \quad \text{(Newton)} \quad \text{(Eq. 2.9)}$$

Many sources of uncertainties should be considered in engineering design in order to achieve an optimal design. Reliability analysis methods provide the basis to account for uncertainties found in predictive models in a realistic manner (Soubra et al., 2015). The failure probability and reliability index are used to quantify risks and assess the probability of failure. In this study structural reliability-based performance is not considered.

Olalusi and Spyridis (2020) investigated uncertainties in modelling concrete edge breakout failure of a single anchor under shear load, using statistical analysis and model uncertainty quantification of the CCD model, ACI318, EN1992, and Grosser model from the database of 366 anchor tests loaded in shear. The conclusions of this study are summarized below:

- The authors revealed that the CCD and ACI 318 models were highly scattered and biased.

- The CCD model uncertainties seem to be very sensitive to the anchor design parameters (anchor nominal diameter, edge distance and embedment depth.
- The Grosser model and EN1992-4 depict low scatter and bias with mild correlation with shear design parameters.
- The model uncertainties derived through statistical analysis can be used as an input in reliability analysis and to derive partial safety factors for anchors subjected to shear loading.

Olalusi et al. (2019) have assessed the reliability of the EN1992-1-1 variable strut inclination method of shear design provision for stirrup using a General Probabilistic method. The authors have evaluated the reliability index of EC2 shear design formulation over a range of practical design situations. The outcomes of these studies were:

- The reliability indices of all the test sections investigated meet the target reliability requirement for the reliability class 2 structure.
- The EC2 reliability analysis indicated uneconomical high reliability at the low level of shear reinforcement.

2.5 Finite Element Analysis (FEA)

The section introduces the basic concept of finite element analysis, Ansys software package and numerical simulation procedures. The section concludes with a summary and findings of previous research on the finite element method (FEM) and its application to analysing nonlinear behavior of reinforced concrete (RC) structures and anchorages system under loading.

2.5.1 Finite Element Analysis (FEA) Concept

Finite Element Analysis (FEA) is a numerical method for solving engineering problems that employs a variety mathematical technique. This technique has gained wide adoption in all engineering disciplines, among others. According to Kurowski (2016), the automotive industry has widely implemented finite element analysis (FEA) as a efficiency tool for design engineers to reduce both development time and costs. The name of the technique implies that it divides a large problem into smaller, simpler parts known as finite elements. The equations that modelled these finite elements are solved and reassemble back into the large system of equations that modelled the entire problem. The method is widely used to analyse structural engineering problems to understand structural components' linear and nonlinear behaviour and their response under various loading conditions.

Numerical simulation models like Finite Element Analysis (FEA) are based on the discretization of the integral form of an equation. The Ansys workbench outlines three major steps to enable engineers or designers to define a problem:

I. Pre-processing: this involves defining the key points such as element types and materials.

II. Processing: has to do with assigning loads, and constraints and solving the model.

III. Post-Processing: this step involves carrying out further processing and viewing of results.

2.5.2 Methods for Solving Engineering Problems

The three methods used to solve engineering problems are:

i. Analytical method: this is considered a theoretical approach to solving engineering problems.

ii. Numerical method: this is the software approach to engineering problem-solving.

iii. Experimental method: this involves carrying out a practical evaluation or testing in the laboratory (e.g. stress, loading, displacement)

2.5.3 FE Program Ansys

Ansys is a practical Finite Element (FE) computer program used to solve problems with complicated geometry, and Multiphysics problems, where obtaining solutions using analytical and experimental approaches is challenging. The program can also ensure safety and provide design insights and optimization, which helps save materials costs and increase the components factor of safety.

Brighton (2011) investigated the damage of prestressed reinforced concrete beam repair with Carbon Fibre Reinforced Polymer (CFRP) using the principle of finite element analysis. The authors modelled the concrete element using the Solid 65 element in Ansys. Brighton’s findings can be summarized as follows:

I. The deflection at the yielding and ultimate load represents the experimental deflections better than the cracking load due to Ansys's ability to model steel more accurately than concrete.
II. Results obtained from finite element analysis showed a strong correlation with the experimental test conducted on the girder.
III. The FE model results demonstrate that CFRP can be used effectively as a retrofit technique.

Using the finite element method (FEM), Cotsovos et al. (2009) investigated the response of supported reinforced concrete beams (RC) under various loading conditions ranging from static to earthquake to rates encountered in blast and impact problems. The study employed three FE software packages (ANSYS, ABAQUS and LS-DYNA) to investigate the applicability of finite element models and their ability to produce convincing predictions of structural concrete behavior. The authors used three case studies which are summarized below:

Case 1: Ductile beam under static monotonic loading

- The LS-DYNA material constitutive law for concrete (Winfrith and Schwer) is more realistic in predicting the behavior of ductile reinforced concrete beams under static monotonic loading. The maximum values of mid-span displacement correlate with experimental values and overestimate the reinforced concrete beam’s the load-carrying capacity.

- The results obtained with the ABAQUS finite element software package are comparable to those obtained with LS-DYNA. ABAQUS employs a concrete constitutive material model that assumes that concrete exhibits an elastic compression behavior. This model assumption explained the discrepancy between the numerical and the test results on the load-carrying capacity and maximum mid-span displacement.

- With the Ansys FE software, the best predictions of the load-carrying capacity and maximum mid-span displacement were obtained by adopting a stress-strain response curve A, describing the uniaxial compression behaviour of the concrete material and using a shear retention factor of 20%. The authors also revealed that using stress-strain B and C reduced the predicted load-carrying capacity and ductility (Cotsovos et al., 2009).

Case 2: Brittle beam under monotonic static loading

In this case, a brittle beam under to monotonic static loading at mid-span results obtained from different finite element predicted models are presented in the load-displacement curves and predicted cracks pattern. Conclusions are summarized as follows:

- LS-DYNA prediction model revealed a response much stiffer than the test results. The predicted load-bearing capacity and ductility are higher than the experimental test results. Adopting the Winfrith concrete constitutive model overestimates the predicted load-carrying capacity (Cotsovos et al., 2009).
- The ABAQUS model predicts the stiffness and maximum displacement realistically while overestimating the load-carrying capacity (Cotsovos et al., 2009).
- ANSYS predictive model revealed the best prediction of ductility and the load-carrying capacity when the authors used the stress-strain response curve C (Cotsovos et al., 2009) and a shear retention factor of 20%. On the other hand, adopting curve A and curve B with a higher shear retention factor overestimated the load-carrying capacity.

Case 3: Ductile beam subject to monotonic higher rate loading

The reinforced concrete beam used in case 1 consists of beams tested under different loading rate conditions varying from 2 KN/msec (monotonic static loading) to 200 KN/msec (impact loading). Conclusions for case 3 can be summarized as follows:

- The prediction model obtained from ANSYS finite element software package form an upper bound to the results of the experimental tests.
- Prediction obtained from LS-DYNA and reinforced concrete finite element RC-FINEL better fits the experimental results.
- The predictive FEA results correlated with the experimental test results under the assumption that in high-rate loading situations, concrete and steel reinforcement material properties are independent of the strain rate, and their effects on the structural response are related to the inertia force developed in the member.

The case studies used in these studies are restricted to simply supported reinforced concrete (RC) beams under axial load at mid-span applied at various load rates varying from static loading to impact loading.

Using finite element analysis Halahla and Abdulsamee (2019) investigated the nonlinear behavior of reinforced concrete (RC) beams under transverse loading. The author developed the concrete material constitutive model using solid 65 elements in ANSYS and investigated the predictive model's ability to yield realistic results.

The conclusions of Halahla, Abdulsamee (2019) can be summarized as follows:

I. The finite element stress's stresses, deflections and initial crack propagation at the centreline compare favourably to the analytical model based on the energy method and the experimental results from an RC beam.

II. There is good agreement between the failure loads from the Finite Element Analysis (FEA) compared to the experimental failure load.

III. A possible numerical solution error may occur during the analysis due to limitations on the mesh size, memory size, contact type, and the concrete and steel model adopted

Al Saeab (2019) used LS-DYNA software package to investigate the behavior of anchorage systems at various strain rates using the finite element method (FEM). Using the LS-DYNA software package, the author investigated the tensile and shear behavior of cast-in-place, undercut, adhesive anchors under various strain rates. Al Saeab (2019) used numerical modelling with a variety of design parameters. In addition, the author determined the ideal mesh size that best simulated the experimental test results from literature using a mesh sensitivity analysis. Furthermore, using these design methods, the author validated the anchorage system's ultimate design capacity by using regression analysis to predict a relationship that accurately represents the FEA results. Saeab (2019) reached following conclusions based on the findings:

I. The numerical models developed for cast-in-place, undercut, and adhesive anchors can predict the tensile and shear behavior, failure load and the failure modes of the anchorage systems at various strain rates.

II. The ultimate shear capacity of the anchors is primarily determined by the diameter of the anchor, the larger the diameter, the greater the ultimate shear capacity.

III. When the pry-out failure mode is the most dominant, the ultimate shear capacity is dependent on embedment depth.

Table 2.1 present a summary of previous research highlighting gaps and studies conducted on concrete element including reinforced concrete beams, Prestressed reinforced concrete beam and anchorage systems using the principle of finite element analysis, experimental investigation, model uncertainty, statistical analysis and regression analysis.

Table 2-1: Various gaps identified in the literatures on headed anchors subjected to shear loading using static solver including affecting parameters on the concrete breakout failure load

	AUTHORS							
Parameters studied	Brighton (2011) [FEA]	Cotsovos et al. (2009) [FEA & EXP]	Halahla et al. (2019) [FEA]	Al Saeab (2019) [FEA, RA]	Olalusi et al. (2020) [MUQ, SA]	Grosser (2011) [EXP, FEA, SA, RA and MUQ]	Anderson et al. (2006) [EXP]	Muledy (2023) [FEA, SA and MUQ]
Damage of PRC beam (Solid 65 model, ANSYS)	√	×	×	×	×	×	×	×
Blast and impact load of RC beams (ANSYS, LS-DYNA and ABAQUS	×	√	×	×	×	×	×	×
Non-linear behavior of RC beams under transverse Loading (solid 65 model, ANSYS)	√	×	√	×	×	×	×	×
Anchorage systems under different strain rate (LS-DYNA)	×	×	×	√	×	×	×	×
Assessment of CCD, EC2 model and Grosser	×	×	×	×	√	√	×	×

predictive model for a single headed anchor under shear loading								
Load-bearing behaviour and design of anchorage systems under shear and torsion loading (Dynamic Analysis, spring model using MASA)	×	×	×	×	√	√	×	×
Non-linear behaviour of a single cast-in place anchor under shear loading using static solver (Solid 65, ANSYS)	×	×	×	×	×	×	×	√

- EXP: Experimental investigation
- RA: Regression Analysis
- FEA: Finite Element Analysis
- MUQ: model uncertainty quantification
- SA: Statistical Analysis
- RA: Reliability Analysis
- RC: Reinforced concrete
- PRC: Prestressed reinforced concrete

CHAPTER 3

RESEARCH METHODOLOGY

3.1 Introduction

In this study, the behavior of a single cast-in-place headed anchor subjected to shear load was investigated by means of the finite element analysis (FEA) package Ansys 2020 R2 commercial software. The investigation focused on the load-displacement behaviour of a single-headed anchor under shear loading. In addition, analytical predictive models from the design standards (CCD and EN1994-2:2009) and predictive models from Anderson and Meinheit (2006) and Grosser (2006) were implemented in this study. This approach was due to the lack of information about the test database used in the development of the concrete model in the numerical analysis.

Numerical modelling of concrete elements is very complex because of its nonlinear behavior in both tension and compression. Because of this complexity, engineers and researchers have rely heavily on empirical formulas to design concrete structures based on numerous experiments (Kwak et al., 1990).

Advances in digital technology, computers, and robust analytical methods like the finite element method (FEM) have reduced the computational effort of experimental tests significantly. The finite element method evolved into a powerful computational tool that enables complex analyses of the linear and nonlinear response of concrete elements to be carried out predictably.

In this thesis, numerical results for a single headed stud were validated with the experimental results from sixty tests on shear-loaded headed studs and compared with results from the analytical models.

This study's methodology is divided into two phases. The first involves using the finite element analysis to predict the concrete breakout failure load of a single cast-in-place headed anchor subjected to shear loading perpendicular to the edge. And the second phase has to do with assessing the adequacy of the analytical predictive models for concrete-headed anchors under shear loading.

This methodology makes it essential to design an approach that answers the hypotheses mentioned in chapter 1 and addresses the weaknesses of the numerical approach used in the present study.

The rest of the chapter is structured as follows:

i. Section 3.2 presents the experimental data source of 366 tests conducted on headed anchors subjected to shear loading.
ii. Section 3.3 presents the Finite Element Analysis and numerical simulation procedure.
iii. Section 3.4 presents different predictive models used for anchors displaying concrete edge breakout failure under shear loading. The section also reports the assessment of each model using statistical analysis and model uncertainties quantification.

3.2 Data Collection

This study used an experimental database collected from previous technical literature research (Olalusi et al., 2020), consisting of 366 tests conducted on headed anchors under shear loading. These experimental tests aim to investigate the concrete breakout capacity of a single cast-in-place headed anchor under shear loading. The study used only 60 tests in the numerical study to validate the results of the experimental tests. A load-displacement response curve was obtained from the dataset investigated by numerical simulation. The design anchor parameters were kept the same as in the experimental studies. The database contains information on a wide range of anchor design parameters. The anchor design parameters of interest were the edge distance C_1 ranging from 50 to 300 mm, the concrete compressive strength f_{cu} ranging from 21.8 to 31.5 MPa, the anchor nominal diameter d_{nom} ranging from 10 to 24 mm, the embedment depth h_{ef} ranging from 50 to 450 mm, as shown in Appendix B.

3.3 Finite Element Analysis

To investigate the concrete breakout capacity of the anchor exhibiting concrete edge breakout failure, a finite element concrete model of a single cast-in-place anchor subjected to shear loading near the edge was created. In addition, the numerical study examines the behavior of a single-headed anchor using a load-displacement response curve and compares the results to experimental studies.

The simulation was carried out incrementally by applying a load in several time steps, with the Ansys 2020 R2 commercial software program to prepare the model and evaluate the results.

3.3.1 Finite Element Type

Ansys software program provides different types of elements. Some of the most commonly used elements include: rod elements, beam elements, Plate elements, shell elements and composite elements, shear panel, solid elements, spring elements, mass elements, rigid elements and Viscous damping elements.

Each element type in the FE program provides an option for element formulation. This provision allows designers or engineers to adequately describe their model's material (Hallquist, 2006).

This study modelled the nonlinear behavior of a single anchor embedded in concrete under shear load using solid element. More details about the concrete model can be found in subsection 3.3.2.

3.3.2 Material Constitutive Law for Concrete and Concrete Model

Concrete is the most difficult material to model, according to research, due to its complex and nonlinear behaviour (Abedini & Zhang, 2020). Therefore, careful consideration is required when modelling concrete. When subjected to compression and tension, concrete, a brittle material, tends to exhibit different behaviour - concrete exhibits both linear isotropic and multi-linear isotropic material properties. The Ansys program used in this study requires the uniaxial compressive stress-strain to describe the concrete behaviour in compression. Other concrete material properties such as the young's modulus, mean tensile strength of concrete and Poisson's ratio have not been provided in the experimental tests in this study, instead they were estimated using the design standards (CEB-FIP model code 90 (1993) or Fib model 2010 (2013)) and previous literature.

In this study, the uniaxial compressive stress-strain response curve of concrete was plotted (as shown in Figure 3.1) using the equations below:

(i) $E_C = 5000\sqrt{f_{cc,200}}$, in GPa Equation 3.1

(ii) $f = \frac{E_c \times \varepsilon}{1+(\frac{\varepsilon}{\varepsilon_0})^2}$ Equation 3.2

(iii) $\varepsilon_0 = \frac{2 \times f_{cc,200}}{E_c}$ Equation 3.3

(iv) $E_c = \frac{f}{\varepsilon}$ Equation 3.4

Where:

E_c is the modulus of elasticity (or Young Modulus) of the concrete (GPa), f is the stress at any strain ε in MPa, ε is the strain at stress f and ε_0 is the strain at the ultimate mean concrete compressive strength $f_{cc,200}$.

Sinđić, (2019) investigated the tensile and shear strength of high strength in concrete, and in the experimental study, the author proposed the following equations that establish the relationship between tensile and compressive strength of concrete:

f_{ctm}= $0.5f_{ck}{}^{0.5}$, where $f_{ck} \geq 50$ MPa

f_{ctm}= $0.738f_{ck}{}^{0.4}$, where $f_{ck} < 50$ MPa

Where:

f_{ctm} indicates the mean tensile strength of concrete, and f_{ck} indicating the characteristic cylinder compressive strength of concrete.

In the absence of experimental data, the mean value of the uniaxial tensile strength of concrete for normal weight concrete can be estimated as below (Fib model 2010 (2013)):

$f_{ctm} = 0.3(f_{ck})^{\frac{2}{3}}$ Equation 3.5

Where f_{ck} is the characteristic compressive strength of concrete in [MPa], which is related to the mean concrete cylinder compressive strength of concrete f_{cm} using the expression below:

f_{ck} = $f_{cm} - \Delta f$ where $\Delta f = 8\ N/mm^2$. Equation 3.5 gives the mean uniaxial tensile strength of 2.18 N/mm^2 which can be used in numerical study.

Studied conducted by Rasoul. N, 2017 on the effect of the mean uniaxial tensile strength of concrete using numerical approaches on anchors loaded in tension has revealed that the anchorage failure loads and behavior of concrete anchors are not influenced by the concrete uniaxial tensile strength. In addition, in the absence of experimental data, the concrete young’s modulus for different mean concrete cube compressive strengths are summarized and estimated in the table 3.1.

The maximum mean concrete compressive strength used for this study is 21.8, 25.5, 26.4 and 31.5.

Table 3.1 and Figure 3.1 respectively give the corresponding Young Modulus calculated and the illustration of the stress-strain plot of concrete in compression using Equations (Eq. 3.1 – 3.4).

Table 3-1: Concrete Compressive Strength – Modulus of Elasticity

Concrete Compressive Strength ($\boldsymbol{f}_{\boldsymbol{cc,200}}$) MPa	Modulus of Elasticity $(\boldsymbol{E}_{\boldsymbol{c}})$ GPa
21.8	23345
25.5	25249
26.4	25690
31.5	28062

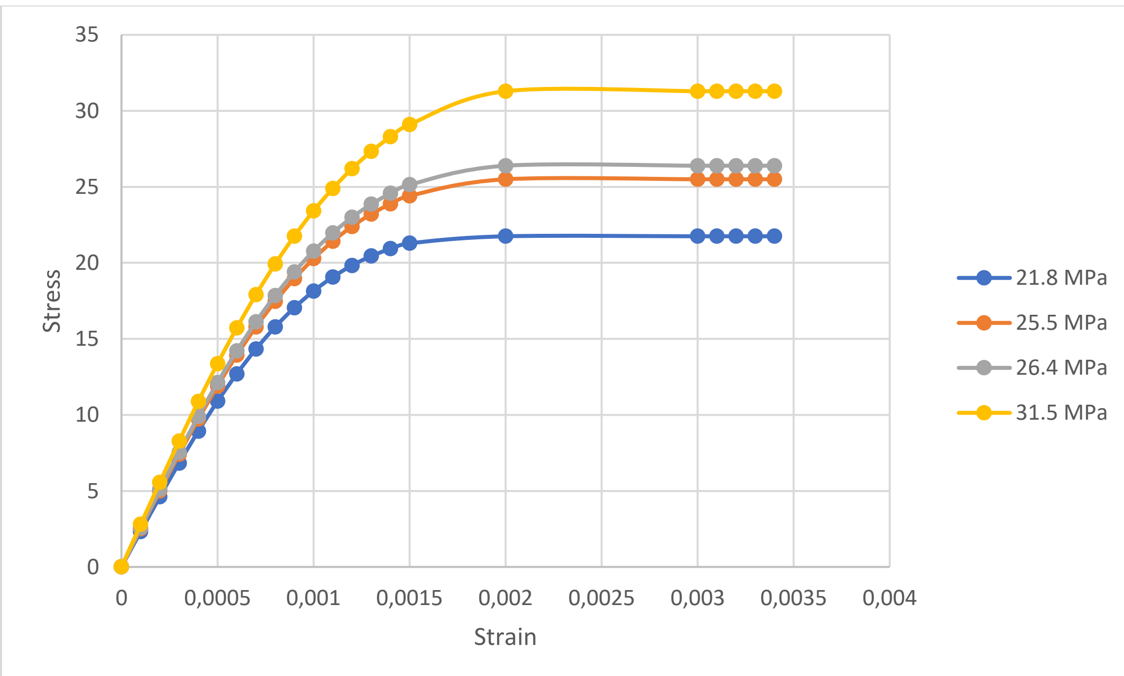

Figure 3.1: Stress-strain Curve for Concrete in Compression using cube strength

The concrete compressive strength (stress-strain curve) is displayed in Figure3.1 using Eq.3.1, Eq.3.2, Eq.3.3 and Eq.3.4 for various ranges of strength ranging from 21.7 to 31.5 MPa

As depicted in Figure 3.2, this study used a solid 65 element to model the behaviour of concrete material. The element has eight nodes exhibiting three degrees of freedom at each node, having translation in the nodal x, y and z directions. Solid 65 element is a mechanism for the three-dimensional modelling of solids with or without rebars. The solid is capable of cracking in tension and crushing in compression.

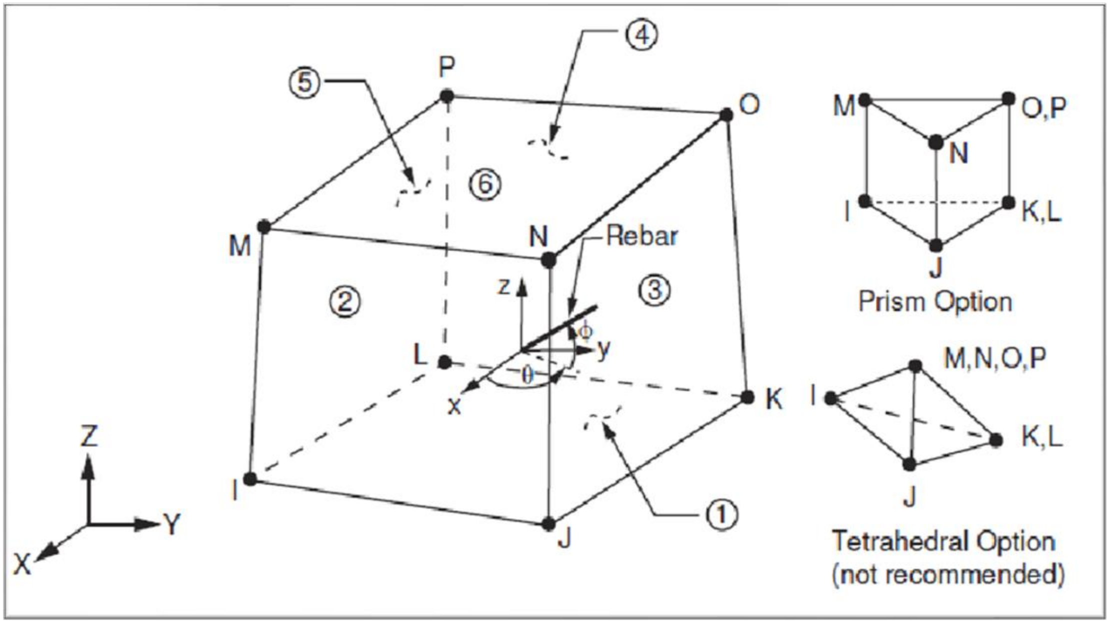

Figure 3.2: Solid 65: Three-dimensional View

Although concrete is similar to a three-dimensional structural solid, it has additional special cracking and crushing properties. The used of solid 65 element to treat nonlinear concrete material properties is its most capability.

The multi-linear isotropic material used to describe the concrete's failure employs the Von-Mises et al. (1974) criterion model (as shown in Table 3.2.). Typically, nine constants were required to implement the solid65 element using the William and Warnke material model on the Ansys Workbench. However, the model proposed in this study implemented only four constants, namely:

i. Shear transfer coefficient for an open crack

ii. Shear transfer coefficient for a closed crack

iii. Uniaxial tensile cracking stress

iv. Uniaxial crushing stress (positive)

Table 3-1: Nonlinear Isotropic Coefficient Used in Ansys Workbench and the Concrete Material Proprieties Using solid 65 Element

Element Type	Material Properties								
	Linear Isotropic		Nonlinear Multilinear Isotropic Concrete Compressive Stress-Strain input		Nonlinear– Inelastic Isotropic Coefficients				
	Modulus of Elasticity	Poisson Ratio	Strain (εs)	Stress (f_y) MPa	Open shear transfer coefficient	Closed shear transfer coefficient	Uniaxial cracking stress	Uniaxial crushing stress	Tensile crack factor (default to
Solid 65	29250 GPa	0.2	0	0	0.3	1	1.5	25.5	0.8
			0,0001	2,95					
			0,0002	5,7					
			0,0003	8,325					
			0,0004	10,8					
			0,0005	13,125					
			0,0006	15,3					
			0,0007	17,325					
			0,0008	19,2					
			0,0009	20,925					
			0,001	22,5					
			0,0011	23,925					
			0,0012	25,2					
			0,0013	26,325					
			0,0014	27,3					
			0,0015	28,125					
			0,0016	28,8					
			0,0017	29,325					
			0,0018	29,7					
			0,0019	29,925					
			0,002	30					
			0,0021	30					
			0,0022	30					
			0,0023	30					
			0,0024	30					
			0,0025	30					
			0,0026	30					
			0,0027	30					
			0,0028	30					
			0,0029	30					
			0,0030	30					
			0,0031	30					

3.3.3 Meshing Technique

As illustrated in Figure 3.3, a numerical analysis aims to produce the size of the element used in the model. This study utilized two strategies to meet this requirement. Firstly, the finite element (FE) model was discretized and simulated using a 10 mm, 15 mm, and 20 mm coarse mesh element. Secondly, an element size sensitivity analysis was conducted to verify results convergence.

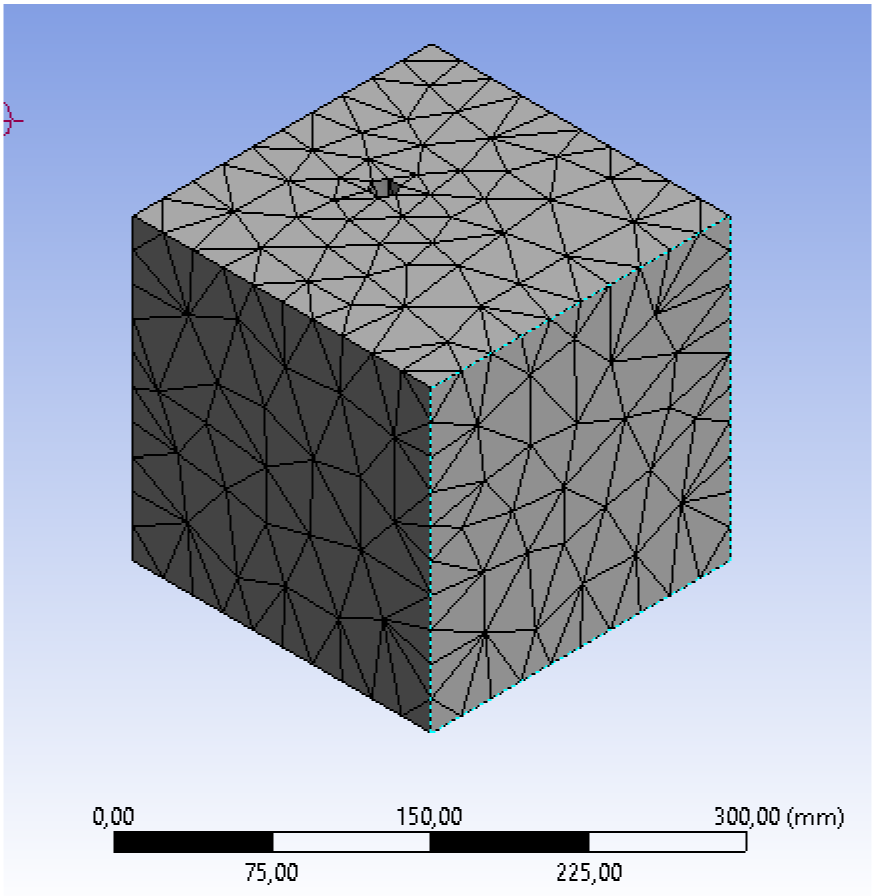

Figure 3.3: Element Size

Mesh size influences the accuracy of the results and the time required to perform the analysis. For example, research has shown that fine mesh size increases the accuracy and computation time resulting in a high overall computation cost (LSTC, 2014a).

Despite this benefit, the license has the numerical problem of limiting the element size to less than 10 mm. Consequently, this study only used element sizes greater than 10 mm. However, the mesh refinement () can reduce discretizing errors (Paultre, 2010).

3.3.4 Contact Modelling

Several contact types are used. These names might be called with different names according to softwares. In Ansys software, contact names are titled frictional, frictionless, rough, bonded and no separation. Choosing the appropriate contact type depending on the problem being solved is often tricky because of the uniqueness of each contact type. Generally, three contact types may be used in Ansys static structural. These include bonded contact, no separations, and frictional. However, this study used bonded contact as illustrated in Figure 3.5. The rationale for this choice is that the bonded contact does not allow penetration, separation or sliding between faces or edges. In addition, in this contact, defined geometries act like one body. Bodies cannot move (no slide and no separate) and rotate between each other.

By default, Ansys uses the full Newton Raphson solution procedure with an MPC contact algorithm that connects all the nodes.

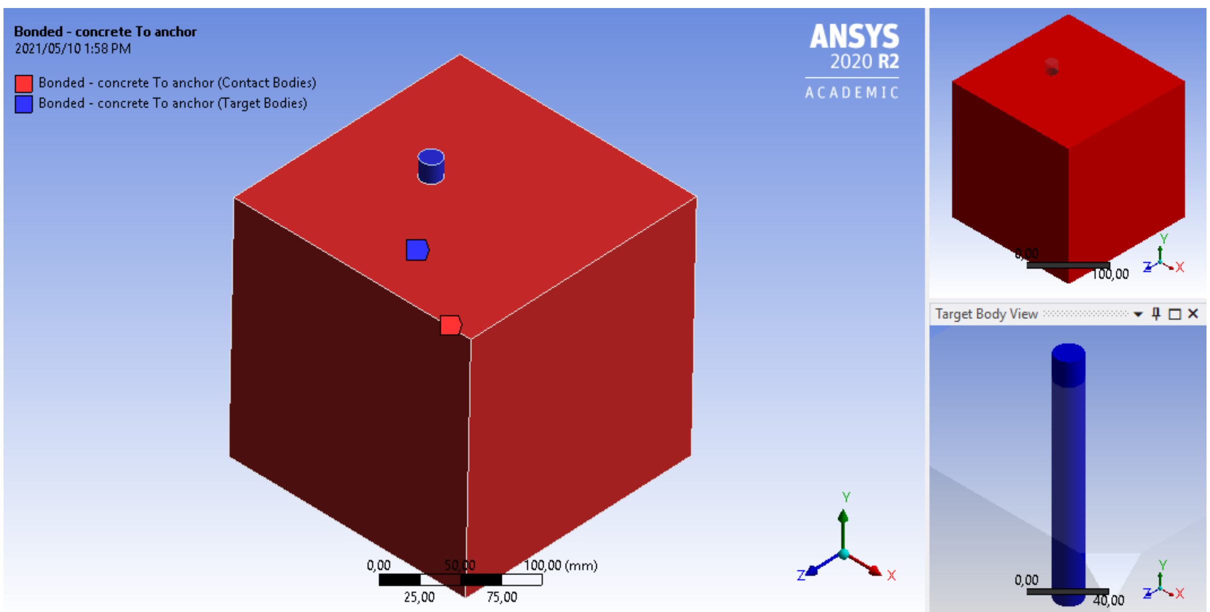

Figure 3.4: Concrete to Anchor Contact Modelling (Bonded contact)

3.3.5 Boundary Condition and Load Condition

For nonlinear analysis, the boundary condition was defined as fixed at the bottom of the concrete element, and the load was applied incrementally using a defined time step

3.3.6 Loading

The simulations were carried out incrementally by applying the load in several time steps. As shown in Figure 3.5, the load was applied at the interface between the concrete and the steel anchor rod. A nodal load was used in several time steps in the model, as illustrated in Figure 3.5.

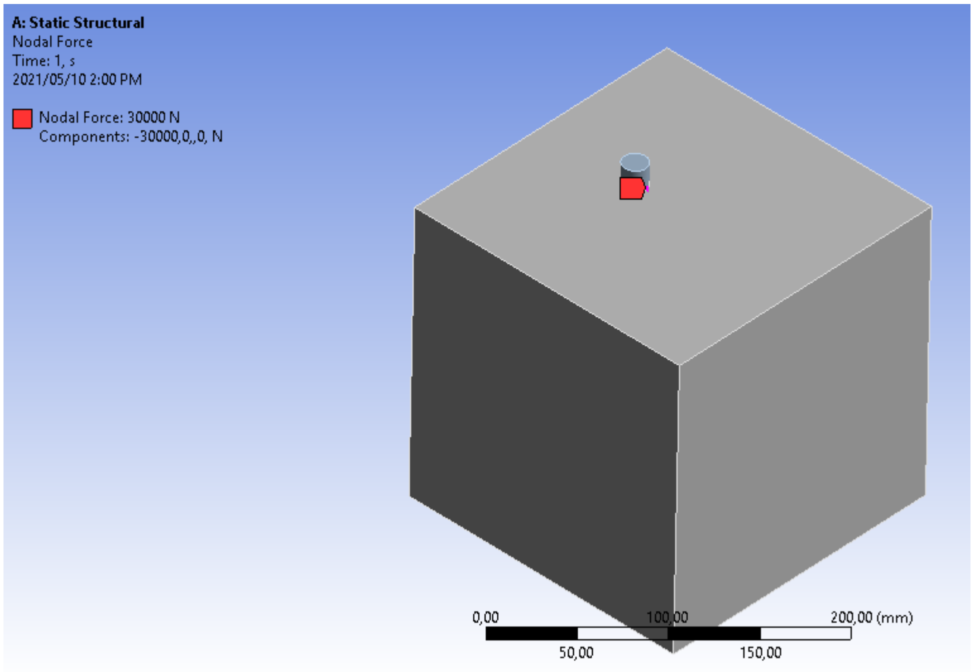

Figure 3.5: Load Application at the Interface Between the Concrete and Steel Anchor Rod

3.3.7 Creation of the Force-displacement Response Curve

To generate a force-displacement curve, the load-bearing node was selected in the model. And a new coordinate system was also created in the mechanical interface. Then, after solving the model, a probe deformation was inserted in the required location in which the deformation is required (Refer to Figure 3.6).

The evaluation results are displayed in a two-column table, the right column showing the required deformation and the left showing the number of time steps used in the analysis. Finally, the time steps were multiplied by the corresponding load to create a force-displacement response curve.

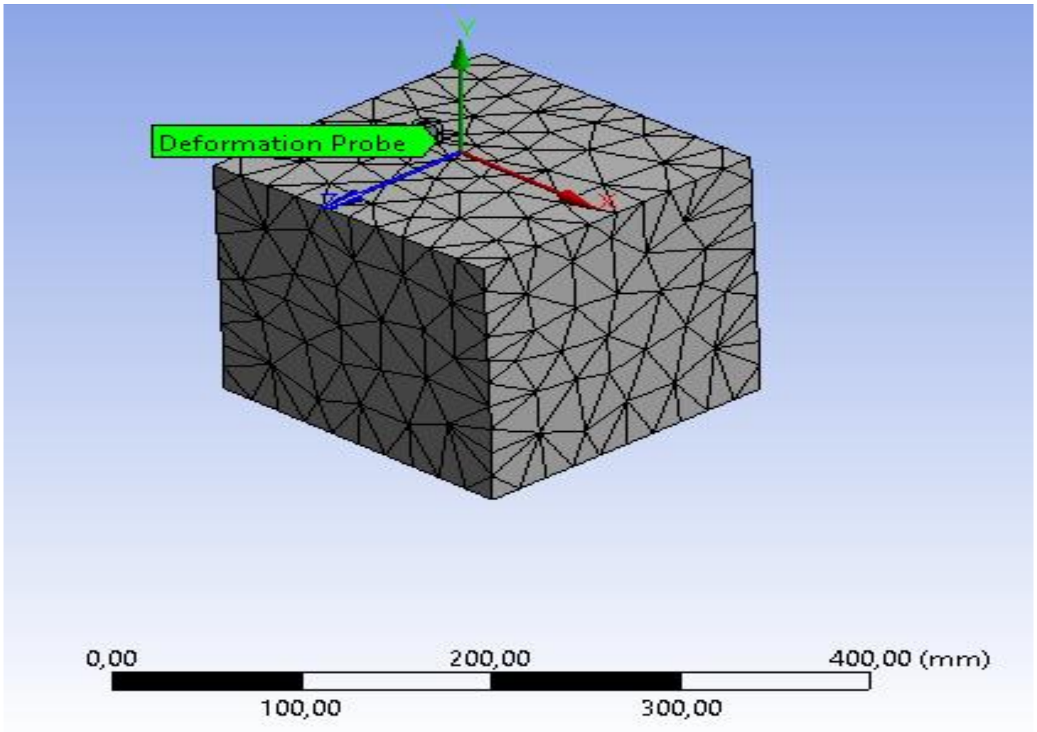

Figure 3.6: Deformation Probe at the Interface Between Concrete and the Steel Anchor

3.3.8 Verification of Numerical Results

The numerical results from FE analysis are presented using contour plots of the total deformation, Equivalent (Von-mises) stress and equivalent strain. And the mean concrete breakout capacity loads were obtained in the numerical studies using a load-displacement response curve as mentioned in section 3.3.7.

The numerical concrete breakout capacity was then compared to the experimental concrete breakout capacity using the same anchor design parameters as displayed in Appendix A.

3.3.9 Geometry and Finite Element (FE) Discretization

A discretization of the concrete element was examined using a solid65 element. A coarse mesh of 20mm in size was used in the model after conducting an element sensitivity analysis reported in section 4.2.1. The size of the concrete block (e.g., width, height, length) was adopted based on the concrete anchor configurations. Three concrete sizes were selected in the numerical study subjected to some limitations:200× 200×200 $(for\ h_{ef}\ \leq 150\ mm\ and\ C_1 \leq 100)$,450× 450450 $\left(for\ h_{ef}\ \leq 350\ mm\ and\ C_1 \leq 300\right)$, $500 \times 500 \times 500$ $(for\ h_{ef}\ \leq 450\ mm\ and\ C_1 \leq 300)$

The accuracy of the predicted FEM depends on the number of parameters (e.g., characteristic strength of concrete in tension and compression, shear retention ability, strain softening, tension softening, etc..) for achieving a realistic correlation between the predicted results from the model and the experimental test results (Cotsovos al., 2009).

The research work omitted some parameters such as the shear retention ability, strain softening, and tension softening because there are no sufficient experimental data available about these parameters.

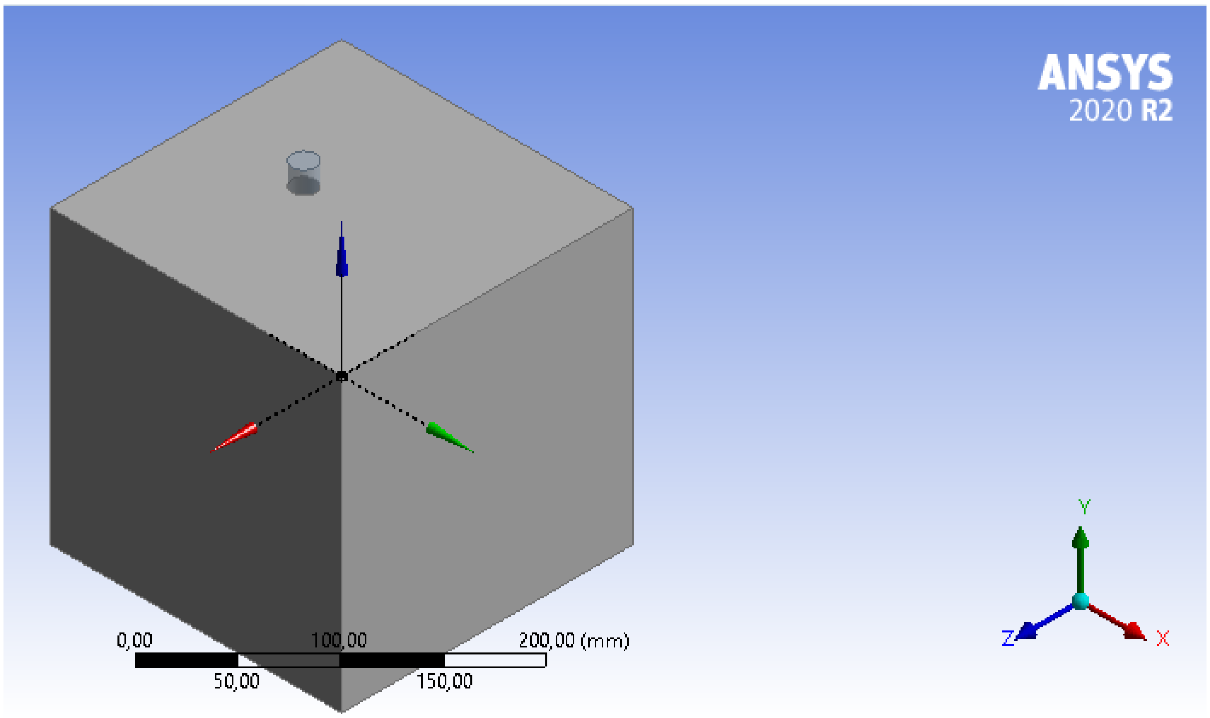

Figure 3.7: Geometry of the Concrete and Steel Anchor

3.4 Statistical Analysis and Model Uncertainty Quantification

Several analytical approaches have been adopted from the codes of practices and previous research to calculate the concrete breakout capacity of a single cast-in-place headed anchor embedded in concrete subjected to shear loading. However, it is often challenging to accurately predict the concrete breakout capacity of a single cast-in-place headed anchor loaded in shear near the edge because of a lack of experimental data required to perform a numerical study.

This section examined the different predictive models used in this study and how to access the adequacy of each model.

3.4.1 Statistical Analysis and Model Uncertainty Assessments

It is crucial to compare the analytical results with experimental tests results in order to determine the accuracy of any predictive models. In this study, the accuracy of the predictive models used were assessed using four statistical tools:

I. A typical comparison method examines the mean tested anchor shear capacity with the mean shear capacity predicted by the models. An analysis can be performed on the ratio of the tested anchor shear capacity to the predictive shear capacity for a set of data. The mean of the ratio indicates bias in the model and indicate how conservative the model is. For example, a mean greater than one on the average suggests that the shear capacity of the anchor will be greater than the predictive shear capacity.

II. Another way to assess the accuracy of a model is to examine the coefficient of variation (COV) or the Standard Deviation (SD). The coefficient of variation is calculated as the standard deviation per percentage of the mean. The standard deviation indicates how far the ratio of the actual shear capacity to the predicted shear capacity is deviates from the mean.

III. The coefficient of determination, R-square, can be used to assess the adequacy of a model. The term R^2 is the proportion of the sum of squares of the deviations of the test values about the test values mean attributed to a linear relationship between the test and predicted values.

IV. Second Order Regression Analysis presents a comparative assessment of the concrete breakout capacity predictions from the experimental test and the mean concrete breakout capacity from alternative models (FEA, CCD, EN2, Anderson and Grosser).

3.4.2 Method for Computation of Model Uncertainties

Model uncertainty characterization was achieved by comparing the concrete edge failure load obtained from the experimental tests of each representative headed anchor to the mean concrete prediction failure load from the CCD model, EN1994-2 model, and analytical models from Anderson and Meinheit and Grosser.

Based on the ratio of the experimental concrete edge failure load ($V_{u,Exp}$) to the predictive concrete edge failure load ($V_{u,pred}$), the Model Uncertainty was assessed using the following expression:

$$\beta = \frac{V_{u,Exp}}{V_{u,pred}}$$

Theoretically, a model is considered ideal if β= 1 – that is, the model has no bias. A model uncertainty of $\beta > 1$ indicates that the model underestimates the accurate concrete edge failure load. Contrarily, a model uncertainty of $\beta < 1$ suggests that the model overestimates the actual concrete edge failure loads (Olalusi et al., 2020).

The study also investigated the influence of anchor design parameters (anchor nominal diameter, stiffness ratio, edge distance and concrete compressive strength) using linear correlation analysis. This analysis considered each predictive model used and provided a brief conclusion on the anchor design parameters' sensitivity.

CHAPTER 4

RESULTS AND DISCUSSION

4.1 Introduction

A database consisting of 360 experimental test results was compiled to facilitate this study, only 60 simulations were run to investigate and validate the proposed model's performance.

Primarily, a mesh sensitivity analysis was executed to verify numerical results convergence. Secondly, verifications of the numerical model accuracy were undertaken. Finally, assessment of the predictive models, and examination of the influence of geometrical parameters (such as the anchor diameter, the edge distance and the stiffness ratio) as well as the mean compressive strength of concrete on the concrete breakout capacity were conducted.

The rest of the chapter is structured as follows:

I. Section 4.2 presents the results from the numerical study, including element size sensitivity analysis and verification of the numerical model.

II. Section 4.3 focuses on alternative empirical predictive models for concrete anchors under shear loading. The section also presents the assessment of each predictive design model and the sensitivity of each anchor design parameter on the concrete breakout capacity, which was investigated through linear correlation.

III. Section 4.4 conclude the chapter by providing the outcomes of each objective.

4.2 Numerical Studies

This study's model was created using Ansys commercial software, and the nonlinear behavior of concrete-headed anchors subjected to shear loading was modelled using solid 65 element, Section 3.3.2 provided more details on the concrete model used. The study utilized several simulations (see Appendix A) and investigated the nonlinear behaviour of concrete using a load-displacement response curve (see appendix B).

The numerical analysis performed in this study will involve the evaluation of the element size sensitivity and the verification of the numerical results using different anchor configurations, ranging from low to high concrete compressive strength, from small to large anchor diameter, from small to large edge distance, from small to large embedment depth.

The simulations were carried out incrementally by applying the load in several time steps. This section only presented a few of the cases studied. The rest of the numerical results can be found in appendix B.

4.2.1 Element Size Sensitivity

Element size sensitivity is a crucial analysis conducted in this study because it enables the convergence of numerical results to be checked. The element size for the concrete and steel anchor rod is depicted in Figure 4.11.

The concrete element used in this study has dimensions of $200\times 200 \times 200$ mm with an anchor nominal diameter of 16 mm.

(a) Concrete block (b) Steel anchor Rod

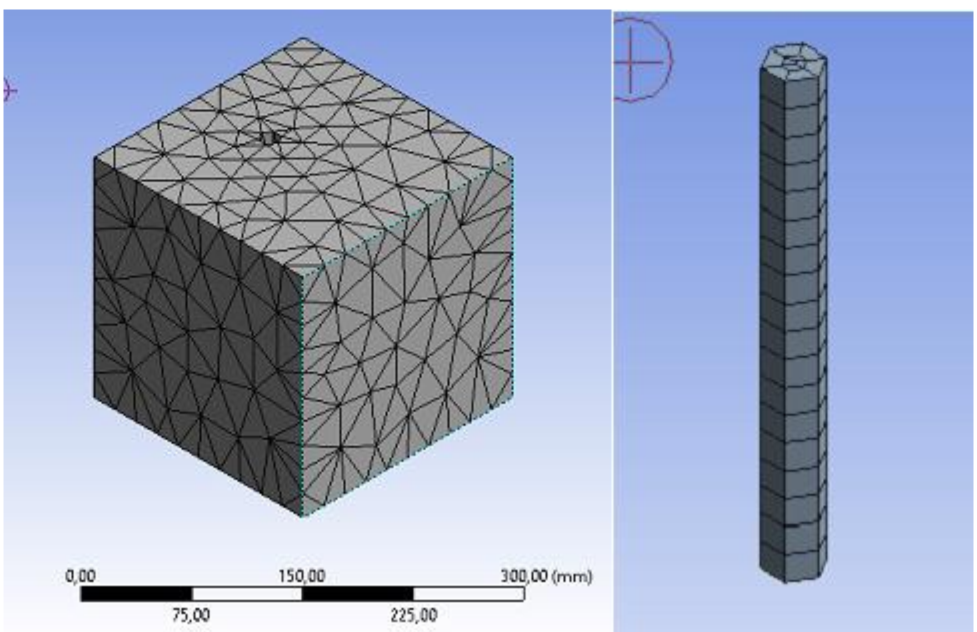

Figure 4.1: Element size Detail for the Concrete Block and Steel Anchor Rod (20 mm mesh size)

This study discretized and simulated the FE model of concrete, using coarse size elements 20mm, 15mm and 10mm. A nodal load of 30 KN was applied at the interface between the concrete and the steel anchor, and the direction of the load is shown in Fig.4.2 and Fig4.3. Such an approach made it possible to achieve the aim of the numerical analysis regarding the size of the elements used in the model. The results from the FE analysis of the model are shown in Figures 4.2 and Figure 4.3.

(a) 10 mm mesh size (b) 15 mm mesh size

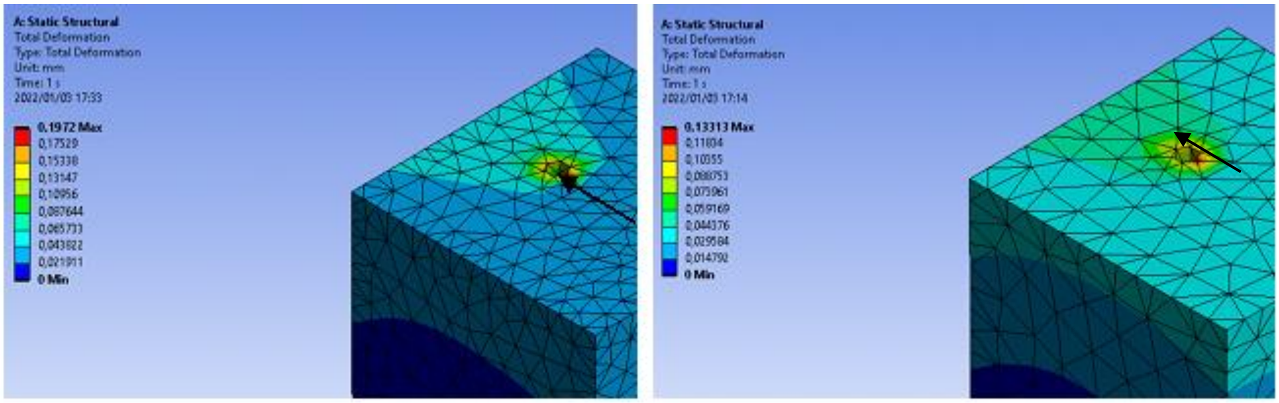

Figure 4.2: Concrete total deformation using: (a) 10 mm mesh size, (b) 15 mm mesh size

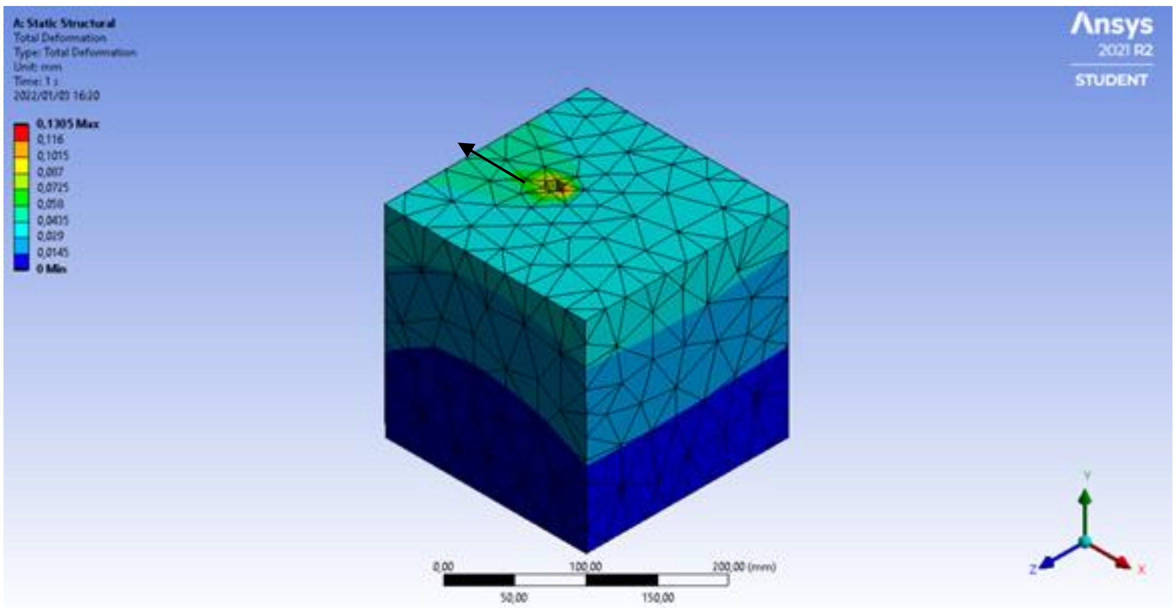

Figure 4.3: Concrete total deformation contour plot using 20 mm mesh size

As demonstrated in Table 4.1, there were no significant changes in the total deformation for a mesh size of 15 and 20 mm (7 % increases in total deformation). As the mesh size varies from 10 to 15 mm, the total deformation decreases by 39% (as shown in Table 4.1). In addition, the result of Table 4.1 indicates that for each mesh size used, there are no changes in the concrete breakout failure loads.

Table 4.1 presents the parameters used in this study and failure loads at the first crack. The Table emphasizes the need to show the details of simulated parameters such as the anchor diameter, embedment depth, edge distance and the concrete compressive strength. Meanwhile, Figure 4.4 represents the load-displacement response curves of concrete element.

Table 4-1: Summary of Results Obtained from Mesh Sensitivity Analysis using Different Mesh Sizes

Mesh size[mm]	d[mm]	h_{ef}[mm]	C_1[mm]	$f_{cc,200}$[MPa]	$V_{experiment}$ [KN]	V_{FEA}[KN]	Total deformation [mm] from FEA
10	16	130	68	25.5	18.84	8	0.197
15	16	130	68	25.5	18.84	8	0.12
20	16	130	68	25.5	18.84	8	0.13

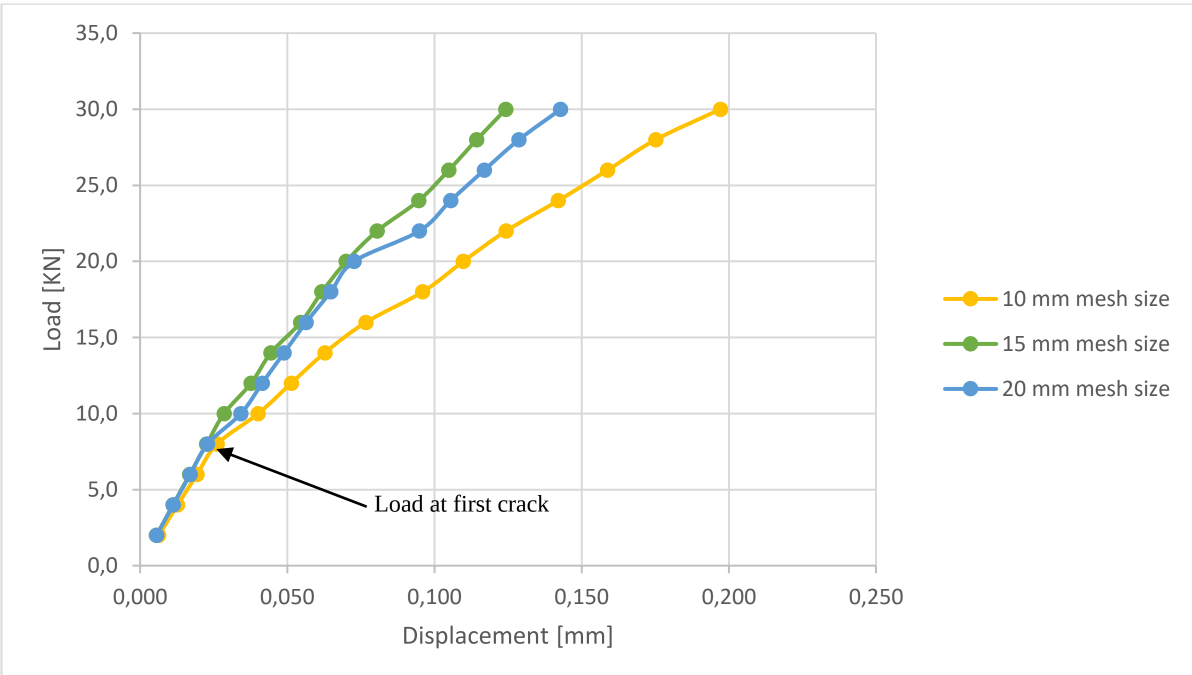

Figure 4.4: Element Size Sensitivity Analysis

From Figures 4-4, it was observed that while using a 10 mm mesh size yielded a corresponding failure load of 8 KN, a 15 mm mesh size generated a failure load of 8 KN and a 20 mm mesh size produced a failure load of 8 KN. Therefore, it can be concluded that there is no significant change in the failure loads and the mesh size has no significant impact on the concrete breakout capacity.

4.2.2 Verification of the Numerical Model

In this study, a single-headed anchor loaded perpendicular to the edge was simulated with the same parameters as the experimental tests to verify the numerical model. The following lines present numerical studies using a few parameters to validate the model's accuracy. Table 4.2 summarized all simulated parameters from the experimental tests database ranging from B_1 to B_8

with concrete compressive strength $\boldsymbol{f_{cc,200}}$ = 25.5 MPa, where $\boldsymbol{f_{cc,200}}$ represents the mean concrete compression strength with the use of cube strength. Appendix A and B offer more details on the anchor design parameters and the corresponding load-displacement response curves plots. The concrete block used has the following dimension: $200\times 200 \times 200$ mm. To increase the accuracy and the computational time, all numerical simulations are conducted using a 20 mm mesh size.

The results from the FE analysis are presented in Figure 4.6 to Figure 4.9 using an Equivalent (von-mises) stress contour plot, total deformation contour plot and the equivalent strain contour plot.

(a) Concrete total deformation contour plot (b) Concrete Equivalent (von-Mises) Stress

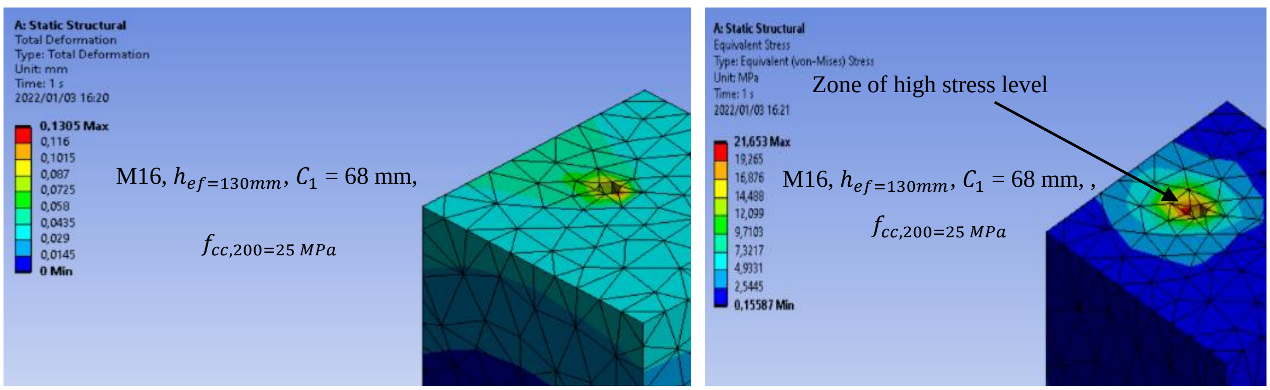

Figure 4.5: Figure 4.5. Concrete Contour plots: (a) Total deformation, (b) Equivalent (Von-Mises) Stress Distribution (Refer to Table 4.2 for the anchor design parameters, Bolt Label B_1)

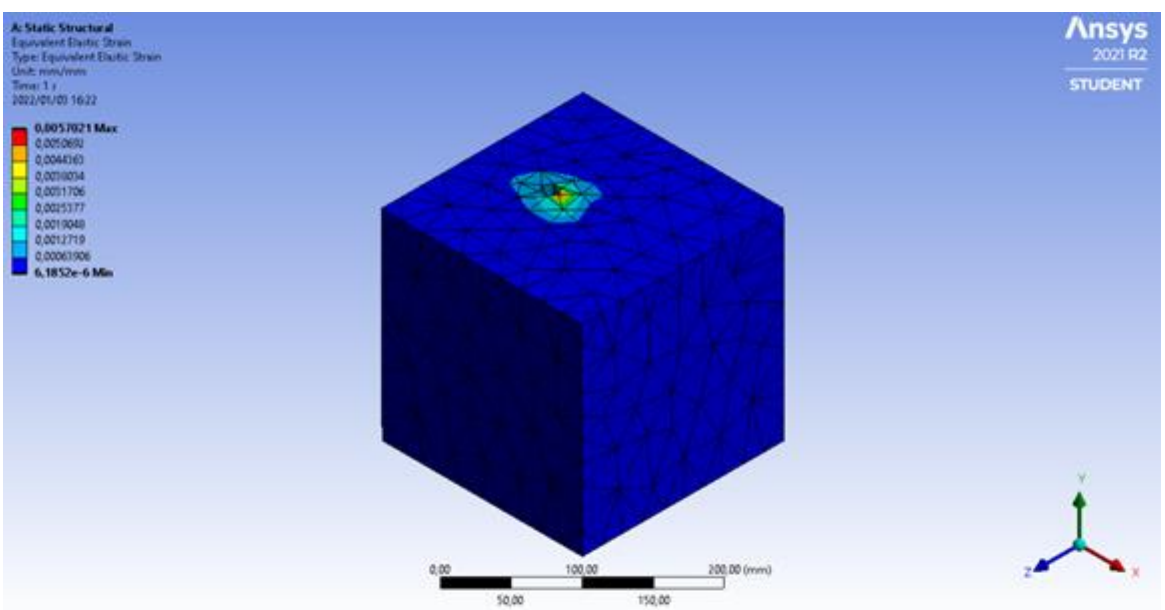

Figure 4.6: Concrete Equivalent strain contour Plot (Bolt Label B_1)

(a) Concrete total Deformation contour plot (b) Concrete equivalent (Von-Mises) stress

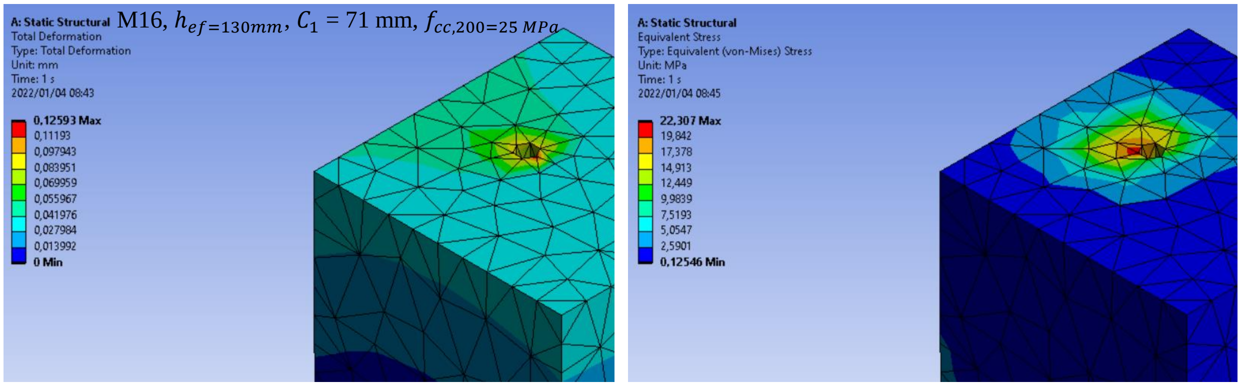

Figure 4.7: Concrete Contour plots: (a) Total deformation, (b) Equivalent (Von-Mises) Stress Distribution (Refer to Table 4.2 for the anchor design parameters, Bolt Label B_2)

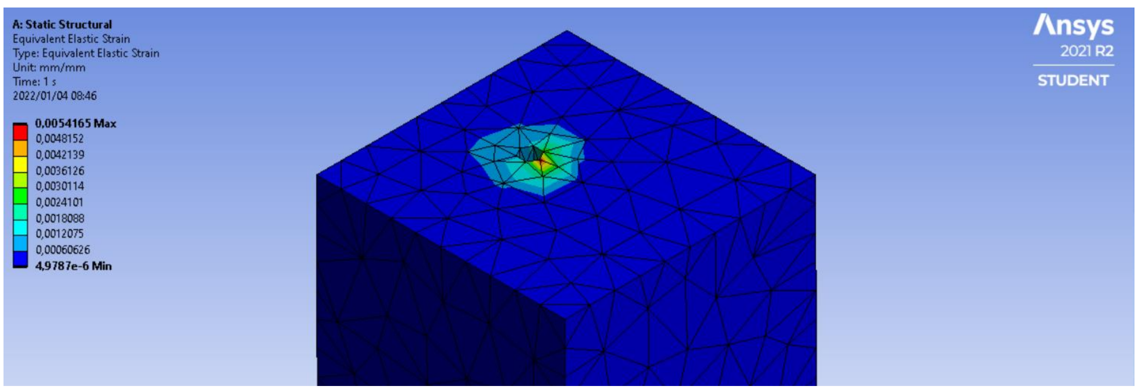

Figure 4.8: Concrete Equivalent strain contour Plot (Refer to Table 4.2, Bolt Label B_2)

(a) Concrete total Deformation contour plot (b) Concrete equivalent (Von-Mises) stress

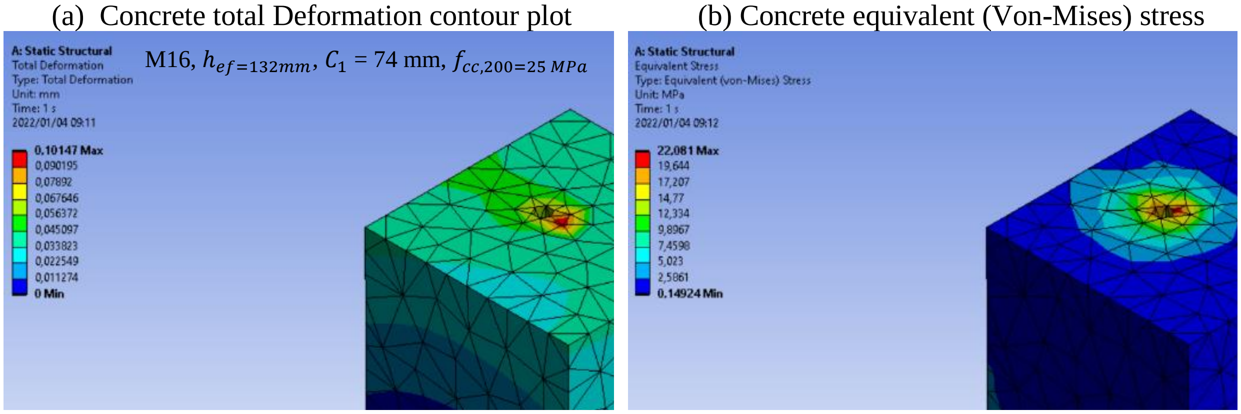

Figure 4.9: Concrete Contour plots: (a) Total deformation, (b) Equivalent (Von-Mises) Stress Distribution (Refer to Table 4.2, Bolt Label B_3)

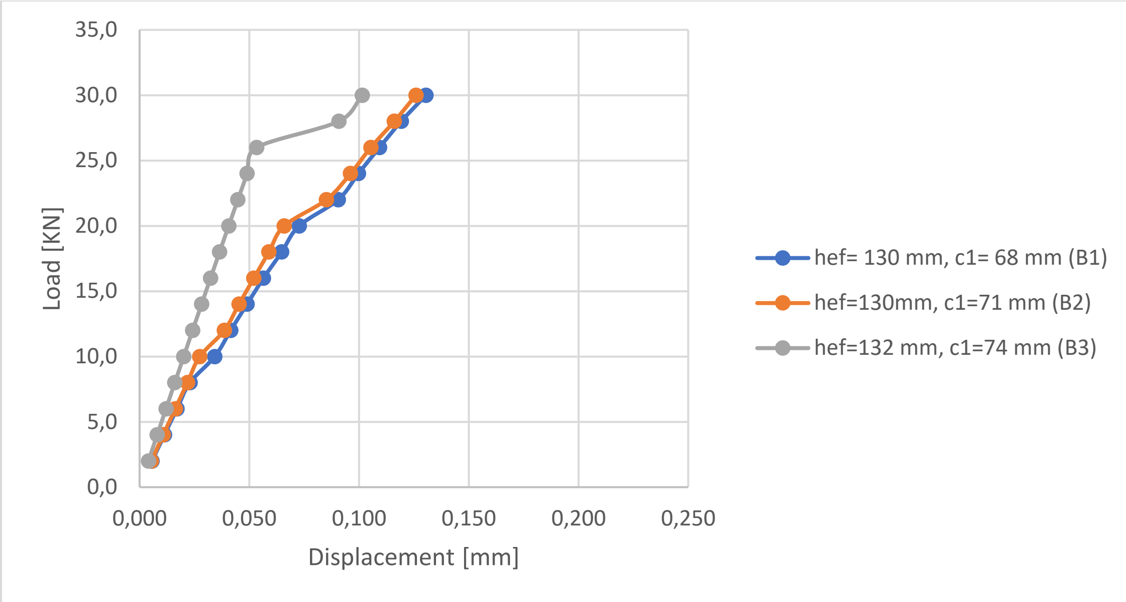

Figure 4.10: Load-displacement behavior of the numerical model for a Single Anchor Loaded Perpendicular to the Edge, f_(cc,200) = 25.5 MPa with Anchor Diameter d= 16 mm

As demonstrated in Figure 4.10, the numerically obtained load-displacement response curves for a single cast-in-place headed anchor display nonlinear behaviour. However, compared with experimental test results obtained from the database (refer to section 3.2) as shown in Table 4.2. The results from the FE analysis as shown in Table 4.2 indicate that some of the failure loads at the first crack are higher compared to the experimental results (Bolt Label B_3, B_5 and B_8), while some are far away from the experimental failure loads. This pattern could be due to the lack of information and assumptions made in the concrete and steel models.

Table 4-2: Comparison Between the Numerical Concrete breakout failure loads from Ansys and Experimental failure loads obtained from Olalusi et al., 2020

No	Bolt Labels	d[mm]	$\boldsymbol{h_{ef}}$[mm]	$\boldsymbol{C_1}$[mm]	$\boldsymbol{f_{cc,200}}$[MPa]	$\boldsymbol{V_{experiment}}$ [KN]	$\boldsymbol{V_{FEA}}$[KN]
1	B_1	16	130	68	25.5	18.84	8
2	B_2	16	130	71	25.5	21.33	10
3	B_3	16	132	74	25.5	20.53	24
4	B_4	16	130	72	25.5	24.98	12
5	B_5	16	131	100	25.5	32.88	40
6	B_6	16	130	103	25.5	29.7	10.70
7	B_7	16	136	105	25.5	34.12	9
8	B_8	16	135	103	25.5	31.17	33.33

The results in table 4.3 indicate that bolt label B_8 experiences a high-stress level reaching a value of 25.07 MPa (refer to figure 4.13) with a corresponding failure load of 33.3 KN, and a total displacement of 0.21 mm as displayed in Figure 4.15. For larger embedment depth and edge distance as displayed in table 4.2, there was an increase in stress and lower equivalent elastic strain. The corresponding load-displacement response curve is given in Figure 4.12. The stress distribution response curve is plotted in Figure 4.13 by applying the load in time step. The curve displayed a linear behaviour up to yield stress of 16.4 MPa, beyond that point the stress in the concrete displayed a non-linear behaviour and reaches a maximum stress value of 25.07 MPa as shown in Figure 4.13.

(a) Concrete total deformation contour plot

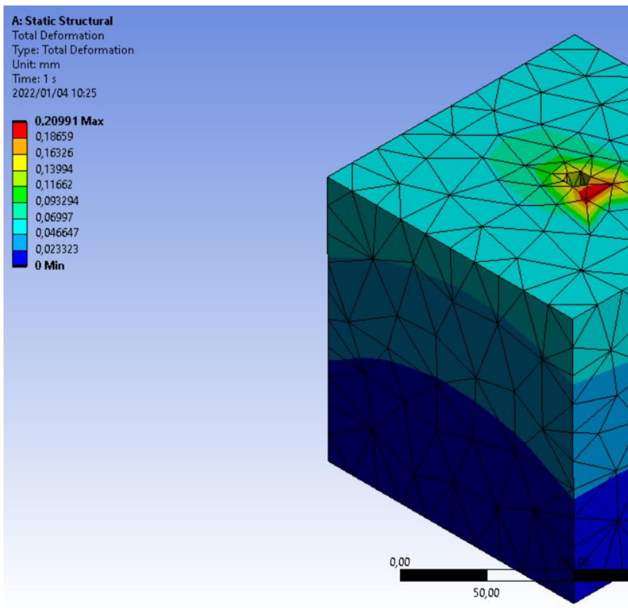

(b) Concrete Equivalent Stress (Von-Mises) contour

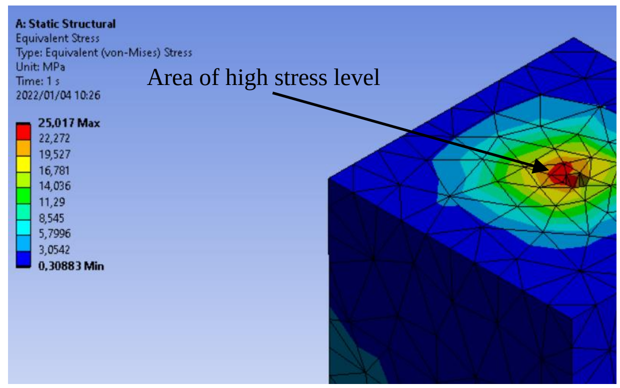

deformation, (b) Equivalent (Von-Mises) Stress
are displayed in Table 4.2, Bolt Label B_8)

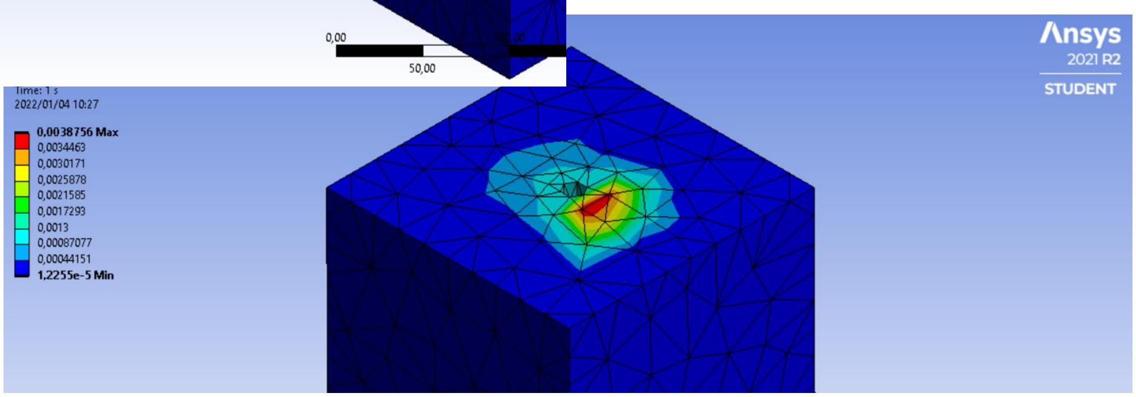

Figure 4.12: Concrete Equivalent strain contour Plot (Refer to Table 4.2, Bolt Label B_8)

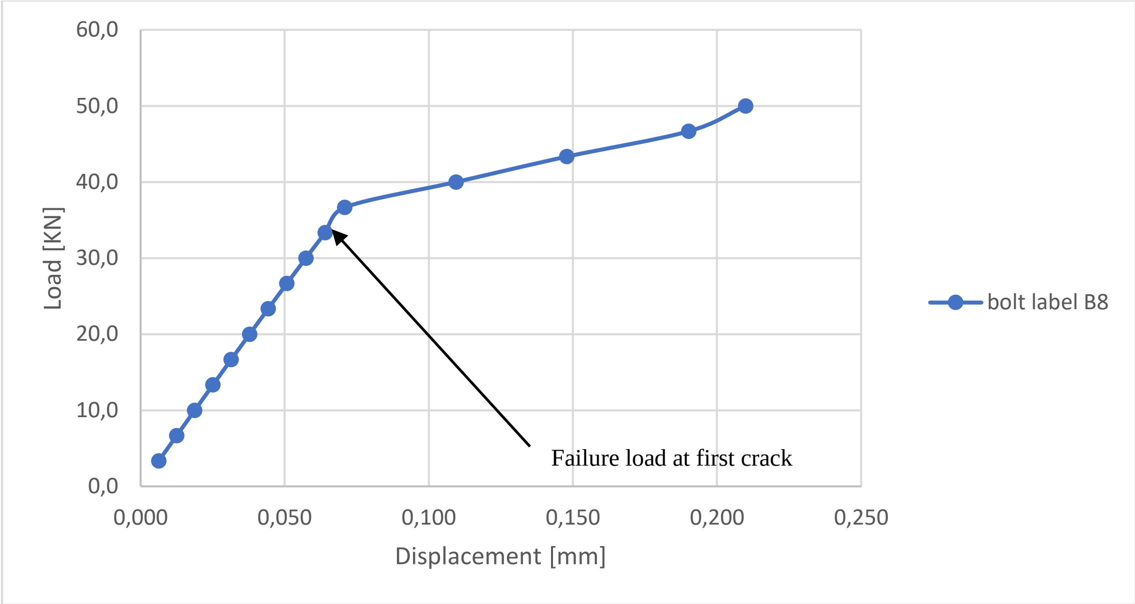

Figure 4.13: Load-displacement behavior of the numerical model for a Single Anchor Loaded Perpendicular to the Edge, f_(cc,200) =25.5 MPa, Bolt Label B_8

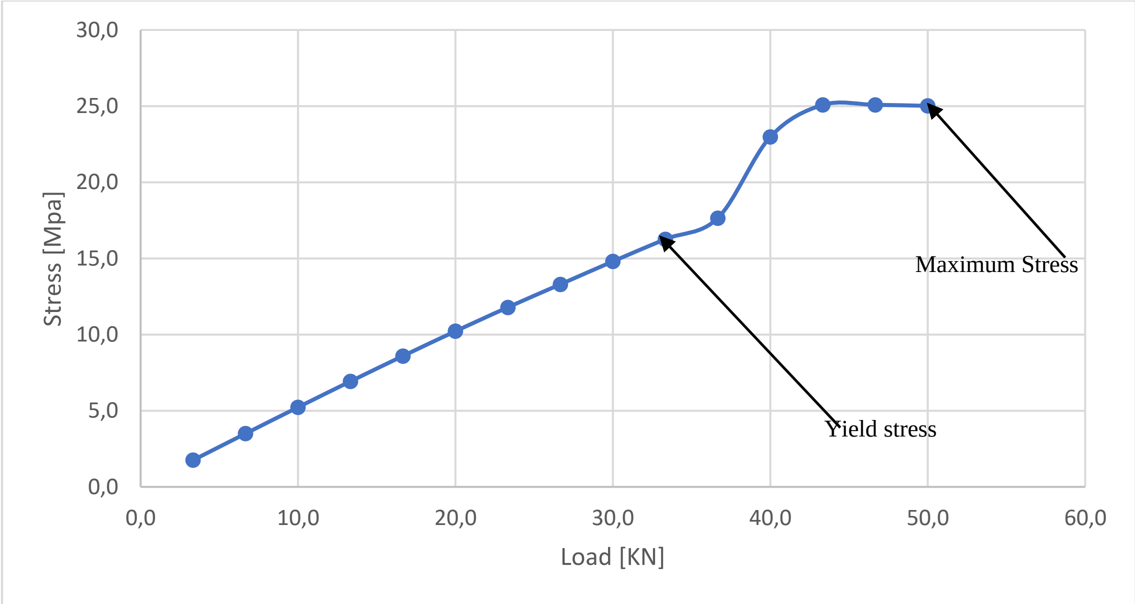

Figure 4.14: Equivalent (Von- Mises) stress distribution plot (Bolt Label B_8)

Table 4-3: Total deformation, equivalent (Von-Mises) stress, and equivalent strain at first cracking

Bolt Labels	$\boldsymbol{V_{experiment}}$ [KN]	$\boldsymbol{V_{FEA}}$[KN]	Max. Total Deformation [mm]	Equivalent (Von-Mises) Stress [MPa]	Equivalent Elastic strain [mm/mm]
B_1	18.84	8	0.13	21.65	0.0051
B_2	21.33	10	0.126	22.31	0.0054
B_3	20.53	24	0.10	22.08	0.0016
B_4	24.98	12	0.13	23.52	0.0043
B_5	32.88	40	0.20	23.60	0.0004
B_6	29.7	10.70	0.18	23.90	0.0055
B_7	34.12	9	0.24	23.12	0.010
B_8	31.17	33.33	0.21	25.07	0.0039

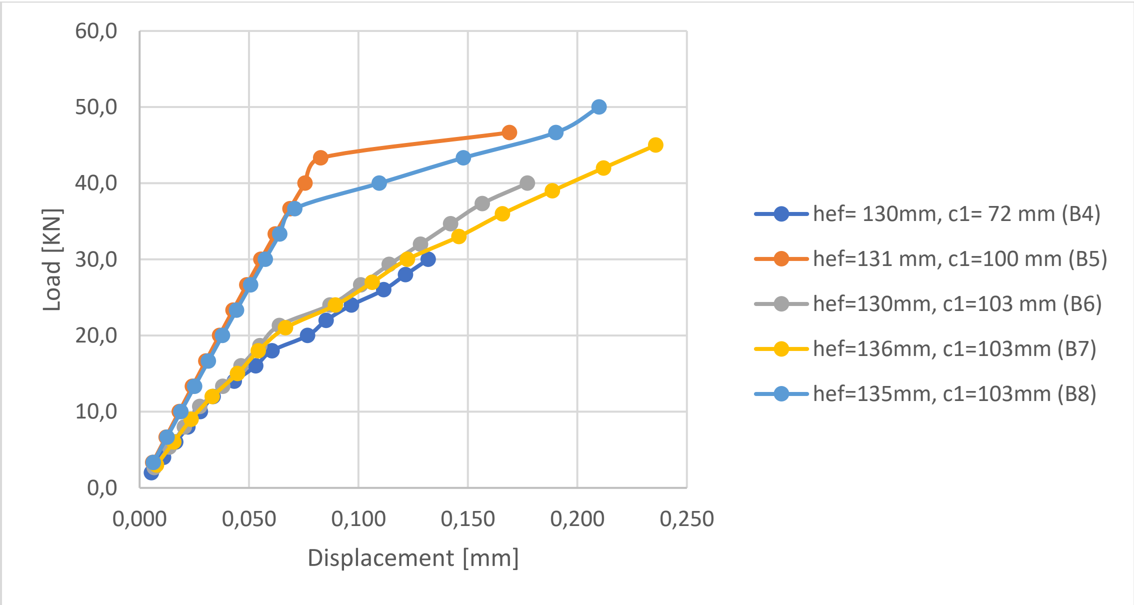

Figure 4.15: Load-displacement behavior of the numerical model for a Single Anchor Loaded Perpendicular to the Edge, f_(cc,200) =25.5 MPa with Anchor Diameter d= 16 mm (Bolt label B_4 to B_8)

From Figure 4.13 and table 4.2, some failure loads from the numerical studies are higher than the experimental failure loads, and in some instances, lower. The difference between the failure loads from the numerical analysis and experimental study can be associated with the fact that the FEA model does not consider the cracked section. This limitation of the concrete model justified that the FEA failure loads are higher than the experimental failure loads in some instances.

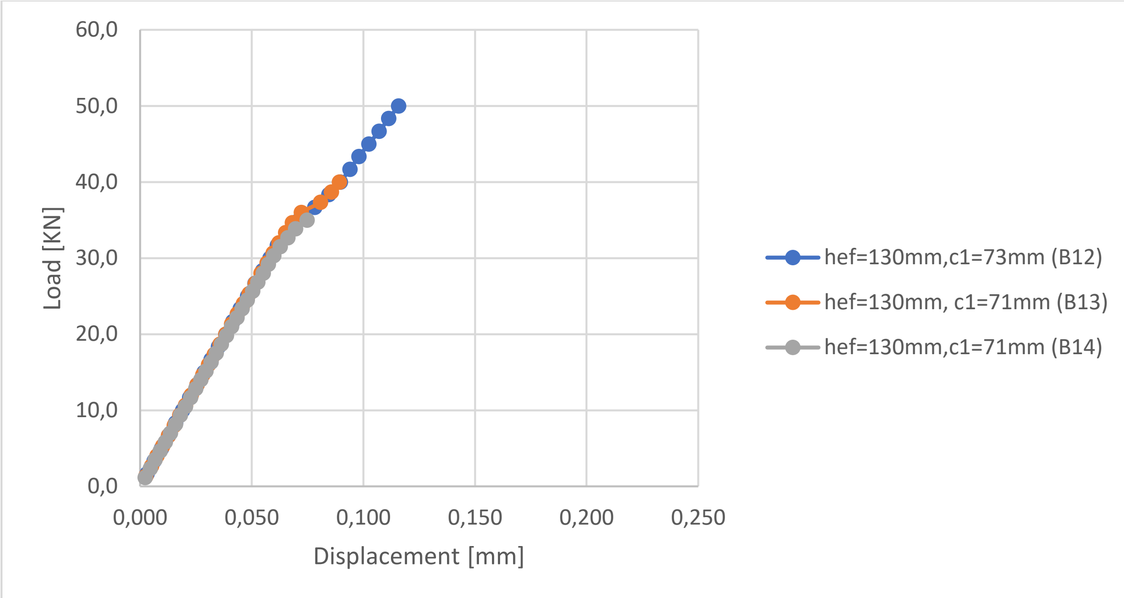

Figure 4.16: Load-displacement behavior of the numerical model for a Single Anchor Loaded Perpendicular to the Edge f_(cc,200) =26.4 MPa with Anchor Diameter d = 24 mm

Table 4-4: Comparison Between the Numerical predictive concrete capacity from Ansys and Experimental Results obtained from Olalusi et al., 2020

No	Bolt Labels	d[mm]	$\boldsymbol{h_{ef}}$[mm]	$\boldsymbol{C_1}$[mm]	$\boldsymbol{f_{cc,200}}$[MPa]	$\boldsymbol{V_{experiment}}$ [KN]	$\boldsymbol{V_{FEA}}$[KN]
12	B_{12}	24	130	73	26.4	21.19	31.7
13	B_{13}	24	130	71	26.4	21.09	34.7
14	B_{14}	24	130	72	26.4	22.36	30.3

Figure 4.16 and Table 4-4 indicate a small variation of the concrete breakout failure loads since there is no significant change in the edge distance In addition, increasing the mean concrete compressive strength leads to an increase in the concrete breakout capacity (refer to Figure 4.15 and Figure 4.16).

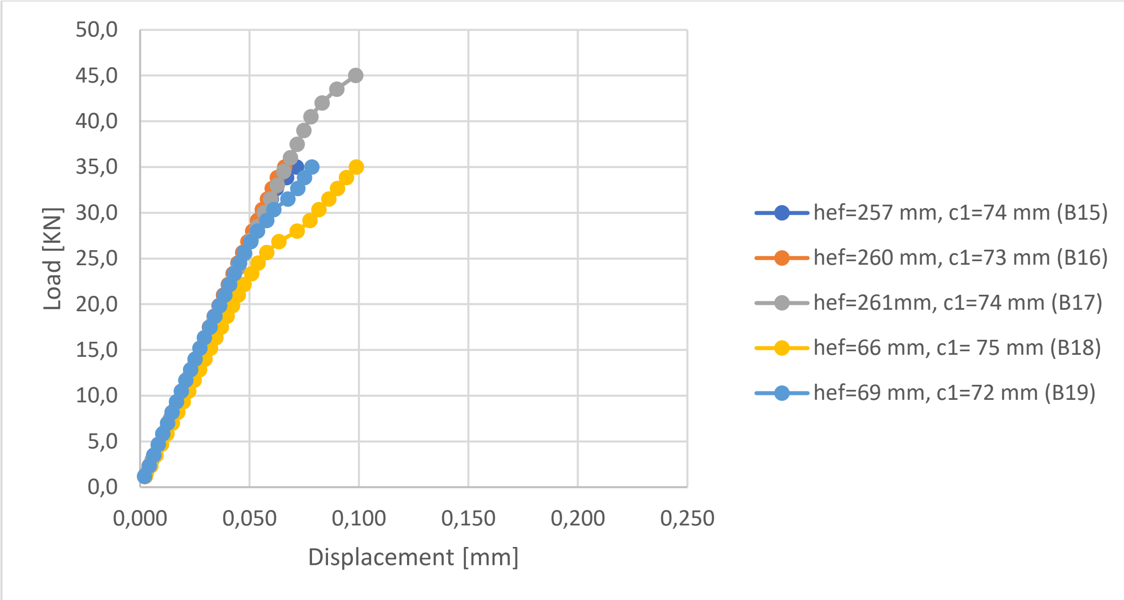

Figure 4.17: Load-displacement behavior of the numerical model for a Single Anchor Loaded Perpendicular to the Edge f_(cc,200) =26.4 MPa with Anchor Diameter d = 16 mm

Table 4-5: Comparison Between the Numerical Predictive concrete breakout failure loads from Ansys and Experimental Results obtained from (Olalusi et al., 2020)

No	Bolt Labels	d[mm]	$\boldsymbol{h_{ef}}$[mm]	$\boldsymbol{C_1}$[mm]	$\boldsymbol{f_{cc,200}}$[MPa]	$\boldsymbol{V_{experiment}}$ [KN]	$\boldsymbol{V_{FEA}}$[KN]
15	B_{15}	16	257	74	26.4	24.03	26.8
16	B_{16}	16	260	73	26.4	21.27	33.8
17	B_{17}	16	261	74	26.4	34.29	40.5
18	B_{18}	16	66	75	26.4	11.77	22.2
19	B_{19}	16	69	72	26.4	15.67	14

Figure 4.16 and Figure 4.17 present the load-displacement response curves obtained from the FE analysis. The corresponding failure loads are given in Tables 4.4 and 4.5. These results revealed that by increasing the mean compressive strength of concrete, the concrete breakout capacity also increases. It was also observed that the Bolts label B_{17} reached a concrete breakout capacity of 40.5 KN with a large embedment depth and edge distance. Very importantly too, the outcome of Table 4.5 confirms that the embedment and the edge distance have a significant influence on the concrete breakout capacity.

The difference in failure loads, as shown in appendix A can be attributed to the assumptions made on the Nonlinear-Inelastic Isotropic Coefficients as provided in Table 3.2. Furthermore, a study would require more detail from the experimental studies about concrete and steel materials properties (Young modulus, the tensile capacity of concrete, the anchor yield strength, poison ratio, etc.) to better predict the concrete breakout capacity of cast-in-place headed anchor under shear loading.

4.3 Statistical Analysis and Models Uncertainties Quantification

The numerical analysis results suggest that this study's concrete model (solid 65 element) cannot realistically predict the concrete breakout capacity of a single cast-in-place headed anchor under shear loading. Therefore, the implication is that the model adopted in this study cannot describe full concrete damage. Consequently, more investigation should be done using the dynamic or microscopic space analysis (MASA) model. Ožbolt et al. (2007) comprehensively discussed the MASA model, arguing that it is more efficient because it requires only the uniaxial stress-strain relationship for each microplane component, and the microscopic response is obtained automatically by integration over all microplane.

This section examined the various predictive models used in this study and discusses how to assess the adequacy of each model. The aim is to understand the validity of applying the five most commonly used methods to predict the shear capacity of headed anchors.

There are several approaches often used to calculate the shear capacity of cast-in-place headed anchor embedded in concrete, as earlier discussed in section 2.4, but this adopts the following models:

I. Concrete Capacity Design (CCD) Method

II. EN1994-2:2009 model (European Standard)

III. Anderson and Meinheit (2006)

IV. Grosser Model (2012)

The discussion here focuses on the predictive capabilities of these models. Therefore, this section examines the features of the models that predict the shear capacity of a single cast-in-place headed anchor, using the concrete compressive strength, the anchor diameter, the embedment depth and the edge distance. Chapter 2 and chapter 3 presented the general discussion of the models in their entirety.

Based on correlation with experimental results in the data available to the author, the accuracy of the predictive design models was assessed using the most suitable statistical tools, which include the mean ratio of the actual test results to the predicted, the coefficient of variation (COV), the coefficient of determination, and standard deviation.

4.3.1 Assessment of the Concrete Breakout Capacity of a Single Headed Anchor Under Shear Loading Using Alternatives Predictive Models

The alternative predictive models adopted for this study include the design equation according to the European standard (EN1992-4:2009), the analytical design equation proposed by Anderson and Meinheit (2006) and Grosser. Table 4.11 provides the summarized predictive design model equations.

Figure 4.9 presents a comparative assessment of each predictive design model used in the study. The evaluation was based on the mean concrete breakout capacity versus edge distance obtained from the best-fit second-order polynomial regression analysis. As shown in Figure 4.9, the results indicate the experimental concrete breakout failure loads and the corresponding alternative model used to evaluate the concrete breakout shear.

For this investigation, the edge distance was limited to 100 mm because, as shown in appendix A, the models yielded unconservative results for an edge distance $C_1 > 100$ mm. Therefore, in this study, the edge distance, C_1 was restricted to 100an mm with an anchor nominal diameter of 25 mm (refer to section 2.4).

As demonstrated in Figure 4.18, the edge distance C_1 is directly proportional to the mean concrete capacity – that is, as the edge distance C_1 increases and the mean concrete capacity increases also. Of all design models, the Grosser analytical predictive model seems to be more conservative when compared to experimental results, as shown in Figure 4.18. Moreso, the best-fit second-order linear regression depicted in Figure 4.18 suggests that the mean concrete breakout failure loads obtained from the Grosser model are very close to the experimental mean concrete breakout failure loads distances distance ranging up to 100 mm since the model takes into account uncertainties of the anchor design parameters which influence the concrete breakout capacity.

Conventionally, the closer the trend lines of the predictive model are to the experimental results, the better the performance of the model. Based on this criterion, the Grosser model seems to be the best predictor of the concrete breakout capacity. However, as presented in Figure 4.18, the trend lines of Anderson and Meinheit, CCD, and EN1992-4 models are far from the experimental trend line. Therefore, these models provide an unconservative approach to computing the mean concrete breakout capacity. This finding could be associated with the uncertainties in the anchor design parameter and with the formulation and limitation of the design models. Due to these uncertainties, reliability-based performance becomes imperative.

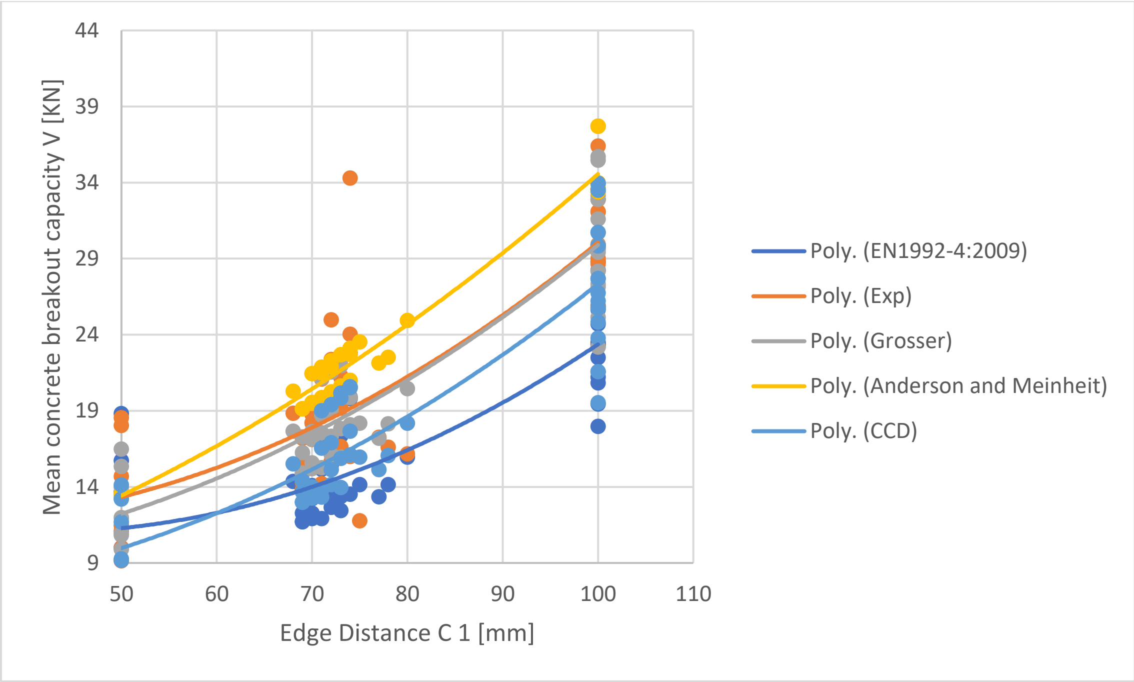

Figure 4.18: Comparison of Mean Shear Breakout Capacity from each Model and Experimental Investigation. Mean Shear Breakout Capacity Plotted Against Edge Distance

4.3.1.1 Concrete Capacity Design (CCD) Model

Following the descriptive and analytical equation, 2.1 given in chapter 3, the concrete breakout shear capacity of a single cast-in-place headed anchor was calculated using the CCD predictive model. This calculation used the same anchor parameters as those used in the experimental tests (e.g. the concrete cube compressive strength, the anchor diameter, the embedment depth and the edge distance). The subsection that follows briefly discusses the effect of these parameters on the concrete breakout capacity.

The results obtained from the concrete capacity design model are shown in Figure 4.19 and Table 4.6. Based on the criterion discussed in subsection 3.4.2, the CCD model underestimated the concrete breakout capacity with a mean of test-to-predicted values of 1.134. The coefficient of variation (COV) of 0.198 indicates a small deviation of the experimental test results- to – predicted shear capacity ratios from the mean. Figure 4.19 shows the best fit line with a coefficient of determination -R^2 equal to 0.831 indicating that the CCD model accounts for 83.1% of variation in the test data.

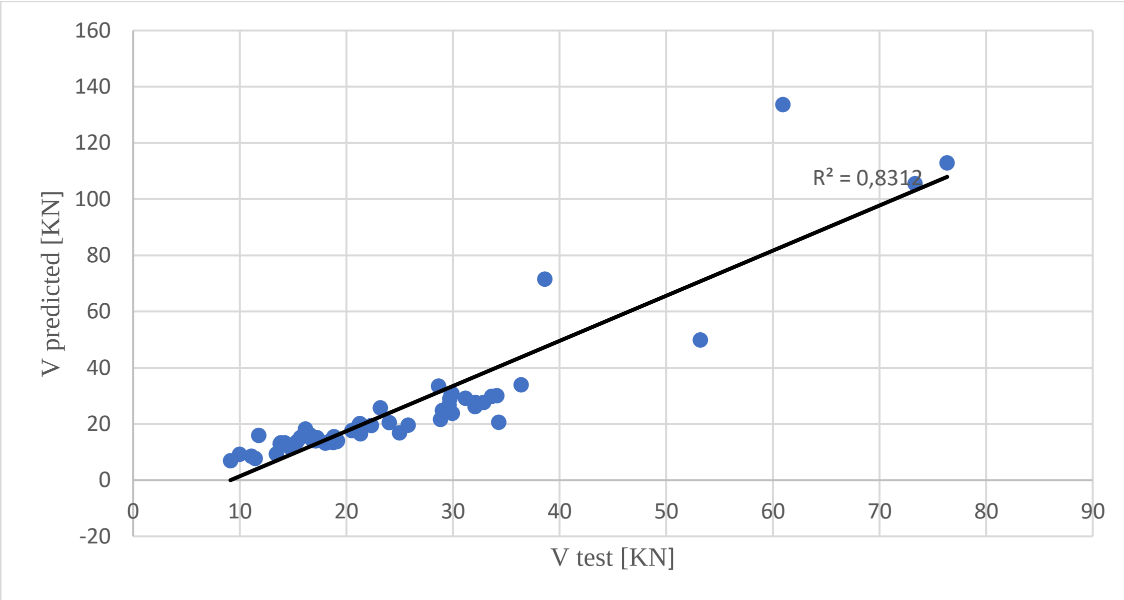

Figure 4.19: Comparison of Experimental Vexp to the Predicted mean concrete breakout Shear capacity Using CCD Method

Table 4-6: Statistical Model Uncertainty Quantification Using CCD Model (Based on the ratio $\frac{V_{Exp}}{V_{CCD}}$)

Mean	1.13
Standard deviation (SD)	0.22
Coefficient of variation (COV)	0.20
Coefficient of determination- $\boldsymbol{R^2}$	0.83

The CCD model employs the mean prediction according to equation 2.1. Table 4.7 shows the mean value of the model uncertainties of the CCD model. This result suggests that the Concrete Design Model (CCD) underestimates the mean concrete breakout resistance. This result can be attributed to the formulation and limitations of equation 2.1, as stated below and supported by Figure 4.19, which displays higher scatter at higher concrete breakout resistance.

Limits:

$d_{nom} \leq$ 25 mm (Nominal diameter of the anchor) and $\frac{hf}{d_{nom}} \leq 8$

4.3.1.2 EN1994-2:2009 Model (European Standard)

This study adopted design equation 2.5, as discussed in subsection 2.4.2 to evaluate the concrete breakout capacity. In this evaluation, the EN 2 model produced a mean of test-to predicted values of 1.134. Therefore, the EN1994-2 design model seems to also underestimate the concrete breakout capacity of a single anchor under shear loading. The coefficient of variation (COV) of 0.159 indicates a small deviation of the experimental test results-to-predicted shear capacity ratios from the mean. From Figure 4.20, there seems to be a higher scatter as the concrete breakout capacity increases. This trend can be attributed to the formulation and limitations of equation 2.5.

Furthermore, Figure 4.20 shows the best fit-line with a coefficient of determination -R^2 equal to 0.851, indicating that the CCD model accounts for 85.1% of the variation in the test data. Table 4.8 displays the statistical model uncertainty used to assess the accuracy of the model.

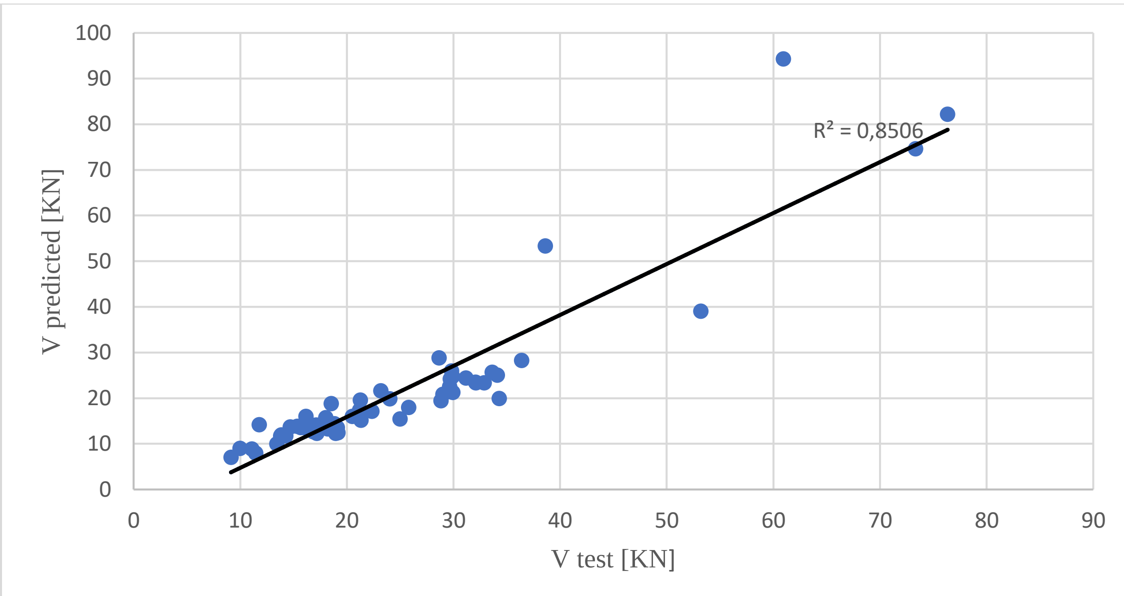

Figure 4.20: Comparison of Experimental Shear Capacity to Predicted Shear Capacity Using EN1994-2:2009

Table 4-7: Statistical Model Uncertainty Quantification Using EN2 (Model (Based on the ratio $\frac{V_{Exp}}{V_{EN2}}$)

Mean	1.25
Standard deviation (SD)	0.20
Coefficient of variation (COV)	0.16
Coefficient of determination- $\boldsymbol{R^2}$	0,85

The mean concrete shear resistance according to EN1994-2 employs the mean prediction according to Equation 2.4, given that $d_{nom} \ll 60$ mm and $h_{ef} \ll 8d_{nom}$. This method is conservative for a small edge distance. However, for a large edge distance, a constant factor of 3 as expressed in equation 2.5 would lead to a conservative prediction of the concrete breakout resistance.

The results in Table 4.7, as illustrated in Figure 4.20, show that the diameter and stiffness ratio showed a high scatter at higher concrete shear resistance when using this approach. Therefore, this result indicates that the EN1994-2 overestimates the mean concrete breakout resistance.

4.3.1.3 Anderson and Meinheit (2006)

The Analytical model used as described in the previous section was to predict the shear capacity of cast-in-place headed anchors with the same parameters as those tested from experimental results. Then the model's results are compared to the experimental test results. The results obtained from Anderson and Meinheit (2006) model are shown in Figure 4.21 and Table 4.8.

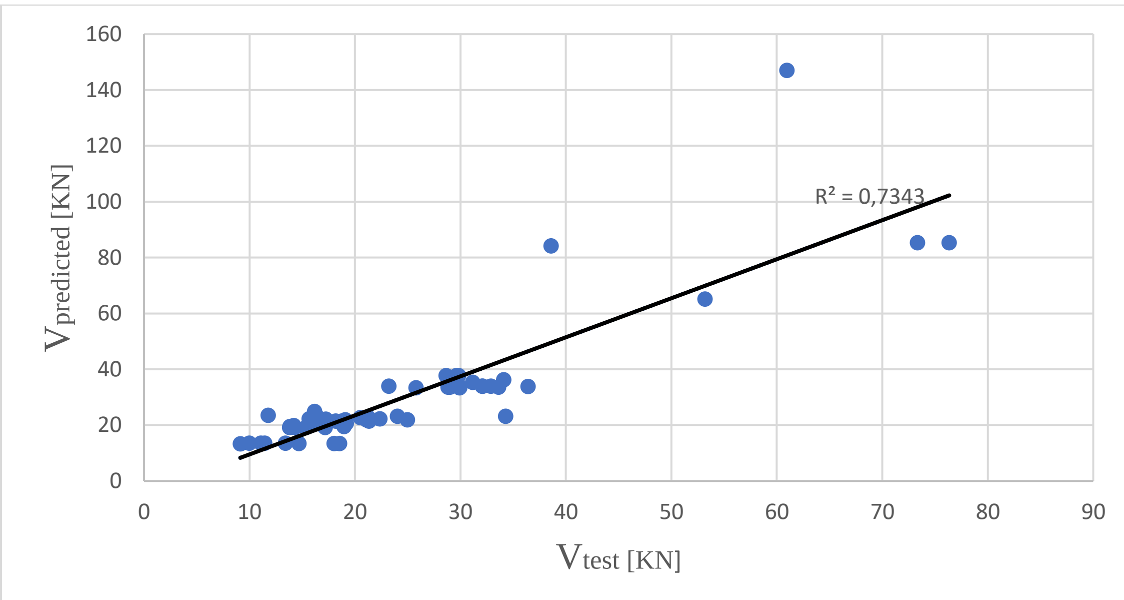

Figure 4.21: Comparison of Experimental Shear Capacity to Predicted Shear Capacity Using Anderson and Meinheit (2006)

The Anderson and Meinheit (2006) predictive model seems to be conservative with a mean of test-to predicted values of 0.872. The model produces a coefficient of variation (COV) of 0.213, which indicates a small deviation of the experimental test results-to-predicted shear capacity ratios from the mean. Figure 4.21 shows the best fit-line with a coefficient of determination, R^2 equal to 0.734. this value reveals that the Anderson and Meinheit (2006) model accounts for 73.4 % of the variation in the test data. All the statistical model uncertainty quantification obtained in this study is summarized in Table 4.8.

Table 4-8: Statistical Model Uncertainty Quantification Using Anderson and Meinheit (2006)

Mean	0.87
Standard deviation (SD)	0.19
Coefficient of variation (COV)	0.21
Coefficient of determination- $\boldsymbol{R^2}$	0,73

4.3.1.4 Grosser Model (2012)

According to Equation 2.7, the concrete mean breakout capacity is strongly influenced and overestimates the mean concrete breakout capacity when the term $\frac{h_{ef}}{d_{nom}}$ (stiffness ratio) increased. Due to this complexity, the authors' proposed equation found using regression analysis required further analysis. Therefore, Grosser (2012) proposed a simpler equation that captures all relevant parameters influencing the concrete breakout capacity. The proposed equation was briefly discussed in subsection 2.4.4.

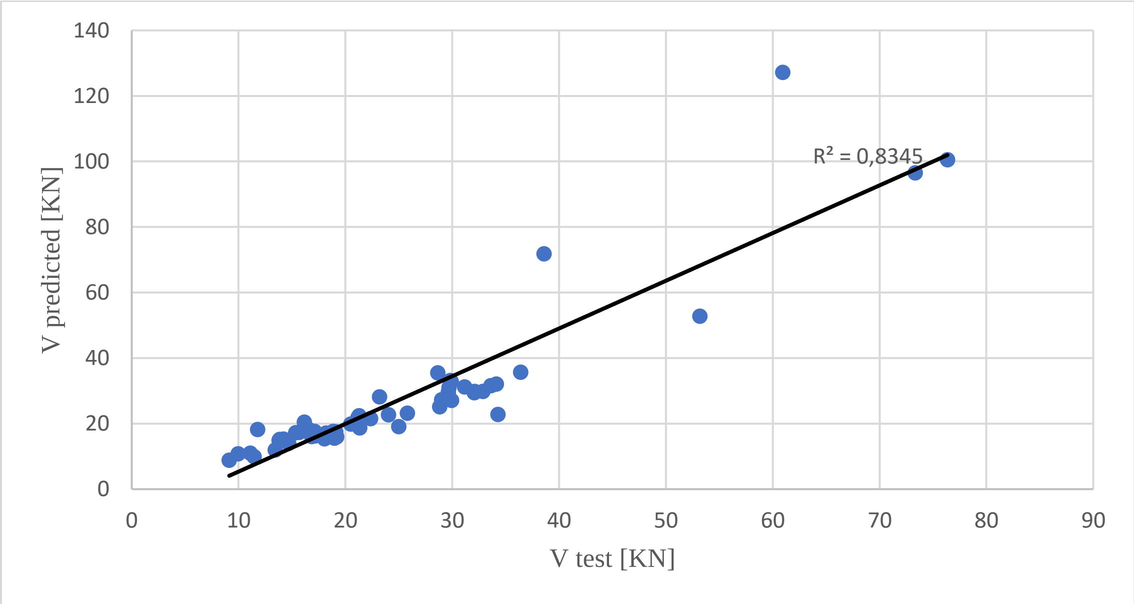

Figure 4.22: Comparison of Experimental Shear Capacity to Predicted Shear Capacity Using Grosser Model

The Grosser (2012) predictive model seems to be more conservative with a mean of test-to-predicted values of 0.997. Based on the criterion discussed in subsection 3.4.2, the Grosser model overestimated the concrete breakout capacity. Furthermore, the coefficient of variation (COV) of 0.165 indicates a small deviation from the mean of the experimental test results-to-predicted shear capacity ratios. Figure 4.23 shows the best fit-line with a coefficient of determination, R^2 equal to 0.835, which suggests that the Grosser model accounts for 83.5 % of the variation in the test data. Table 4.9 summarizes all the statistical model uncertainty quantification obtained in this study.

Table 4-9: Statistical Model Uncertainty Quantification using Grosser's (2012) Model

Mean	0.99
Standard deviation (SD)	0.17
Coefficient of variation (COV)	0.17
Coefficient of determination- $\boldsymbol{R^2}$	0,84

Although Equation 2.7 is a more accurate, it overestimates the mean concrete breakout capacity as the stiffness ration $\frac{h_{ef}}{d_{nom}}$ increases.

Another observable trend, as shown in appendix A, is that each design model had a mean concrete breakout capacity that is different from each other and the experimental mean concrete breakout capacity. Limiting the applicability of the design model equations to certain ranges and calibration can improve the performance of the design models.

This investigation reveals that of the models examined in this study (CCD, EN1994-2, Anderson and Meinheit and Grosser model), the Grosser method provides the most realistic approach for cast-in-place headed anchor under shear loading exhibiting concrete edge breakout failure. The basis for this conclusion is that the model captures all relevant uncertainties found in the anchor design parameters influencing the concrete mean breakout strength.

4.3.2 Effect of the Anchor Parameters on the concrete breakout Capacity

4.3.2.1 Introduction

This study employed simulations to investigate the influence of anchor parameters. A range of numerical simulations was performed to investigate the anchor parameters' effect on the breakout capacity. The parameters considered are:

I. The anchor diameters

II. The stiffness ratio

III. The edge distance

IV. The concrete compressive strength.

A linear correlation analysis was performed on the datasets of the model uncertainty to investigate the influence of the design anchor parameters on the concrete breakout strength. The main reason for performing linear correlation was to improve the performance and formulation of the anchor design models and investigate the sensitivity of each anchor design parameter, which is then used to calculate the safety margin in reliability analysis. The calculated linear correlation coefficients between model uncertainty and concrete breakout design parameters are summarized in Table 4.11. In this study, the parameters of interest influencing the concrete breakout capacity are the anchor nominal diameter(d_{nom}), the mean concrete compressive strength(f_{cu}), the edge distance(C_1), the stiffness ratio ($\frac{h_{ef}}{d_{nom}}$).

4.3.2.2 Linear correlation analysis of model uncertainties and concrete anchor design parameters

Table 4.7 and Figure 4.20 show that the model uncertainty related to the CCD model has a bias factor of 1.134. Based on the assessment criteria discussed in chapter 3, the CCD model underpredicts the concrete breakout capacity since the mean concrete breakout strength of test-to predicted value is more than 1. Among all predictive models investigated, the Concrete design Capacity (CCD) model yields the largest dispersion with a standard deviation (SD) of 0.224 and underestimates the mean concrete breakout resistance, as shown in Table 4.7. Also, based on the linear correlation analysis as presented in Table 4.11 and Figure 4.23, Figure 4.24 – 4.33, the model uncertainty variables investigated reveal that the concrete breakout capacity is more sensitive to the anchor nominal diameter d_{nom} (correlation coefficient r = -0.373), edge distance C_1 (Correlation coefficient r = -0.703), Concrete compressive strength $f_{cc,200}$ (Correlation coefficient r = -0.081). The stiffness ratio correlation seems to have a mild positive correlation (r = 0.237).

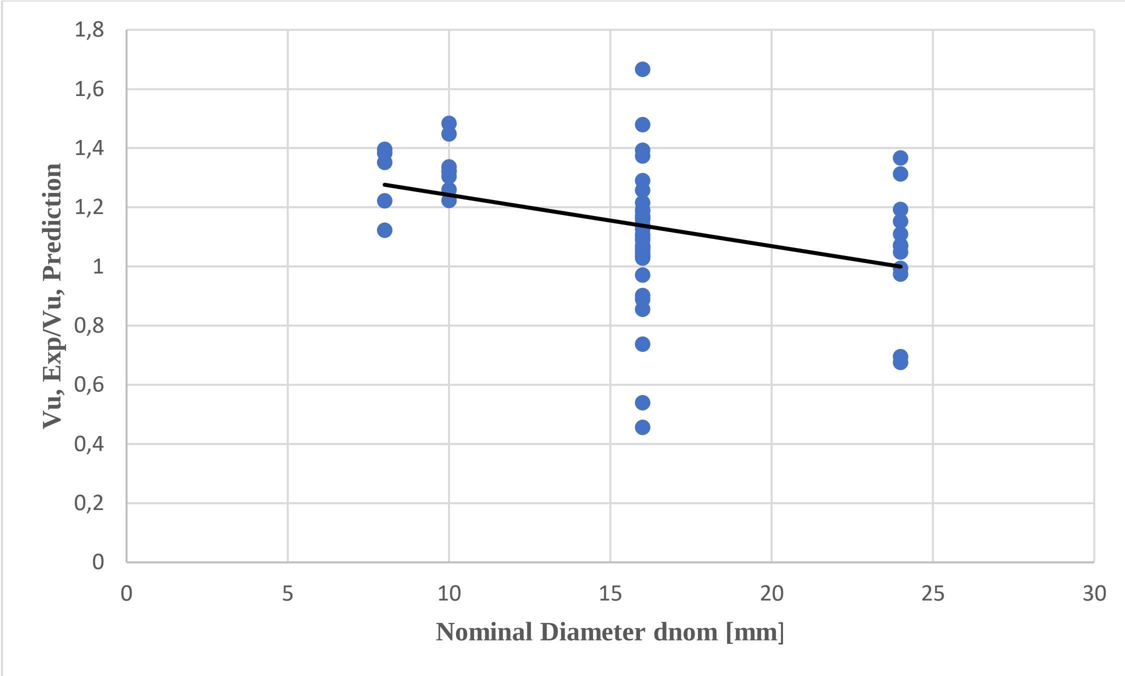

Figure 4.23: Evaluation of the Model Uncertainty Versus Nominal Anchor Diameter Using the CCD Model

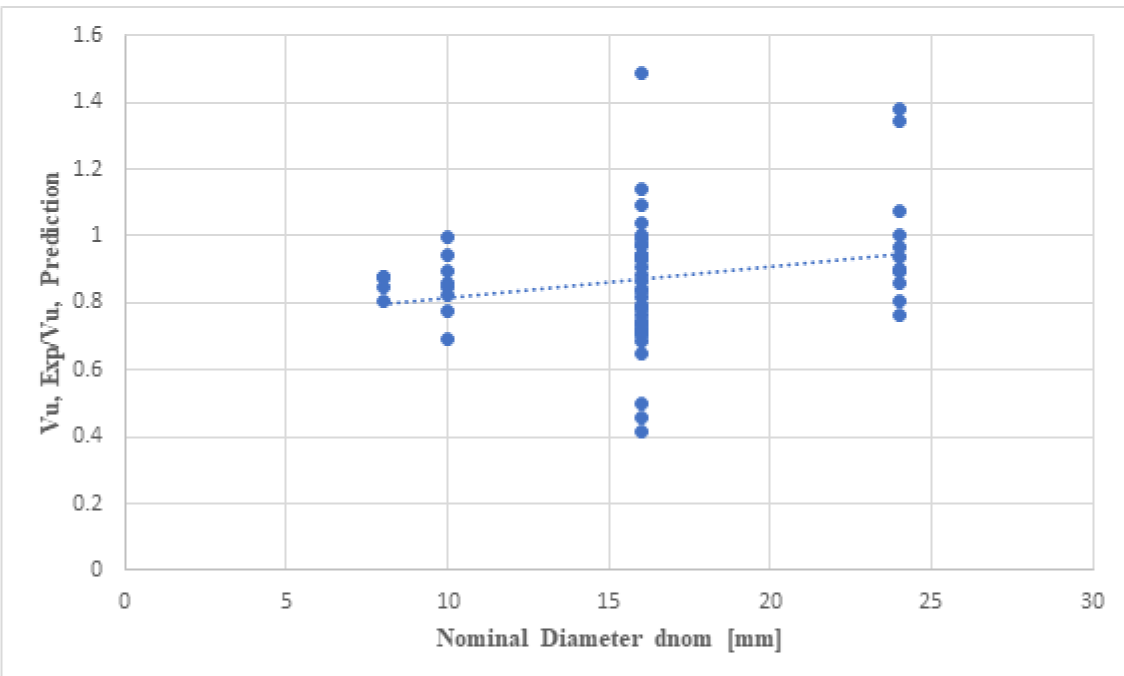

Figure 4.24: Evaluation of the Model Uncertainty Versus Nominal Anchor Diameter Using Anderson and Meinheit (2006) Model

Table 4.8 and Figure 4.21 show that the model uncertainty related to Anderson and Meinheit (2006) has a bias factor of 0.872. The Anderson and Meinheit (2006) analytical model overpredicts the concrete breakout capacity since the mean of the test-to the predicted value is less than 1. Table 4.8 shows that the model has a low dispersion with a standard deviation of 0.186. At the same time, Figure 4.25, and Figure 4.21 – 4.23 demonstrate that the model uncertainty associated with anchor parameters mildly influences the concrete breakout capacity (see Table 4.11).

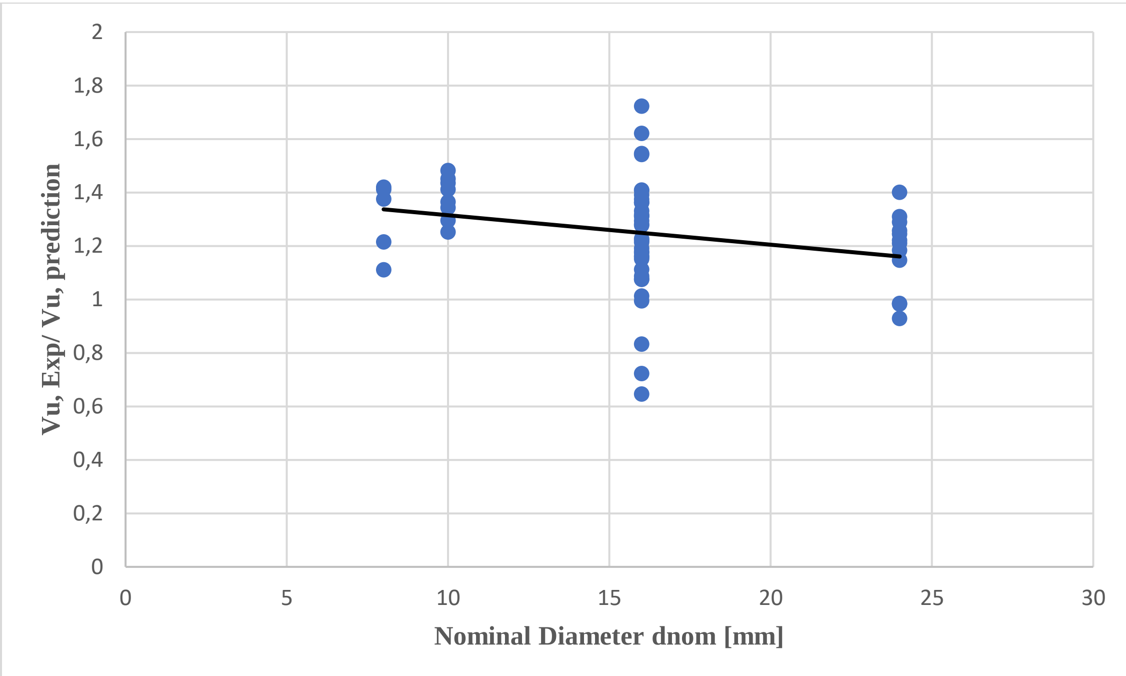

Figure 4.25: Evaluation of the Model Uncertainty Versus Nominal Anchor Diameter Using EN1992-4:2009

The model uncertainty related to EN1992-4:2009 has a bias factor of 1.247 (see Table 4.7 and Figure 4.20). EN1992:4-2009 model underpredicts the concrete breakout capacity since the mean of the test-to the predicted value is more than 1. The linear correlation analysis presented in table 12 shows that the EN1992-4:2009 model uncertainty variable associated with the edge distance is sensitive with a correlation coefficient r = -0.476. All other parameters have a mild correlation (refer to Table 4.12, figure 4.17, figure 4.21 – 4.23). In addition, the EN1992-4:2009 design model has a low dispersion with a standard deviation of 0.198.

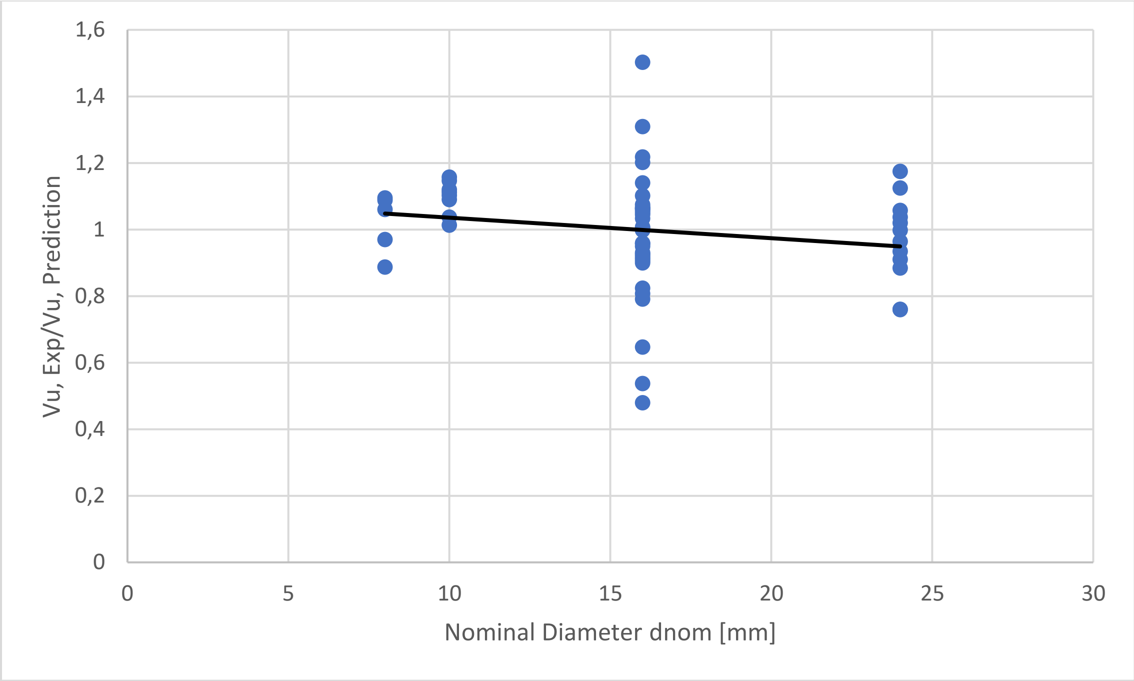

Figure 4.26: Evaluation of the Model Uncertainty Versus Nominal Anchor Diameter for Grosser Model

The model uncertainty related to the Grosser model has a bias factor closer to 0.998 (closer to 1) with a low dispersion of 0.165 (see Table 4.9 and Figure 4.23). From linear correlation analysis (refer to Table 4.12, Figure 4.18, and Figure 4.30 – 4.33), model uncertainty associated with the stiffness ratio has a low correlation coefficient, therefore an insignificant influence on the concrete breakout capacity. The CCD and the Grosser models seem sensitive to the edge distance with a correlation coefficient r = -0.703 and r = -0.587. All other parameters in the Grosser model do not influence the concrete breakout capacity, making the Grosser model the best predictor of the mean concrete breakout resistance.

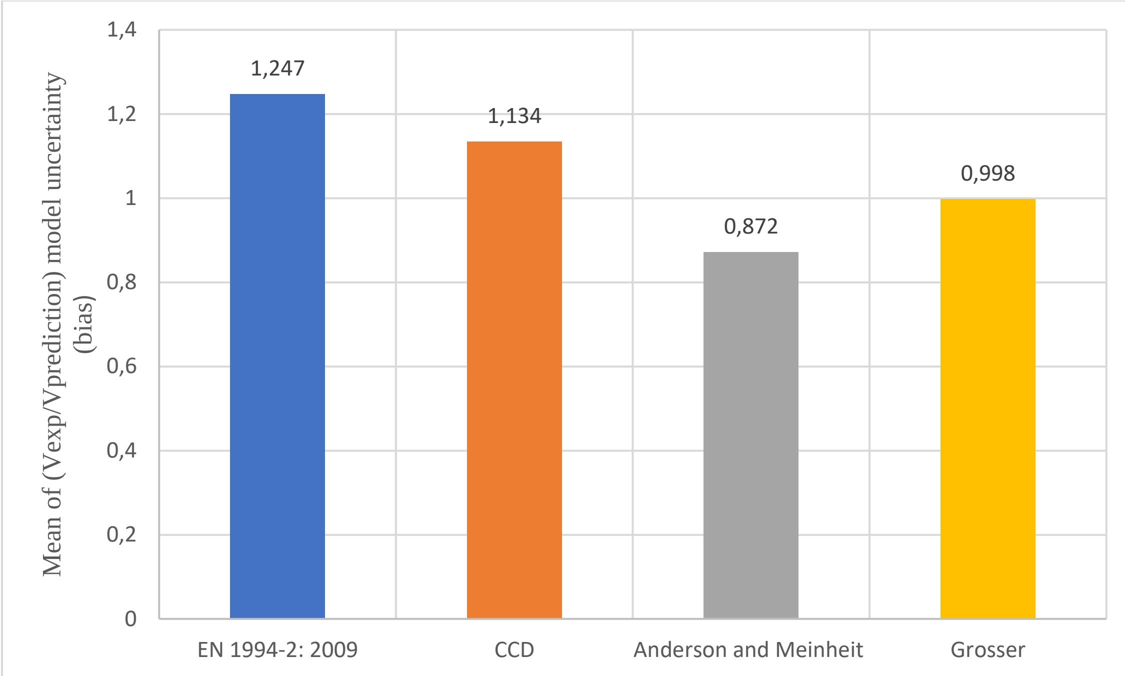

Figure 4.27: Mean of the Models Uncertainty (bias)

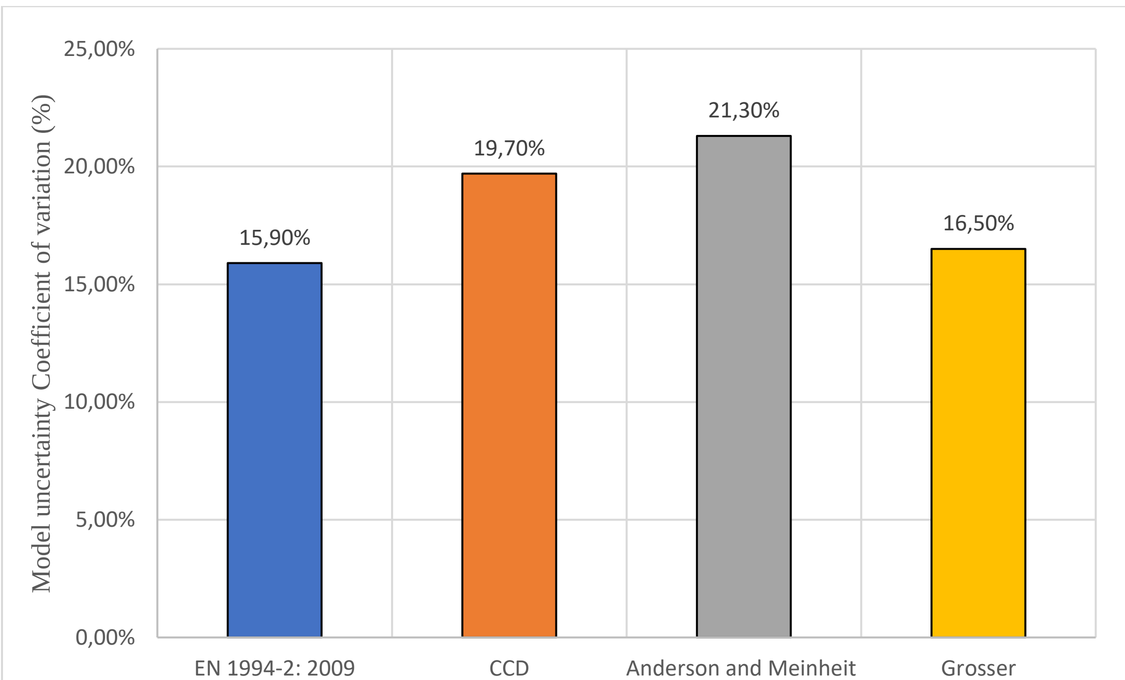

Figure 4.28: Model Uncertainty Coefficient of Variation

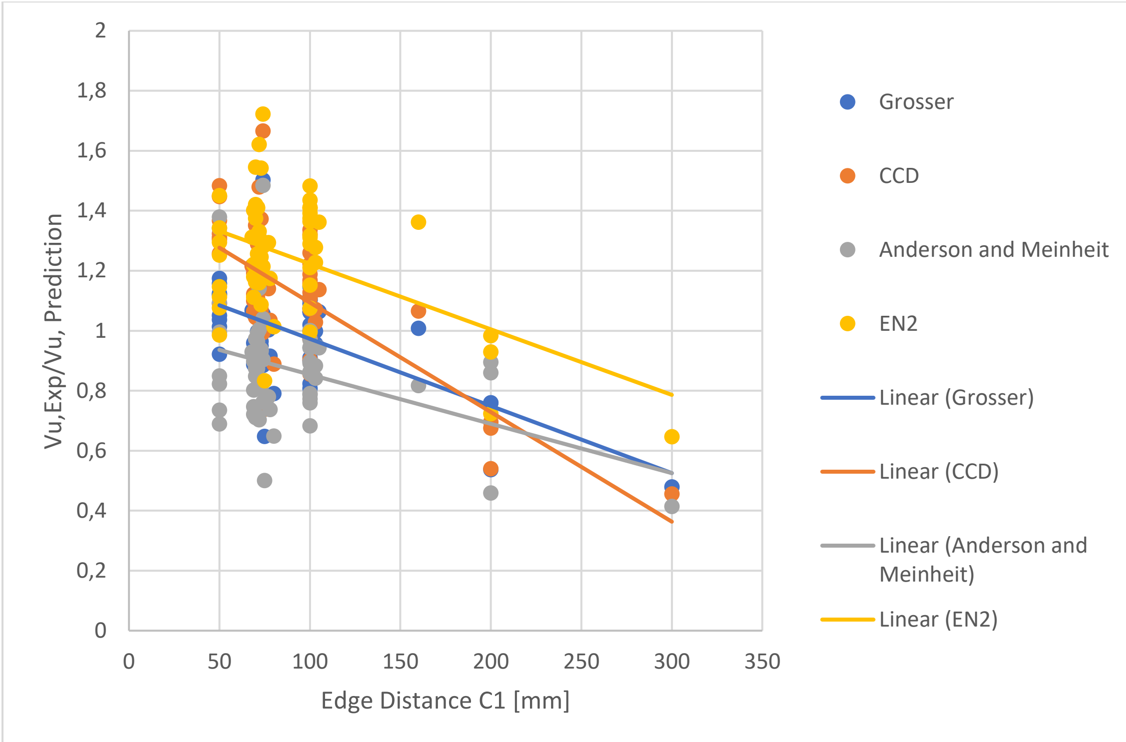

Figure 4.29: Evaluation of the Model Uncertainty Versus Edge Distance C_1

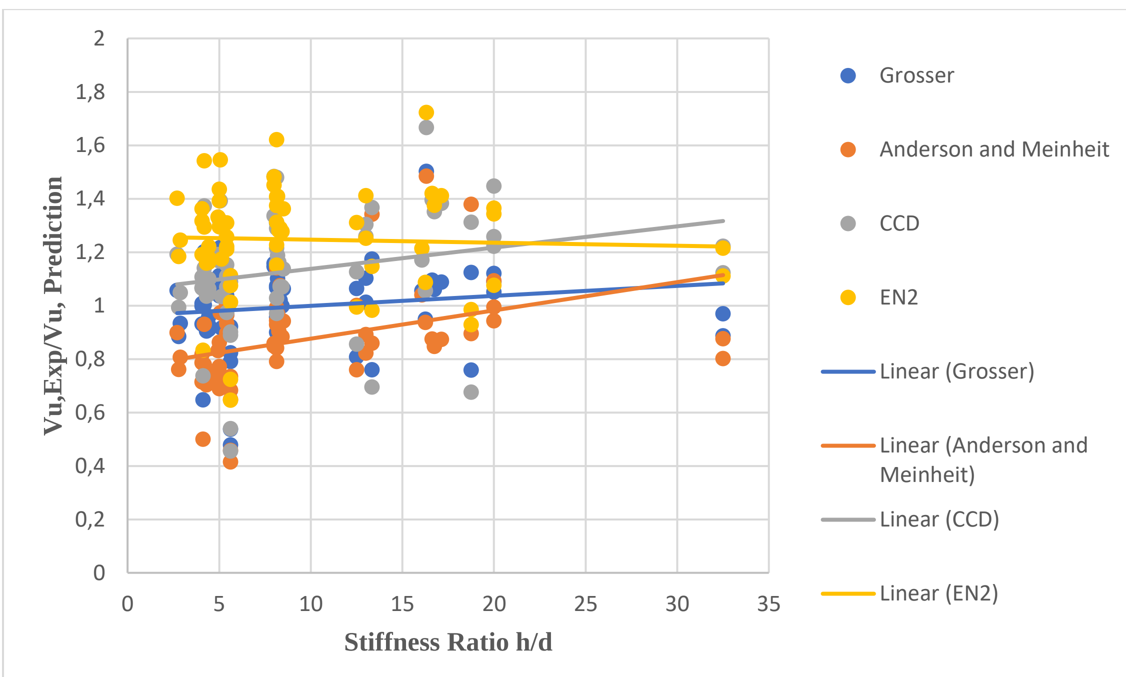

Figure 4.30: Evaluation of the Model Uncertainty Versus the Stiffness Ratio

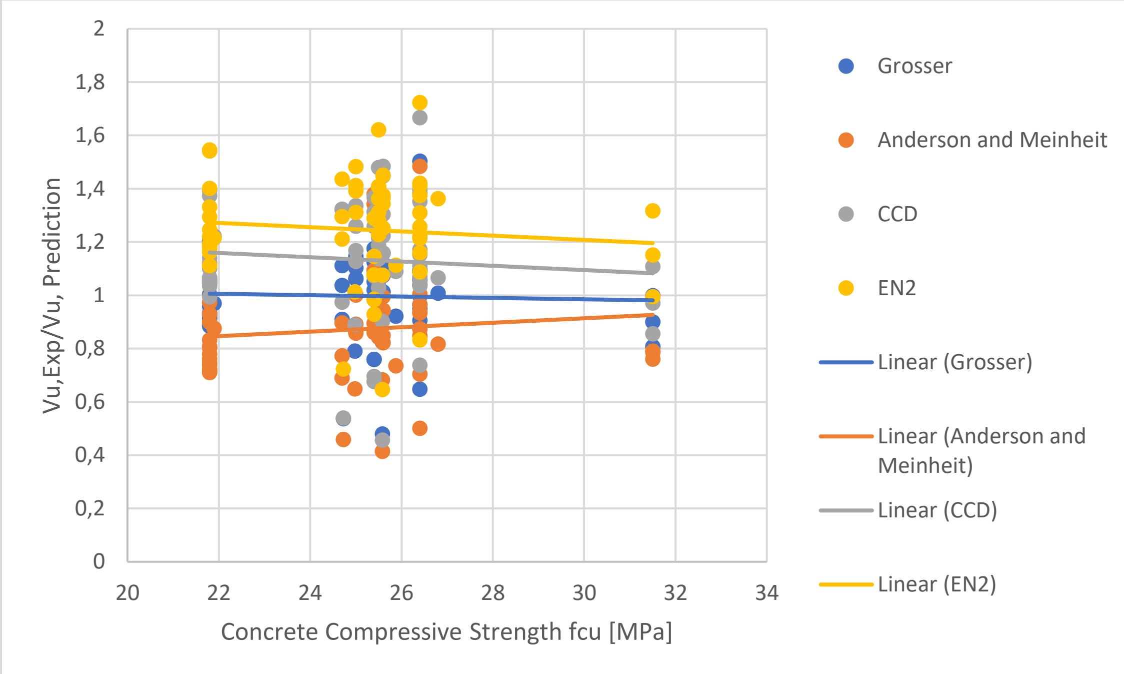

Figure 4.31: Evaluation of the Model Uncertainty Versus Concrete Compressive Strength

Table 4-10: Comparison of Different Prediction Equations Used to Calculate the Shear Capacity of a Cast-in Place Headed Anchor and Statistical Model Uncertainty Quantification (number of tests= 60)

Prediction model	$Vu_{Experiment}/Vu_{Prediction}$			Coefficient of determination -R^2
	Mean	Standard deviation	COV	
V_u=0.9×$(\frac{hf}{d})^{0.2}$×$d^{0.5}$×$C^{1,5}$×$\sqrt{f_{cc,200}}$ **CCD model**	1.02	0.201	0.198	0.831
$V_{u,c,o}$= 14.47×$C^{\frac{4}{3}}$.$\sqrt{f_{cc,200}}$ **Anderson and Meinheit (2006)**	0.87	0.186	0.213	0.734
$V_u = 2.4 \times d^{\alpha} \times {l_f}^{\beta} \times \sqrt{f_{cc}} \times c^{1.5}$ **EN1992-4**	0.99	0.165	0.165	0.835
V_u= 16.5×$\sqrt{f_{cc,200}}$ ×$C^{\frac{4}{3}}$×(0.02d+0.5)×$(\frac{h}{12d})^{c^{-0.4}}$ **Grosser (2011a)**	1.24	0.198	0.159	0.851

Table 4-11: Linear Correlation Coefficients and Anchor Parameters Influencing the Concrete Breakout Capacity

Concrete Breakout parameters	Grosser	Anderson and Meinheit	CCD	EN2
Nominal diameter ($\boldsymbol{d_{nom}}$)	**-0.181**	**0.235**	**-0.373**	**-0.269**
Edge Distance ($\boldsymbol{C_1}$)	**-0.587**	**-0.382**	**-0.703**	**-0.476**
Stiffness Ratio ($\frac{\boldsymbol{h_{ef}}}{\boldsymbol{d_{nom}}}$)	**0.151**	**0.379**	**0.237**	**-0.038**
Concrete Compressive Strength ($\boldsymbol{f_{cu}}$)	**-0.035**	**0.101**	**-0.081**	**-0.091**

4.5. Summary

Following this study's assessment of each predictive model, the Grosser model was rated the best predictor of concrete breakout capacity of single-headed anchor subject to shear loading. The Anderson and Meinheit (2006) model follow the Grosser model on this same rating. The basis for this conclusion is that for the Grosser model, all the crucial anchor design parameters had no significant influence on the concrete breakout capacity.

In terms of uncertainty quantification, the outcomes of this investigation proved that with the Grosser analytical model, the anchor parameters (anchor nominal diameter, embedment depth and the stiffness ratio) exert less influence on the concrete breakout capacity. Nonetheless, the EN1992-4:2009 model can be used as a predictor by carefully limiting the anchor design parameters such as the anchor nominal diameter and the embedment depth,

Of the investigated models, the Concrete Capacity Design (CCD) model was rated a poor predictor based on the model uncertainty quantification and linear correlation analysis. Specifically, the CCD model's trend line as shown in Figure 4.10 is far from the experimental trend line and the model appeared to be more sensitive to the edge distance.

Consequently, the applicability of each design model required that the anchor design parameters be limited and carefully calibrated. Moreso, due to the complexity of uncertainties and the bias found in each investigated design model, a reliability assessment is highly recommended for future studies to enhance the performance of the models investigated. Such an assessment can involve using the EN1992-4:2009 as a general probabilistic representation of the concrete of the limit state function on reliability assessment.

Another interesting finding was that all the design models produced different mean concrete breakout capacities compared to the experimental mean concrete failure loads. This finding suggests that limiting the applicability of the design model equations to certain ranges and calibration can improve the performance of these design models.

From the numerical studies, the element size did not influence the mean concrete breakout resistance, and the solid 65 element did not realistically display the full concrete damage as explained in subsection 4.2.2. Based on this conclusion, further investigations are required to be conducted on numerical analysis and more relevant information from the experimental investigation is required.

CHAPTER 5

CONCLUSIONS AND FUTURE WORK

5.1 Summary of the Work

This study investigated the load-bearing capacity of a single cast-in-place headed anchor under shear loading. The methodological approach of the study involved first, the principle of finite element analysis in Ansys workbench. Second, the assessment of the concrete breakout capacity using four predictive design models for concrete anchor subjected to shear loading, namely the Concrete Capacity Design model (CCD), European standard (EN1994-2:2009), Anderson and Meinheit (2006), and the Grosser (2012) model.

This section summarizes the objectives of this study and how they were achieved:

5.1.1 Objective One: To Create a Model that Displays a Nonlinear Behaviour of Concrete in Ansys Workbench

This objective was achieved using solid 65 element for the concrete model while the steel anchor model was used in default mode in Ansys program. The developed concrete and steel anchor models were subjected to several assumptions and limitations from the experimental studies on the materials' properties.

5.1.2 Objective Two: To Conduct a Mesh Sensitivity Analysis

This objective was achieved numerically by using three selected mesh sizes of 10 mm, 15 mm and 20 mm. Then a load-displacement curve was plotted for each selected mesh size by applying load in time steps to examine the convergence of the results.

5.1.3 Objective Three: To Validate the Numerical Model’s Results

The third objective was achieved by comparing results from numerical simulations with experimental test results using different anchor configurations as depicted in appendix A and B.

5.1.4 Objective Four: To Perform Statistical Analysis and Models Uncertainty Quantifications

The study achieved the above objective by using four concrete breakout capacity design models, namely the Concrete Capacity design model (CCD), the European standard (EN1994-2:2009), and the Anderson and Meinheit (2006), and the Grosser model. Furthermore, each of these predictive models were assessed using the statistical tools discussed in subsection 3.4.1.

5.1.5 Objective Five: To Investigate the Relevant Anchor Parameters Influencing the Concrete Breakout Capacity

This objective was achieved by using linear correlation analysis to examine the sensitivity of each anchor design parameter influencing the concrete breakout capacity as comprehensively discussed in chapter 4. The parameters investigated in this study include the anchor nominal diameter, edge distance, concrete compressive strength, and the stiffness ratio. Each of these parameters was carefully analysed and their influence on the concrete breakout capacity is assessed.

5.2 Findings

The study's findings can be summarized as follows:

I. According to the mesh sensitivity analysis, the mesh size has no effect on the concrete breakout capacity.

II. A Solid 65 element model cannot predict the concrete breakout capacity of headed anchor under shear loading near the edge in the realistic manner. Overall, it was discovered that some of the failure loads obtained from numerical studies were higher than the loads obtained from the experimental tests, though in some cases, numerical analysis were much lower than the experimental tests results.

III. Based on the assessments of each predictive models, the Grosser analytical predictive model is rated the best predictor of concrete breakout capacity of single headed anchor under shear loading because the associated predictive equation takes into account the limitation of the design anchor parameters.

IV. The predictive model assessments also revealed that the Concrete Capacity Design (CCD) model is a poor predictor of the concrete breakout capacity. Moreso, the CCD's analytical predictive equation seems to be very sensitive to the edge distance.

5.3 Future Work

Although the study yielded some interesting findings, such findings are subject to the limitations outlined in section 1.6. Therefore:

I. More numerical research is needed to understand the behavior of concrete anchor subjected to shear loading using dynamic solver or microscopic space analysis (MASA) model for anchorage systems. The MASA model is more efficient because it only required the uniaxial stress-strain relationship for each microplane components, and the microscopic response is obtained automatically through integration across all microplanes. Ožbolt et al., (2007) provided details information about the model. In addition, dynamic analysis and time dependent load analysis can also be use to improve results from the finite element model.

II. Due to the complexity on the formulation of each analytical predictive model and the sensitivity of the anchor design parameters that influence the concrete breakout capacity, reliability-based performance is required in future studies.

References

Abedini, M., & Zhang, C. (2020): Performance Assessment of Concrete and Steel Materials Models in LS-DYNA for Enhanced Numerical Simulation, A State of the Art Review. Archives of computational Methods in Engineering 2020 28:4, 28 (4), 2921-2942)

Al Saeab, L.T.A., (2019): Finite Element Modelling of Anchorage to Concrete Systems at Different Strain Rates (Doctoral dissertation, Carleton University).

Anderson, N.S. and Meinheit, D.F., (2006): Design Criteria for Headed Stud Groups in Shear: Final Report. Wiss, Janney, Elstner Associates, Inc., Northbrook, I.

Anderson, N. S.; Meinheit, D. F. (2001): Steel Capacity of Headed Studs Loaded in Shear. In Eligehausen, R. (Editor): RILEM Proceedings PRO 21 „Connections between Steel and Concrete ", RILEM Publications s.a.r.l. Cachan Cedex, pp. 202–211.

Anderson, N. S.; Meinheit, D. F. (2000/1): PCI Sponsored Headed Stud Research Program: Test Results and Comparisons to Existing Models.

A.Bashir, K. Ahmad, H.U. Khan, M.N. Rafique and S. Karam. (2014): Identification of Shear Cracks in Reinforced Beams Using Finite Element Method, Pakistan Journal of Science, Vol. 66, No. 1, March 2014.

Brighton, D. A. (2011): Finite element analysis of an intentionally damaged prestressed reinforced concrete beam repaired with carbon fiber reinforced polymers (Doctoral dissertation, University of Toledo).

Cotsovos, Demetrios M., Christos A. Zeris, and Ali A. Abbas. (2009): Finite element modelling of structural concrete. COMPDYN 2009 (2009).

EN 1990: 2002 (2002): Basis of design for structural Eurocodes. European Committee for Standardisation (CEN), Brussels, 2002.

Eligehausen, R., Mallée, R. and Silva, J.F., (2006): Anchorage in concrete construction (Vol. 10). John Wiley & Sons.

European Organisation for Standardization: CEN TS (2004): Design of Fastenings for Use in Concrete. Final draft, 2004. Part 1: General. Part 2: Headed Anchors. Part 3: Anchor Channels. Part 4: Post-installed Anchors – Mechanical Systems. Part 5. Post-installed Anchors – Chemical Systems.

Eligehausen, R., Mallée, R., & Silva, J. (2012): Anchorage in Concrete Construction. Anchorage in Concrete Construction (First). Ernst und Sohn.

Eriksson, D. and Gasch, T., (2011): Load capacity of anchorage to concrete at nuclear facilities: Numerical studies of headed studs and expansion anchors.

EN 12390-3. (2009): Testing hardened concrete – Part 3: Compressive strength of test specimens, 19 pp.

EN 12390-6. (2009): Testing hardened concrete – Part 6: Tensile splitting strength of test specimens, 11 pp.

EN 1992-1-1. (2004): Design of concrete structures – Part 1–1: General rules and rules for buildings, European Committee for Standardization (CEN), Brussels, Belgium, 225 pp.

Fuchs, W. (1990): Load-bearing behaviour of fastenings under shear loading in non-cracked concrete. Doctor thesis, Universität Stuttgart, 1990.

Fuchs, W.; Eligehausen, R.; Breen, J. E. (1995/1): Concrete Capacity Design (CCD) Approach for Fastening to Concrete. ACI Structural Journal, Vol. 92 (1995), No. 1, pp. 73–94.
Fuchs, W.; Eligehausen, R.; Breen, J. E. (1995/2): Concrete Capacity Design (CCD) Approach for Fastening to Concrete, Authors' Closure to Discussions. ACI Structural Journal, Vol. 92 (1995), No. 6, pp. 794–802.

Fuchs, W., Eligehausen, R., and Breen, J. E. (1995): Concrete capacity design (CCD) approach for fastening to concrete. ACI Struct. J., 92(1), 73–94.

Grosser, Philipp R. (2012): Load-bearing behavior and design of anchorages subjected to shear and torsion loading in uncracked concrete. (2012).

Halahla, Abdulsamee. (2019): Identification of Crack in Reinforced Concrete Beam Subjected to Static Load Using Non-linear Finite Element Analysis. Civil Engineering Journal 5.7 (2019): 1631- 1646.

Kwak, H.G. and Filippou, F.C., (1990): Finite element analysis of reinforced concrete structures under monotonic loads (pp. 33-39). Berkeley, CA: Department of Civil Engineering, University of California.

Kurowski, P. M. (2016): Finite Element Analysis for Design Engineers, Second Edition. Finite Element Analysis for Design Engineers, Second Edition (2nd ed., pp. i–xiii). SAE International.

Lee, J.H., Choi, E. and Cho, B.S., (2020): Shear Failure Mode and Concrete Edge Breakout Resistance of Cast-In-Place Anchors in Steel Fiber-Reinforced Normal Strength Concrete. Applied Sciences, 10(19), p.6883.

Liu, Q., French, C. W., & Sritharan, S. (2021): Comparative response of rocking-wall systems with cast-in-place and precast floor systems in buildings. Engineering Structures, 234, 111942

Olalusi, Oladimeji B., and Panagiotis Spyridis. (2020): Uncertainty modelling and analysis of the concrete edge breakout resistance of single anchors in shear. Engineering Structures 222 (2020).

Meyer, R., Ahrens, H. and Duddeck, H., (1994): Material model for concrete in cracked and uncracked states. *Journal of engineering mechanics*, *120*(9), pp.1877-1895.

Nilforoush, Rasoul. (2017): Anchorage in Concrete Structures: Numerical and Experimental Evaluations of Load-Carrying Capacity of Cast-in-Place Headed Anchors and Post-Installed Adhesive Anchors. Diss. Luleå University of Technology, 2017.

Ožbolt, J., Eligehausen, R., Periškić, G., & Mayer, U., (2007): 3D FE Analysis of Anchor Bolts with Large Embedment Depths. Engineering Fracture Mechanics, 74(1-2), pp.168-178.

Shuvalov, A., Gorbunov, I., & Kovalev, M. (2021): Anchorage strength and ductility in shear tests. E3S Web of Conferences, 263, 02016.

APPENDIX A: Mean concrete breakout capacity from numerical study and predictive design models

No	Bolt Labels	d [mm]	h_{ef} [mm]	c_1 [mm]	$f_{cc,200}$ [MPa]	$f_{cc,150}$ [MPa]	EXPERIMENTAL [KN]	FEA [KN]	EN1992-4[KN]	CCD [KN]	Anderson and Meinheit [KN]	Groser [KN]
1	B1	16	130	68	25,50	26,84	18,84	16,70	14,36	15,50	20,28	17,64
2	B2	16	130	71	25,50	26,84	21,33	17,00	15,14	16,54	21,48	18,71
3	B3	16	132	74	25,50	26,84	20,51	17,00	16,01	17,65	22,70	19,85
4	B4	16	130	72	25,50	26,84	24,98	12,00	15,41	16,89	21,89	19,07
5	B5	16	131	100	25,50	26,84	32,88	40,00	23,34	27,68	33,92	29,85
6	B6	16	130	103	25,50	26,84	29,70	25,00	24,19	28,89	35,28	31,03
7	B7	16	136	105	25,50	26,84	34,12	12,00	25,05	30,01	36,20	32,08
8	B8	16	135	103	25,50	26,84	31,17	8,00	24,40	29,11	35,28	31,22
9	B9	8	133	70	26,40	27,79	18,76	13,50	13,21	13,44	21,45	17,13
10	B10	8	137	71	26,40	27,79	19,10	18,00	13,53	13,81	21,86	17,55
11	B11	8	134	70	26,40	27,79	18,19	9.3	13,23	13,46	21,45	17,16
12	B12	24	130	73	26,40	27,79	21,19	31,70	17,35	19,81	22,68	21,97
13	B13	24	130	71	26,40	27,79	21,09	34,70	16,78	19,00	21,86	21,14
14	B14	24	130	72	26,40	27,79	22,36	30,30	17,07	19,40	22,27	21,55
15	B15	16	257	74	26,40	27,79	24,03	26,80	19,80	20,52	23,10	22,75
16	B16	16	260	73	26,40	27,79	21,27	33,80	19,57	20,15	22,68	22,40
17	B17	16	261	74	26,40	27,79	34,29	40,50	19,90	20,58	23,10	22,82
18	B18	16	66	75	26,40	27,79	11,77	22,20	14,13	15,95	23,52	18,19
19	B19	16	69	72	26,40	27,79	15,67	15,04	13,52	15,14	22,27	17,31
20	B20	16	71	69	21,80	22,95	14,28	31,50	11,70	12,98	19,12	14,89
21	B21	16	71	69	21,80	22,95	13,80	31,50	11,70	12,98	19,12	14,89
22	B22	16	71	70	21,80	22,95	13,85	33,00	11,92	13,26	19,49	15,19
23	B23	16	67	73	21,80	22,95	19,17	25,70	12,43	13,96	20,61	15,95
24	B24	16	65	71	21,80	22,95	14,20	29,20	11,92	13,31	19,86	15,25
25	B25	16	67	77	21,80	22,95	17,25	32,7	13,33	15,12	22,13	17,19
26	B26	24	69	73	21,80	22,95	16,64	31,50	13,36	15,86	20,61	17,82
27	B27	24	65	69	21,80	22,95	17,18	26.80	12,26	14,40	19,12	16,25
28	B28	24	67	74	21,80	22,95	15,99	8,20	13,50	16,09	20,99	18,07
29	B29	8	260	70	21,90	23,05	17,11	9,30	14,08	14,00	19,54	17,64
30	B30	8	260	69	21,80	22,95	15,34	22,22	13,80	13,67	19,12	17,28
31	B31	16	81	70	21,80	22,95	18,96	23,30	12,27	13,62	19,49	15,56
32	B32	16	79	72	21,80	22,95	16,84	34,70	12,65	14,13	20,24	16,12
33	B33	16	82	78	21,80	22,95	16,61	41,70	14,14	16,06	22,52	18,14
34	B34	16	65	100	31,50	33,16	29,63	30,00	22,50	26,74	37,70	29,69
35	B35	16	130	100	31,50	33,16	29,82	14,00	25,89	30,72	37,70	33,13
36	B36	16	200	100	31,50	33,16	28,65	12,00	28,78	33,48	37,70	35,48
37	M37	10	50	50	24,70	26,00	9,13	12,00	7,05	6,90	13,25	8,80
38	M38	10	80	50	25,60	26,95	11,45	14,00	7,89	7,72	13,49	9,89
39	M39	10	130	50	25,60	26,95	11,09	12,00	8,86	8,50	13,49	10,95
40	M40	10	200	50	25,60	26,95	13,42	12,00	9,99	9,27	13,49	11,98
41	M41	10	50	100	24,70	26,00	25,79	14,00	17,97	19,52	33,38	23,19
42	M42	10	80	100	25,00	26,32	28,82	11,20	19,44	21,57	33,58	25,14

43	M43	10	130	100	25,00	26,32	29,94	12,80	21,21	23,77	33,58	27,15
44	M44	10	200	100	25,60	26,95	32,06	12,00	23,49	26,22	33,98	29,41
45	M45	16	320	50	25,40	26,74	14,69	20,00	13,65	11,68	13,43	13,98
46	M46	16	80	100	25,00	26,32	29,00	28,00	20,83	24,84	33,58	27,33
47	M47	16	130	100	25,60	26,95	32,09	22,00	23,34	27,69	33,98	29,87
48	M48	16	200	100	25,00	26,32	33,62	20,00	25,64	29,83	33,58	31,60
49	M49	24	320	200	25,40	26,74	73,35	36,00	74,59	105,51	85,30	96,53
50	M50	24	450	200	25,40	26,74	76,35	31,5	82,19	112,96	85,30	100,57
51	M51	16	90	50	25,88	27,24	9,97	22,50	8,96	9,15	13,56	10,82
52	M52	16	90	80	24,98	26,29	16,17	13,80	15,96	18,19	24,93	20,44
53	M53	16	90	100	25,58	26,93	23,20	18,00	21,57	25,72	33,97	28,17
54	M54	16	90	200	24,73	26,03	38,60	17,50	53,34	71,53	84,16	71,85
55	M55	16	90	300	25,58	26,93	60,95	26,30	94,30	133,65	146,98	127,19
56	M56	24	320	50	25,40	26,74	18,03	28,00	15,72	13,19	13,43	15,35
57	M57	24	450	50	25,40	26,74	18,53	29,80	18,80	14,12	13,43	16,48
58	M58	24	130	100	24,70	26,00	29,92	29,80	24,71	30,72	33,38	32,88
59	M59	24	200	100	25,40	26,74	36,40	28,00	28,23	33,96	33,85	35,70
60	B60	16	65	160	26,80	28,21	53,19	24,80	39,05	49,92	65,07	52,77

APPENDIX B: **L**oad-displacement response curves from the numerical study (FEA) on a Single Anchor Loaded Perpendicular to the Edge. Refer to Appendix A for the anchor design Parameters.

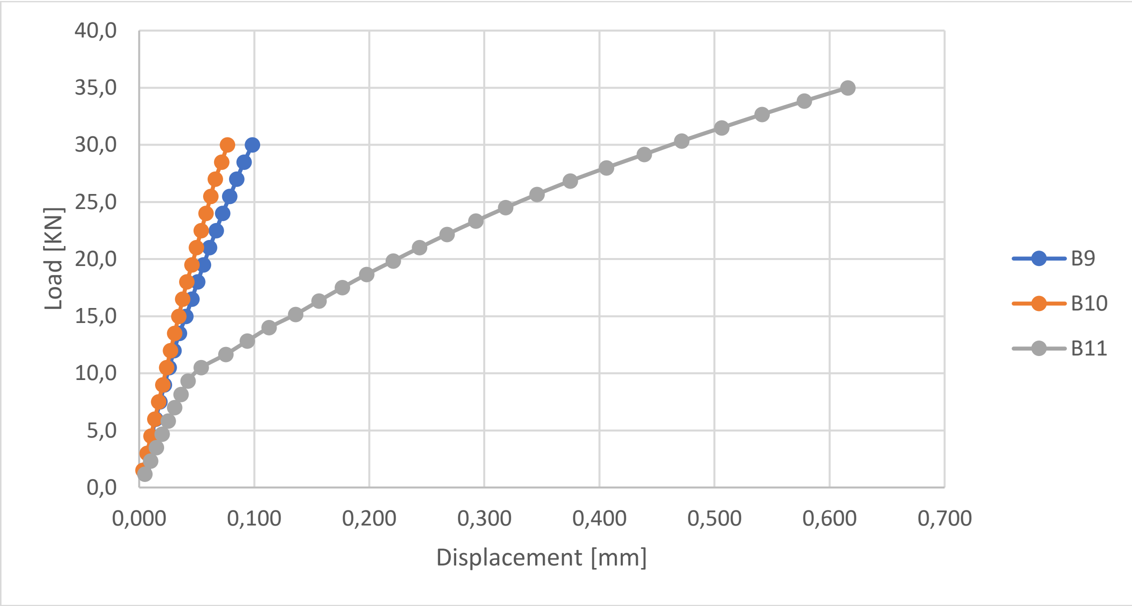

Figure B.1. Load-displacement behaviour of the numerical model for a Single Anchor Loaded Perpendicular to the Edge (Refer to Appendix A for the anchor design parameters)

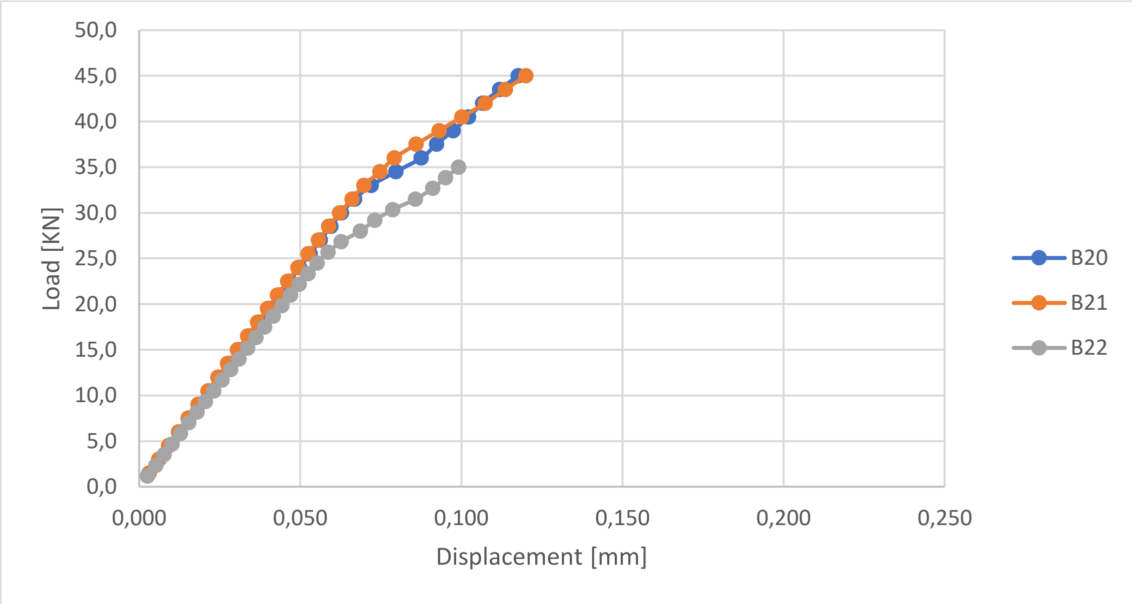

Figure B.2. Load-displacement behaviour of the numerical model for a Single Anchor Loaded Perpendicular to the Edge (Refer to Appendix A for the anchor design parameters)

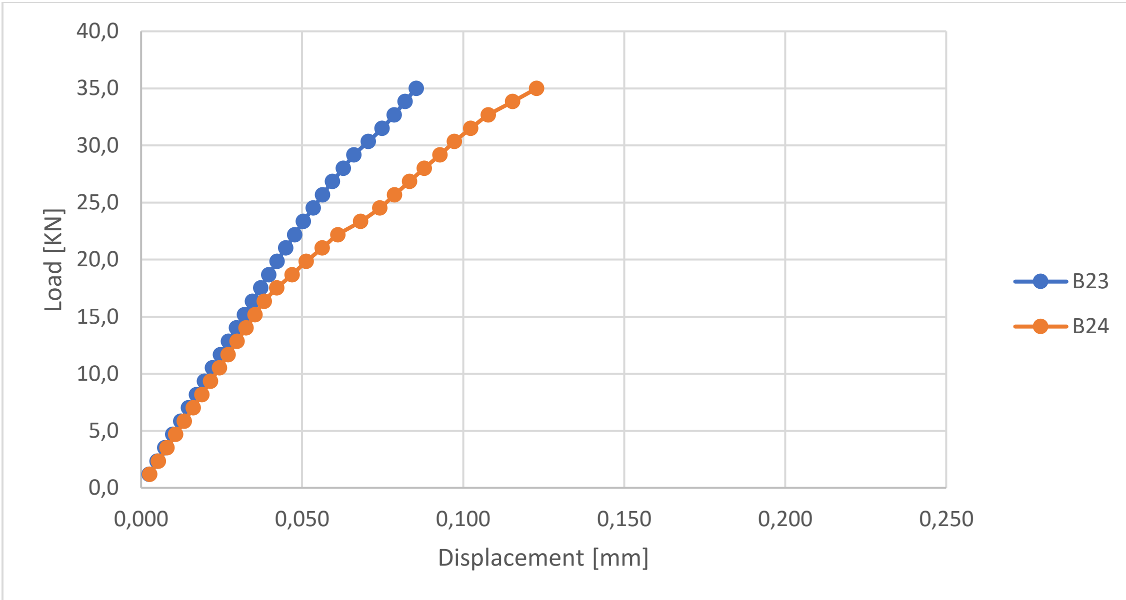

Figure B.3. Load-displacement behaviour of the numerical model for a Single Anchor Loaded Perpendicular to the Edge (Refer to Appendix A for the anchor design parameters)

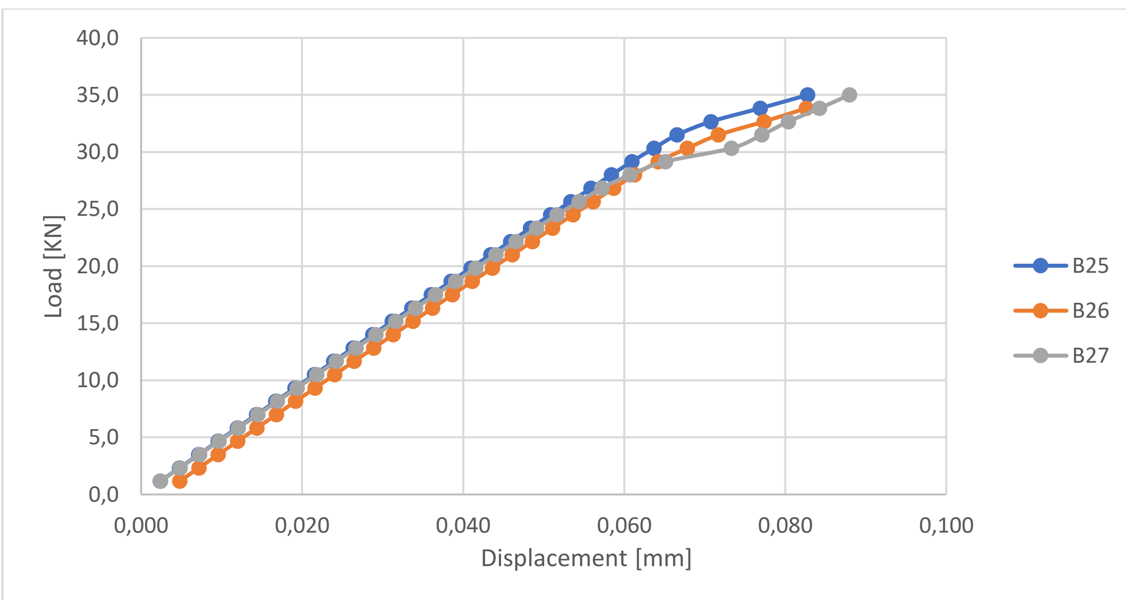

Figure B.4. Load-displacement behaviour of the numerical model for a Single Anchor Loaded Perpendicular to the Edge (Refer to Appendix A for the anchor design parameters)

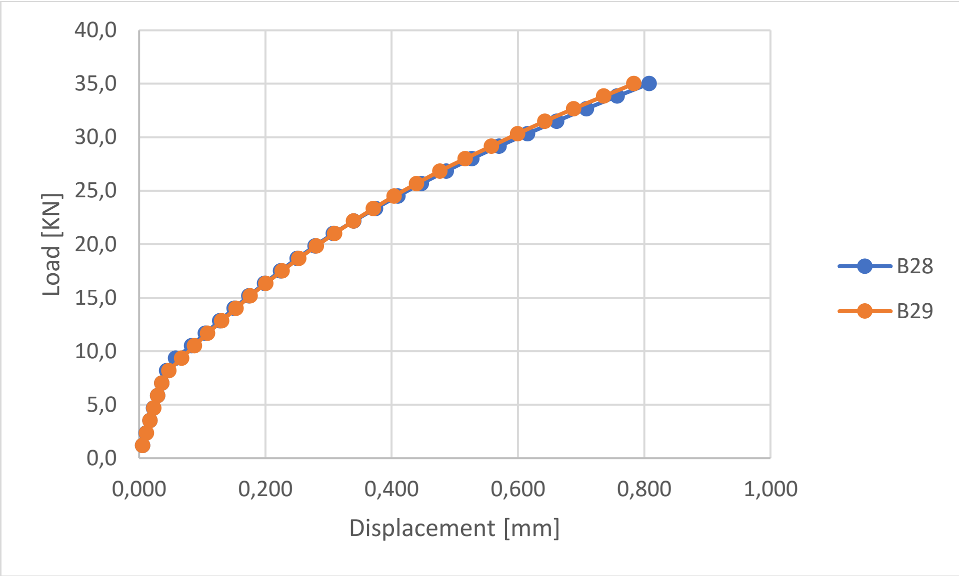

Figure B.5. Load-displacement behaviour of the numerical model for a Single Anchor Loaded Perpendicular to the Edge (Refer to Appendix A for the anchor design parameters)

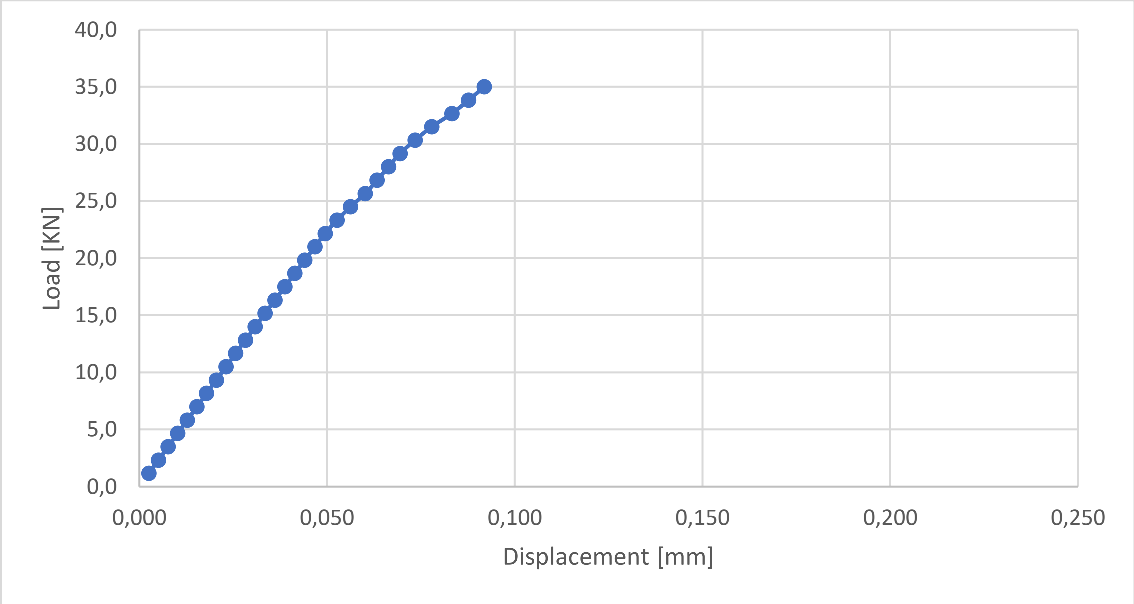

Figure B.6. Load-displacement behaviour of the numerical model for a Single Anchor Loaded Perpendicular to the Edge (Refer to Appendix A for the anchor design parameters). Bolt label:B30

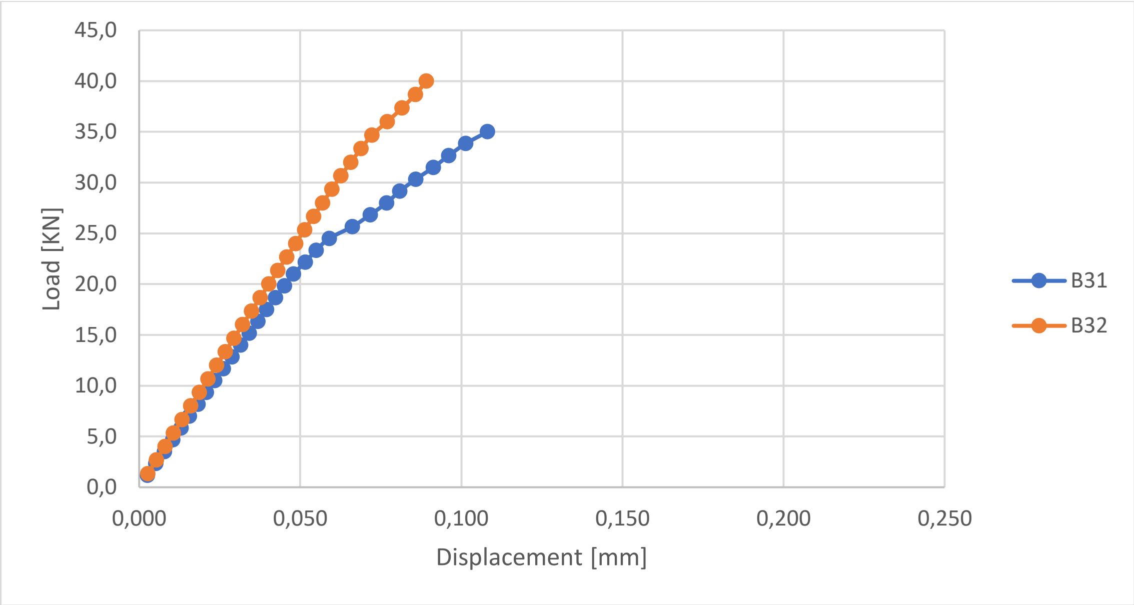

Figure B.7. Load-displacement behaviour of the numerical model for a Single Anchor Loaded Perpendicular to the Edge (Refer to Appendix A for the anchor design parameters)

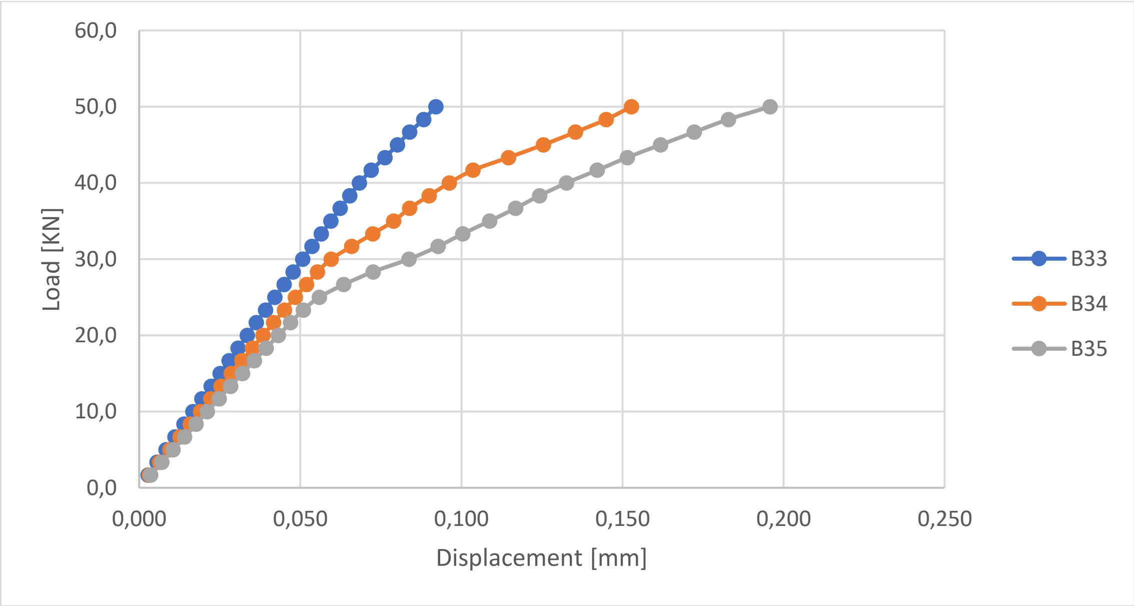

Figure B.8. Load-displacement behaviour of the numerical model for a Single Anchor Loaded Perpendicular to the Edge (Refer to Appendix A for the anchor design parameters)

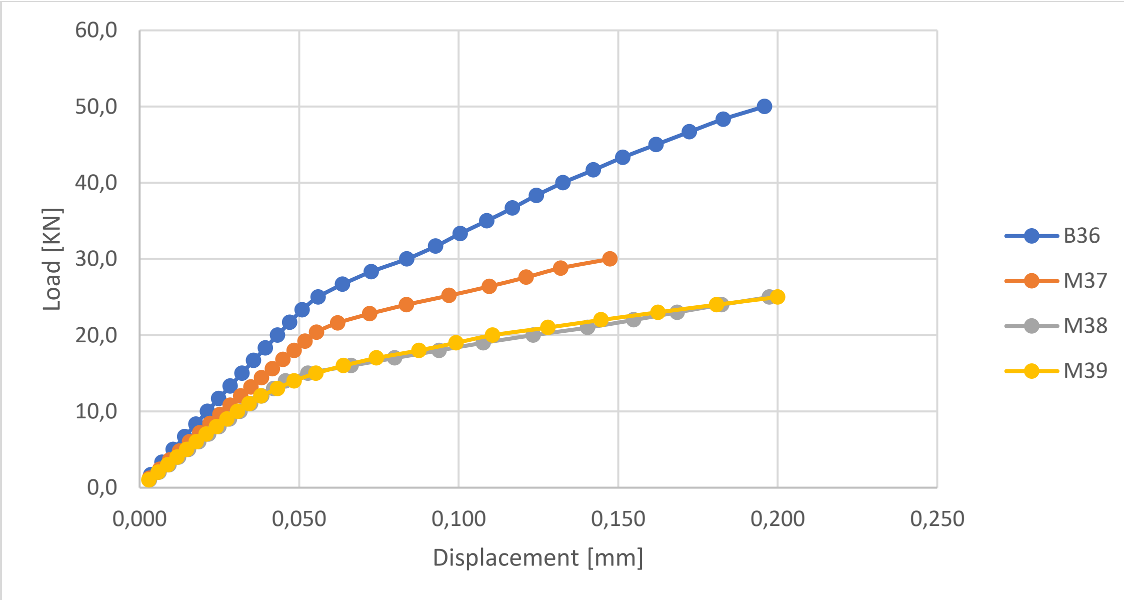

Figure B.9. Load-displacement behaviour of the numerical model for a Single Anchor Loaded Perpendicular to the Edge with Anchor Diameter ranging from 10 mm to 16 mm (Refer to Appendix A)

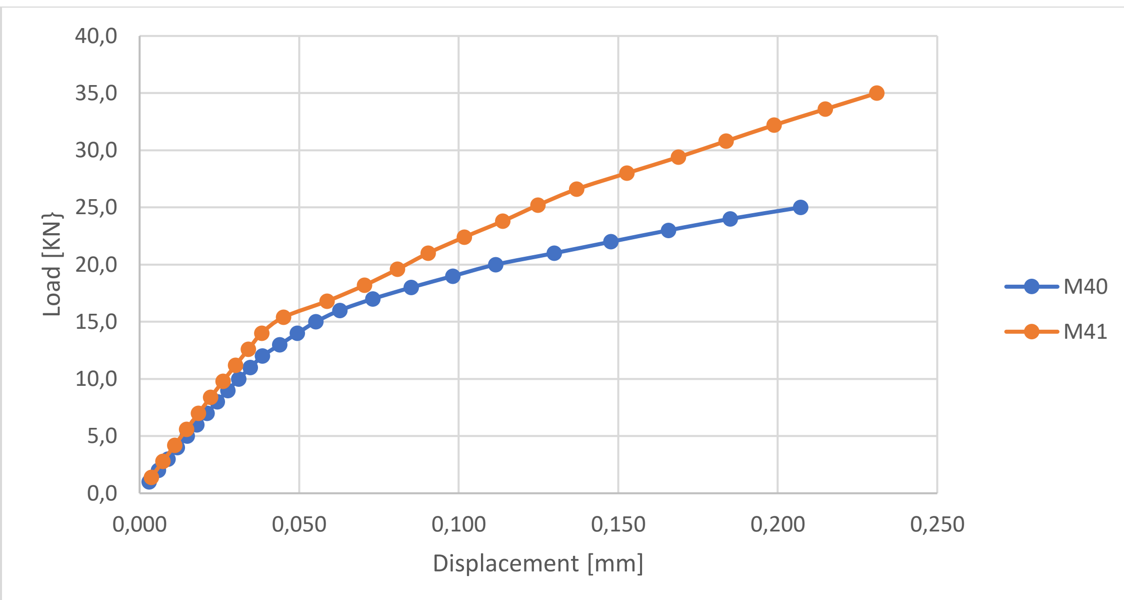

Figure B.10: Load-displacement behaviour of the numerical model for a Single Anchor Loaded Perpendicular to the Edge with Anchor Diameter d = 10 mm (Refer to Appendix A for the anchor design parameters)

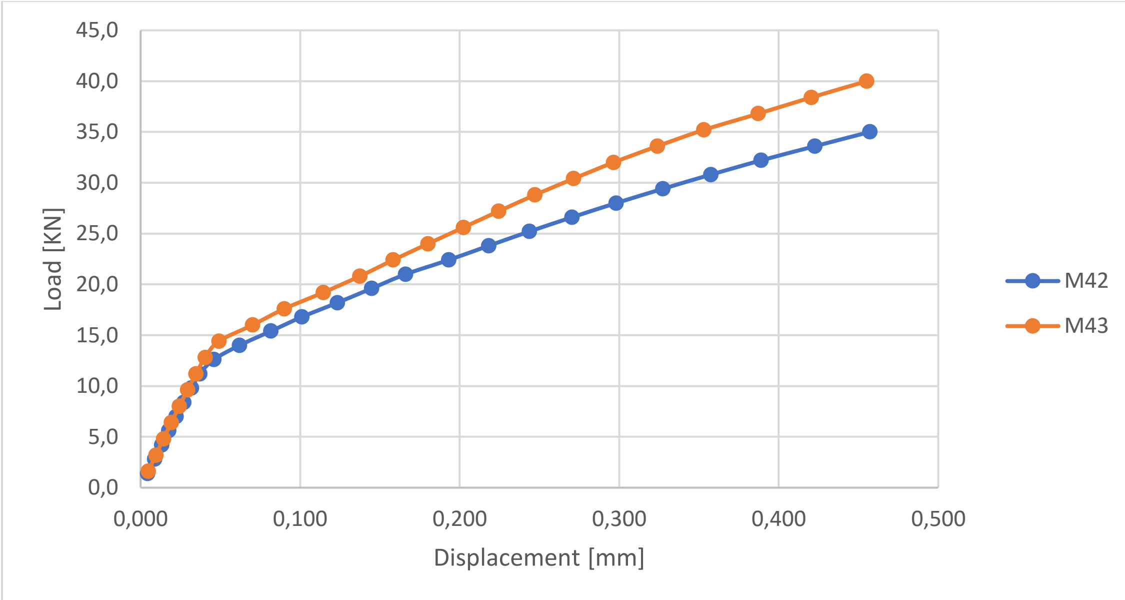

Figure B.11 Load-displacement behaviour of the numerical model for a Single Anchor Loaded Perpendicular to the Edge with Anchor Diameter ranging from 10 to 16 mm (Refer to appendix A for the anchor design Parameters)

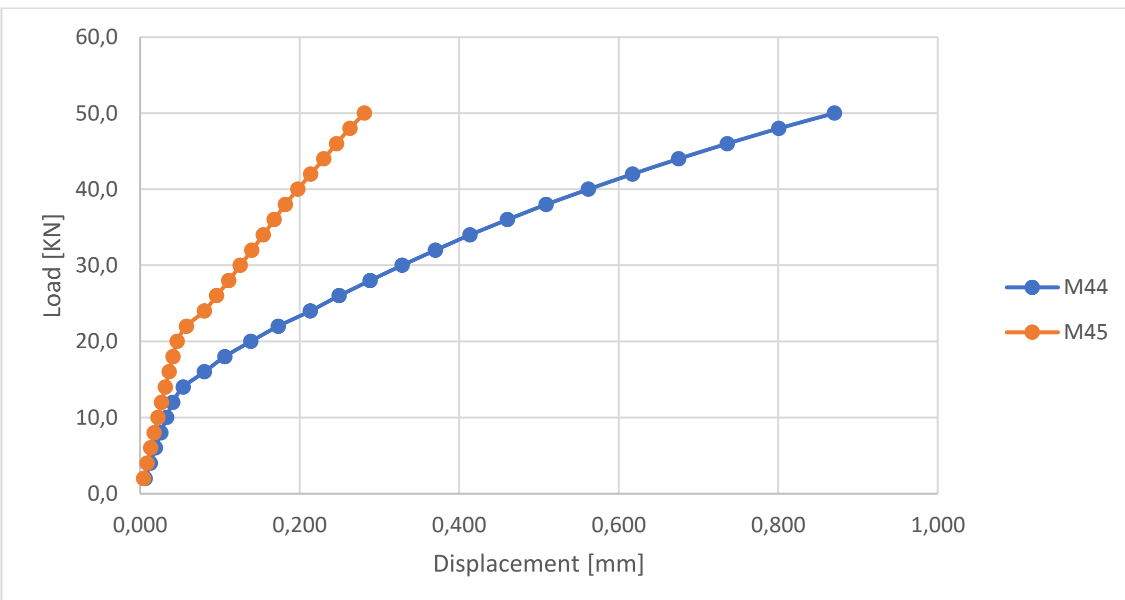

Figure B.12 Load-displacement behaviour of the numerical model for a Single Anchor Loaded Perpendicular to the Edge with Anchor Diameter ranging from 10 to 16 mm (Refer to appendix A for the anchor design Parameters)

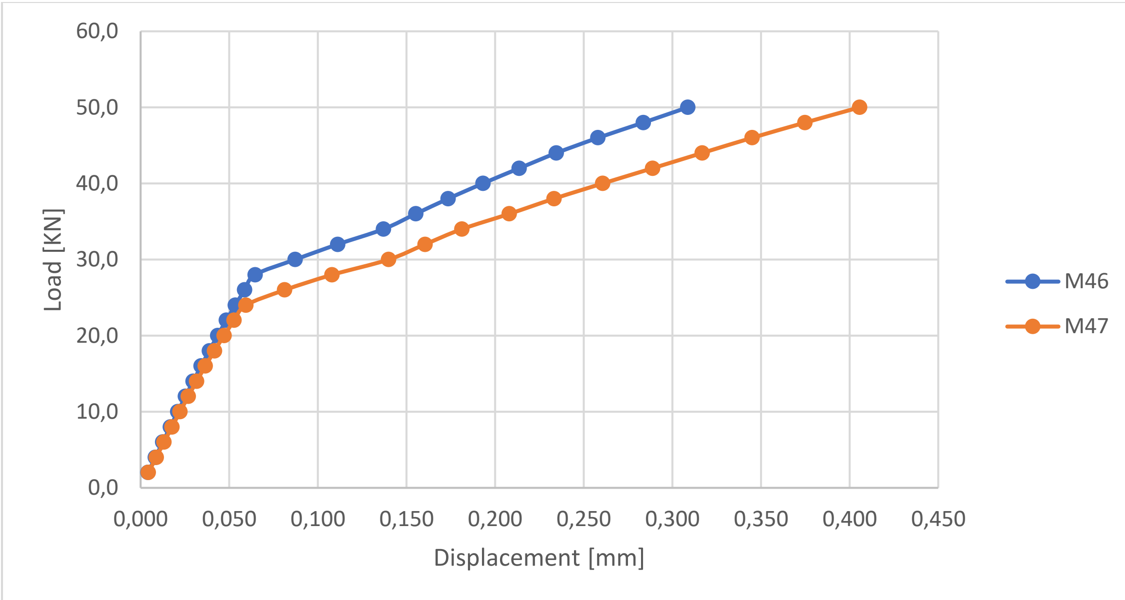

Figure B.13: Load-displacement behaviour of the numerical model for a Single Anchor Loaded Perpendicular to the Edge with Anchor Diameter d = 16 mm

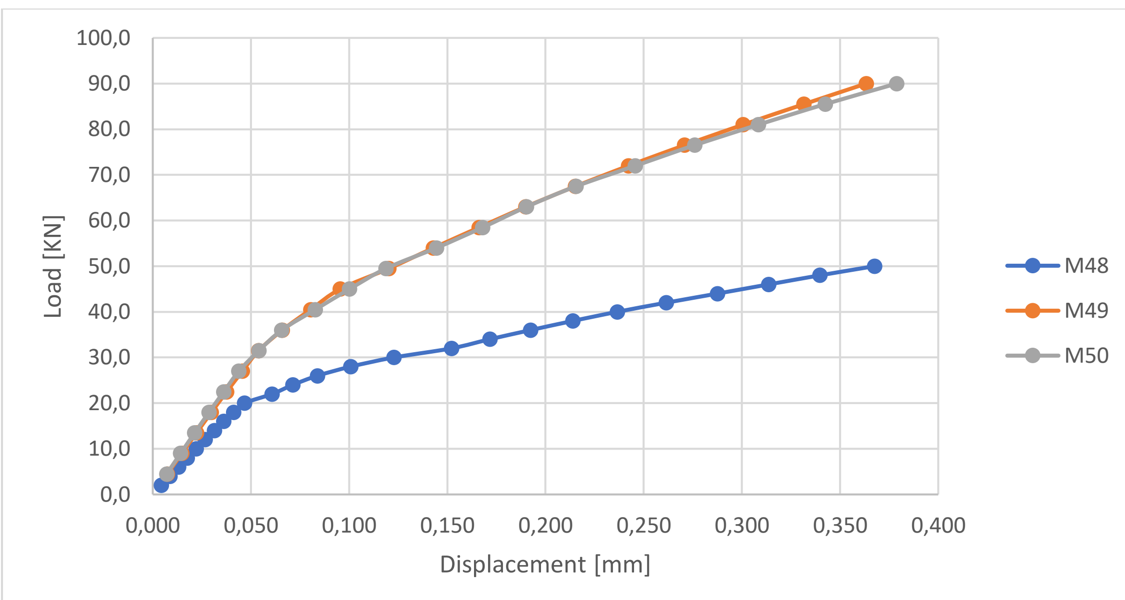

Figure B.14: Load-displacement behaviour of the numerical model for a Single Anchor Loaded Perpendicular to the Edge with Anchor Diameter ranging from 16 to 24 mm

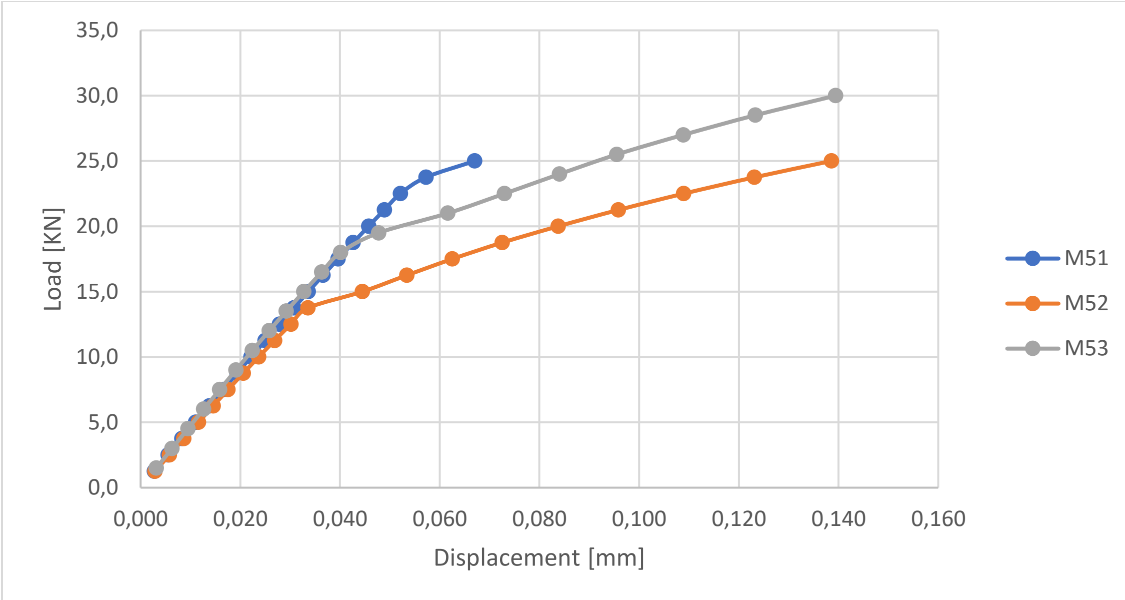

Figure B.15: Load-displacement behaviour of the numerical model for a Single Anchor Loaded Perpendicular to the Edge with Anchor Diameter d = 16 mm

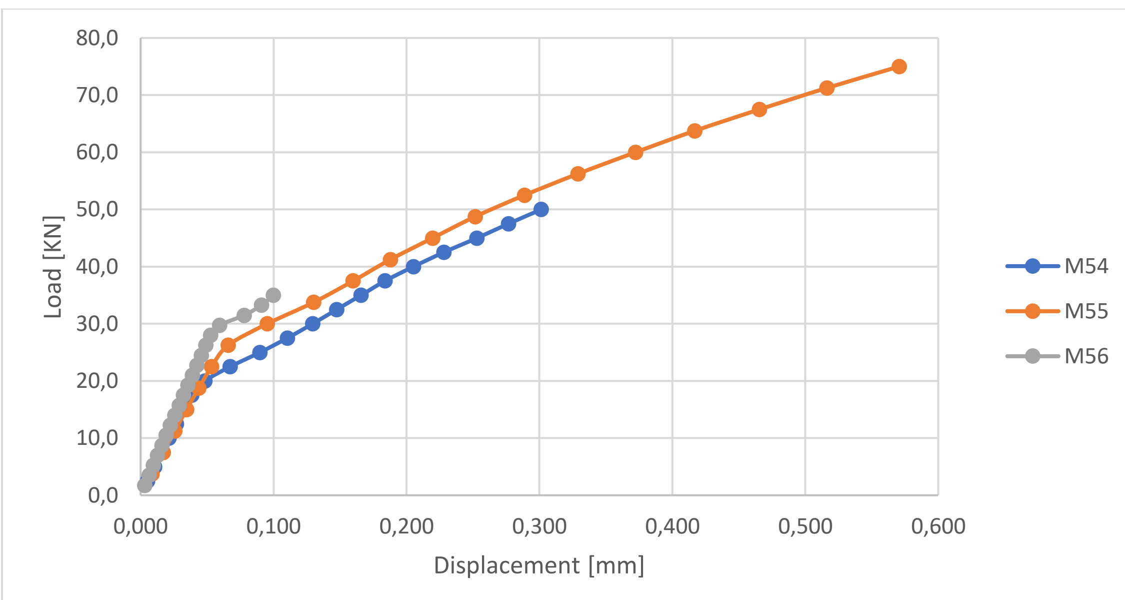

Figure B.16: Load-displacement behaviour of the numerical model for a Single Anchor Loaded Perpendicular to the Edge with Anchor Diameter ranging from 16 to 24 mm (Refer to Appendix A for the Anchor design Parameters)

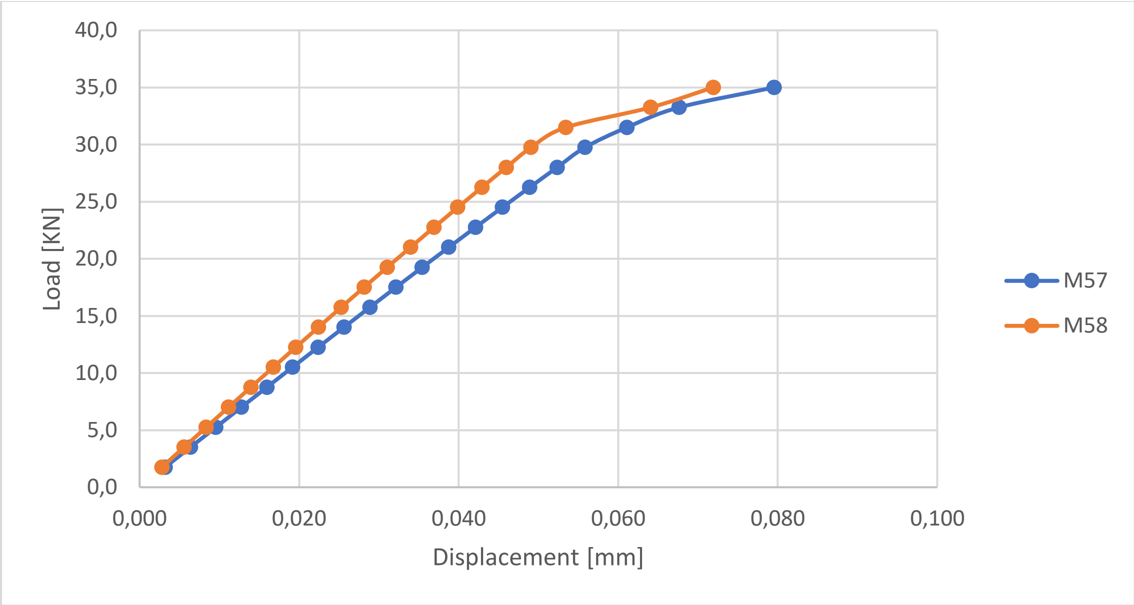

Figure B.17: Load-displacement behaviour of the numerical model for a Single Anchor Loaded Perpendicular to the Edge with Anchor Diameter d = 24 mm

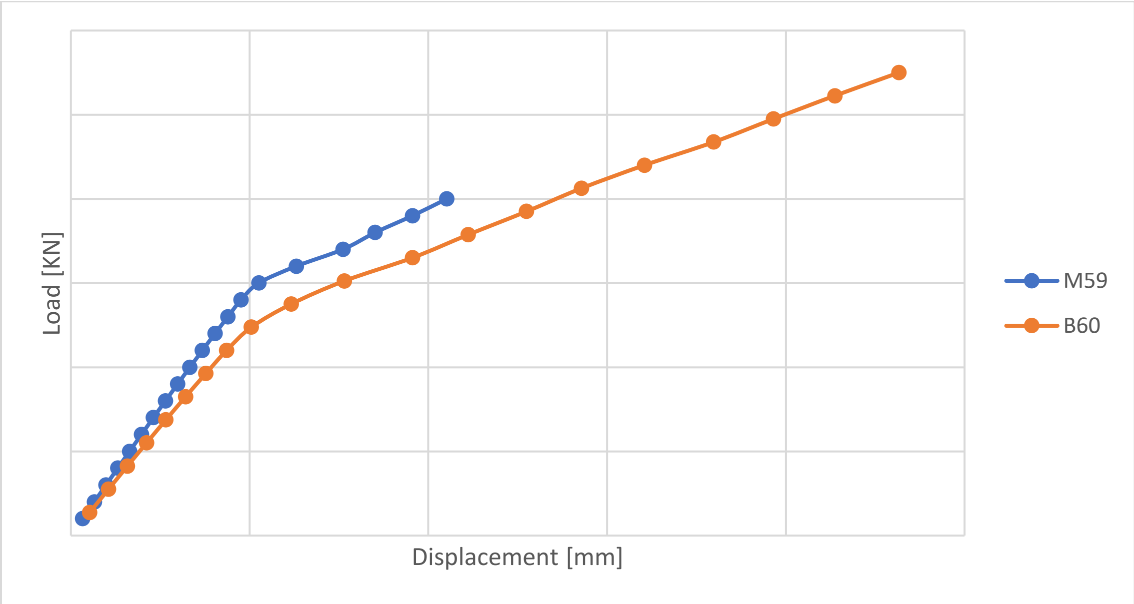

Figure B.18: Load-displacement behaviour of the numerical model for a Single Anchor Loaded Perpendicular to the Edge $f_{cc,200}$ =26.8 MPa with Anchor Diameter d = 16 mm: